1998

Inactivation of the JAK-STAT Pathway

Richard Lawrence Haspel

Inactivation of the JAK-STAT Pathway

A thesis presented to the faculty of
The Rockefeller University
in partial fulfillment of the requirements
for the degree of Doctor of Philosophy

by

Richard Lawrence Haspel

For my parents

Acknowledgments

I would like to thank all the members of the Darnell lab who have helped me these last few years. I would especially like to thank Curt Horvath who has been a constant source of critical insight. Most of all, I would like to thank my advisor, James Darnell, for his support. He has always taken the time to discuss my project and to teach me the fundamentals of scientific research.

Table of Contents

Abstract 1

Chapter 1 Introduction 3

1.1 The Interferons--A Model for Cytokine-Induced Gene Transcription 4
1.2 The STATs: Purification of GAF and ISGF-3 5
1.3 Other STAT Family Members 6
1.4 The STATs: Transcriptional Activation 8
1.5 The JAKs 10
1.6 IFN-γ Induced Signal Transduction--A Model of JAK-STAT Pathway Activation 11
1.7 The Transiency of Cytokine-Induced Gene Transcription 13
1.8 Downregulation of the Receptor-JAK Complex--The Role of the Ubiquitin-Proteasome Pathway 14
1.9 Downregulation of the Receptor-JAK Complex--The Role of Phosphatases 16
1.10 Inactivation of the STATs 17
1.11 The Effects of Aberrant JAK-STAT Pathway Activation 19
1.12 Guide to the Thesis 20

Chapter 2 The Kinetics of Stat1 Inactivation 27

2.1 The IFN-γ Time Course 27
2.2 The Half-Life of Activated Stat1 28
2.3 The Effect of Staurosporine Treatment on Inactivation Defective Stat1 Mutants 30
2.4 N-terminal Stat1 Mutants Translocate to the Nucleus 31
2.5 Discussion 33

Chapter 3 Mechanisms of JAK-STAT Pathway Inactivation 43

3.1 Inhibitors of Transcription Prolong IFN-γ Signaling 43
3.2 RNA and Protein Synthesis is Not Required for Stat1 Inactivation 44

3.3 Proteasome Inhibitors Prolong IFN-γ Signaling 45
3.4 The Effect of the Proteasome Inhibitor MG132 is Upstream From the Stat1 Molecules 46
3.5 MG132 Prolongs Activation of the IFN-γ Cell Surface Receptor 47
3.6 The Effect of Proteasome Inhibitor on Stat5 Activation 48
3.7 The Effect of the Proteasome Inhibitor MG132 is Upstream From the Stat5 Molecules 49
3.8 Vanadate Prolongs the Stat1 Signal In the Presence of Staurosporine 50
3.9 Direct Evidence For Cytoplasmic-Nuclear Cycling of Stat1 Involving a Tyrosine Phosphatase 51
3.10 Treatment with Staurosporine Also Reveals the Presence of a Stat1 Phosphatase 52
3.11 Discussion 53

Chapter 4 Localizing the Stat1 Phosphatase.....68

4.1 Cells Lacking SHP-1 Have a Prolonged IFN-γ Time Course 68
4.2 The Effect of SHP-1 on IFN–γ Signaling is Upstream of Stat1 69
4.3 The IFN-γ Time Course in Cytoplasts 70
4.4 The Effect of Staurosporine on the IFN-γ Time Course in Cytoplasts 72
4.5 The Flow of Activated Stat1 Upon Receptor-JAK Inactivation is from Cytoplasm to Nucleus 73
4.6 Flow of Activated Stat1 Upon Staurosporine Addition 74
4.7 Vanadate Prolongs Stat1 DNA Binding Activity in the Nucleus As It Decreases in the Cytoplasm 75
4.8 ^{35}S Labeling Reveals Nuclear Trapping of Phosphorylated Stat1 76
4.9 Discussion 77

Chapter 5: Perspectives and Future Directions.....94

5.1 What controls the duration of cytokine signaling? 94
5.2 How is the IFN-γ receptor-JAK complex inactivated? 95
5.3 What controls STAT inactivation? 98

5.4 What is the nature of the Stat1 phosphatase? 100
5.5 How is Stat1 exported from the nucleus? 102
5.6 What is the role of the N-terminus in Stat1 inactivation? 103
5.7 A model and future directions 104

Appendix A Experimental Procedures.....107

A.1 Cell Culture 107
A.2 Preparation of Cytoplasts 108
A.3 Antibodies, Inhibitors and Oligonucleotides 109
A.4 Cell Extracts, Immunoprecipitations and SDS-PAGE 110
A.5 Western Blotting 111
A.6 Electrophoretic Mobility Shift Assay 112
A.7 Pulse-Chase Experiments 113
A.8 Quantitation Using the PhosphorImager 113

Appendix B References.....115

List of Figures

Figure 1.1	Properties of STAT Molecules	25
Figure 1.2	A Model for IFN-γ Induced Signal Transduction	26
Figure 2.1	Effect of Staurosporine Treatment on Pre-induced IFN-γ DNA Binding Activity	36
Figure 2.2	Western Blots of Stat1 in IFN-γ Treated Cells with and without Staurosporine	37
Figure 2.3	The Staurosporine Pulse-Chase Experiment	38
Figure 2.4	Stat1 Constructs Stably Transfected into U3A Cells	39
Figure 2.5	The IFN-γ Time Course in U3A Cells Complemented with Wild-type and N-terminal Mutants of Stat1	40
Figure 2.6	Effect of Staurosporine Treatment on U3A Cells Complemented with Wild-type and N-terminal Mutants of Stat1	41
Figure 2.7	EMSA and Western Blot Analysis of Cytoplasmic and Nuclear Extracts from U3A Cells Complemented with p91 and Δ154	42
Figure 3.1	Actinomycin D Prolongs IFN-γ Signaling but not in the Presence of Staurosporine	59
Figure 3.2	Proteasome Inhibitors Prolong IFN-γ Signaling	60
Figure 3.3	MG132 Does Not Prolong Signaling in the Presence of Staurosporine	61
Figure 3.4	MG132 Prolongs Phosphorylation of the IFN-γ Receptor α Chain	62
Figure 3.5	MG132 Prolongs IL-2 Signaling	63
Figure 3.6	MG132 Does Not Prolong IL-2 Signaling in the Presence of Staurosporine	64
Figure 3.7	Vanadate Prolongs IFN-γ Signaling Even in the Presence of Staurosporine	65
Figure 3.8	The Stat1 Activation/Inactivation Cycle Analyzed by ^{35}S Labeling	66

Figure 3.9	The Effect of Staurosporine on the Stat1 Activation-Inactivation Cycle Analyzed by ^{35}S Labeling	67
Figure 4.1	Western Blots of SHP-1 Macrophages from Motheaten Mice and Littermate Controls	83
Figure 4.2	IFN-γ Time Course in Macrophages from Motheaten Mice and Littermate Controls	84
Figure 4.3	IFN-γ Signaling in Macrophages from Motheaten Mice is not Prolonged in the Presence of Staurosporine	85
Figure 4.4	Preparation of Cytoplasts	86
Figure 4.5	The IFN-γ Time Course in Cytoplasts and Control Cells	87
Figure 4.6	The Effect of Staurosporine on the IFN-γ Time Course in Cytoplasts and Control Cells	88
Figure 4.7	Western Blots of Stat1 in IFN-γ and Staurosporine Treated Cytoplasts and Control Cells	89
Figure 4.8	The Decay in Stat1 DNA Binding in Cytoplasmic and Nuclear Extracts During an IFN-γ Time Course	90
Figure 4.9	The Decay in Stat1 DNA Binding in Cytoplasmic and Nuclear Extracts Upon Staurosporine Addition	91
Figure 4.10	The Effect of Vanadate on Stat1 DNA Binding in Cytoplasmic and Nuclear Extracts	92
Figure 4.11	The Effect of Vanadate on the Stat1 Activation-Inactivation Cycle Analyzed by ^{35}S Labeling	93
Figure 5.1	The Stat1 Activation-Inactivation Cycle	106

List of Tables

Table 1.1	Phenotypes of Mice with Targeted Disruptions of Mouse STAT Genes	22
Table 1.2	JAKs and STATs Activated by Various Growth Factors and Cytokines	23
Table 1.3	Mutant Cell Lines Defective in Response to IFNs and the Complementing Proteins	24

List of Abbreviations

EGF	epidermal growth factor
EMSA	electrophoretic mobility shift assay
EPO	erythropoietin
GAF	gamma activated factor
GAS	gamma activated site
GM-CSF	granulocyte, macrophage-colony stimulating factor
IFN	interferon
IL	interleukin
ISGF	interferon-stimulated gene factor
ISRE	interferon-stimulated response element
JAK	Janus kinase
kD	kilodalton
LIF	leukemia inhibitory factor
MAPK	mitogen-activated protein kinase
MPF	M phase promoting factor
NES	nuclear export signal
NA	not available
NLS	nuclear localization signal
OSM	oncostatin M
PAGE	polyacrylamide gel electrophoresis
PDGF	platelet derived growth factor
PTP	protein tyrosine phosphatase
SH	src homology
SHP	SH2 containing protein tyrosine phosphatase
STAT	signal transducer and activator of transcription

Abstract

Signaling pathways involving Janus kinases (JAKs) and Signal Transducers and Activators of Transcription (STATs) play an important role in cytokine-induced gene transcription. Aberrant stimulation of this pathway can lead to abnormal development and cellular transformation demonstrating the importance of understanding mechanisms of downregulation.

After interferon-γ (IFN-γ) treatment of cells the appearance of tyrosine phosphorylated Stat1 in the nucleus was maximal within 20-30 minutes, remained for 2-2.5 hours and activated molecules disappeared by 4 hours. In the absence of continued signaling from the IFN-γ receptor (imposed by staurosporine treatment) previously activated Stat1 disappeared within 30-60 minutes, implying continuous generation and removal of tyrosine phosphorylated molecules during extended IFN-γ treatment. The proteasome, induced inhibitory proteins and the SHP-1 protein tyrosine phosphatase were all shown to play a role in the inactivation of the IFN-γ receptor-JAK complex but not in the direct inactivation of Stat1 molecules.

By analyzing the flow of phosphorylated Stat1 from cytoplasm to nucleus and utilizing ^{35}S labeling to examine the distribution of total Stat1 and activated Stat1 during a 4 hour IFN-γ time course, we concluded that the Stat1 molecules cycle into the nucleus as tyrosine phosphorylated molecules, are retained in the nucleus until dephosphorylated and then return to the cytoplasm. Our work with

Stat5 activation by IL-2 suggests similar mechanisms of downregulation are involved in other JAK-STAT pathways. Therefore, the removal of the activated STAT molecules appears not to be proteolytic but must depend on a nuclear protein tyrosine phosphatase(s).

Chapter 1 Introduction

Ligand-receptor interactions modulate a cell's response to its environment. Each of these interactions initiates a cascade of intracellular signaling events and frequently the induction of specific genes (1-4). The balance of activation and inactivation of intracellular signaling is crucial in determining a cell's phenotype. Overactive receptors, kinases or transcription factors can lead to abnormal growth and differentiation (reviewed in (5)). In addition, only two- to three-fold differences in the activity of components of a signaling pathway can lead to significant downstream effects (6).

This thesis focuses on the inactivation of signaling pathways involving Janus kinases (JAKs) and Signal Transducers and Activators of Transcription (STATs). JAKs are tyrosine kinases associated with the intracellular domains of numerous cytokine receptors, and are activated upon ligand binding to the receptor. The activated JAKs phosphorylate the receptor chains to which the STATs bind. The STATs then become phosphorylated on tyrosine, dimerize, translocate to the nucleus and activate transcription (reviewed in (7-15)).

In contrast to activation of the JAK-STAT pathway, the mechanisms for inactivation of this pathway are not well understood. While phosphatases, proteases and the induction of novel inhibitory proteins have all been implicated in JAK-STAT pathway inactivation, it is not clear in most instances where and how in the pathway these

different proteins function. Aberrant activation of JAKs or STATs can lead to cellular transformation and abnormal development, which demonstrates the importance of understanding mechanisms of downregulation. The interferons (IFNs), the first cytokines shown to activate the JAK-STAT pathway, will serve as a model system throughout much of this introduction.

1.1 The Interferons--A Model for Cytokine-Induced Gene Transcription

The IFNs were discovered over 40 years ago as secreted factors that induce resistance to viruses (reviewed in (16)). They are now classified into Type I (α and β) and Type II (γ) based on the agents that promote their secretion and the cells from which they are produced. IFNs bind to two major transmembrane receptors. All Type I IFNs bind the Type I IFN receptor while Type II IFN binds the IFN-γ receptor (16, 17). Interaction of ligand with receptor leads to novel gene transcription and numerous changes in cell function, including enhanced viral resistance and growth control (16).

In order to understand the mechanisms of IFN signaling, genes were cloned that were transcriptionally induced within minutes of Type I IFN treatment (1, 2, 18). This induction did not require new protein synthesis and promoter analysis identified a short region sufficient to drive the expression of these genes upon the addition of IFN-α (19, 20). This region was named the IFN-stimulated response element (ISRE). Using electrophoretic-mobility shift assays with an

ISRE probe, an IFN–α induced DNA binding factor was discovered, the IFN-stimulated gene factor 3 (ISGF-3) (20). This factor was not present in untreated cells but appeared within minutes after IFN–α addition.

While work with Type I IFNs was proceeding, a number of IFN-γ induced genes were discovered (reviewed in (4)). One of these genes coded for a guanylate binding protein whose transcript was induced to a higher degree by IFN-γ than by IFN–α (4). Analysis of the promoter region of this gene revealed an ISRE as well as a novel site required for maximal response to IFN–γ (21). This novel site was called the gamma activated site (GAS). A factor that bound to the GAS site within minutes after IFN–γ treatment was identified using exonuclease III assays and called GAF for gamma-activated factor (22).

Using enucleated cells, it was shown that both GAF and ISGF-3 became rapidly activated in the cytoplasm (22, 23). It was also known that ISGF-3 consisted of a component that was rapidly activated by IFN–α and a non-activated component (24). The stage was now set for the purification of these novel DNA-binding proteins.

1.2 The STATs: Purification of GAF and ISGF-3

Using an ISRE oligonucleotide, the protein components of ISGF-3 were purified, subjected to peptide sequencing and cloned (25-28). All four were novel proteins and named after their molecular weight (p112, p91, p84 and p48). p48 was the unactivated factor and

belonged to a family of proteins called IFN- regulatory factors (IRFs) for their supposed role in the regulation of the IFN-β gene (reviewed in (29)). The other three proteins in ISGF-3 belonged to a new protein family, with p84 being a splice variant of p91 lacking 38 C-terminal amino acids (25).

Purification with a GAS oligonucleotide also yielded a protein in the 90 kD range; it was later confirmed using specific antiserum that this protein was the same as the p91 component of ISGF-3 (25). Whereas IFN–α induced rapid tyrosine phosphorylation of p112 and p91 which then complexed with p48, IFN–γ only led to the tyrosine phosphorylation and homodimerization of p91 (30, 31). p84 was also activated by IFN-α and IFN-γ and could substitute for p91 in regard to DNA binding (8, 15).

Through a number of techniques, p91 was shown to be a component of GAF, and both p91 and p112 proteins were shown to be components of ISGF-3 (30, 31). It was demonstrated that these proteins were activated in the cytoplasm by tyrosine phosphorylation and then translocated to the nucleus to bind to GAS and ISRE sites and activate specific genes (reviewed in (8, 15)). Due to their dual function these proteins were named STATs for Signal Transducers and Activators of Transcription (10). The p91, p84 and p112 proteins were called Stat1α, Stat1β and Stat2 respectively.

1.3 Other STAT Family Members

Since the discovery of Stat1 and Stat2, five other STAT genes have been cloned (Table 1.1). Stat4 and Stat5b were discovered by homology screening of a cDNA library (32, 33). Stat5a and Stat6 were isolated through purification of a DNA binding activity (34, 35). Stat3 was discovered by both techniques (33, 36). As with Stat1, alternative splicing can lead to different forms of some of these proteins (reviewed in (13)).

The STATs are all believed to have certain features in common ((Figure 1.1), reviewed in (9, 13, 15)) . All of the STATs are activated by tyrosine phosphorylation on a single residue near amino acid 700. This phosphorylation leads to dimerization, entry into the nucleus and activation of transcription. The phosphorylation of the STATs is induced by numerous cytokines and growth factors (Table 1.2). In addition, while homodimerization occurs for all the STATs except Stat2, only certain heterodimers form *in vivo*, Stat1:2 and Stat1:3 being particularly prominent examples. Tests of all heterodimerization possibilities, however, have yet to be carried out.

All of the STATs contain an SH2 (src homology 2) domain between amino acids ~600 and 700. SH2 domains are, of course, known to function as binding sites for phosphorylated tyrosine residues (37). The STATs are no exception as the dimerization of these proteins occurs through phospho-tyrosine-SH2 interactions (38). The phospho-tyrosine of one STAT protein (located at amino acid ~700) binds the SH2 domain of its dimeric partner and vice versa. Utilizing the fact that different STATs preferentially bind different DNA sequences, chimeric proteins were used to determine that the DNA binding domains for Stat1, Stat3 and Stat6 lie between

amino acids ~400 and 500 (39, 40). The crystal structures of Stat1 and Stat3 homodimers bound to DNA confirm much of the earlier work on dimerization and DNA binding and provide a firm foundation for dividing the STAT proteins into functional domains (Figure 1.1) (41, 42). One point that was immediately clarified by the crystal structures was the identification of a linker domain between the DNA binding and SH2 domains that was originally thought to be an SH3 domain (43).

Specificity of signaling is achieved to some extent by different ligands activating different STATs ((Table 1.2), reviewed in (9, 12)). For example, only interleukin-4 (IL-4) activates Stat6 while only IL-12 activates Stat4. "Knockout" mice, homozygous for deletions of the different STATs, further reveal how specificity of signaling is achieved ((Table 1.1), reviewed in (9, 11, 12)). As expected, Stat4 and Stat6 knockout mice have defects in T cell development related to IL-12 and IL-4 respectively (44-48). Surprisingly, even though in cell culture Stat1 is activated by numerous ligands, including several growth factors, the Stat1 knockout mice have only defects in innate immunity (15, 49, 50). This result indicates Stat1 primarily functions in the IFN pathway. The Stat3 knockout, however, is an embryonic lethal and recent studies on the importance of Stat3 in apoptosis in T cells and oncogenic transformation suggest a broad role for this STAT in cell growth (51-53). How physiological specificity is achieved upon activation of Stat3 remains uncertain.

1.4 The STATs: Transcriptional Activation

The finding that Stat1α, and not Stat1β, promotes IFN-γ induced transcription implicated the C-terminus as a transcriptional activator (54). In fact, the 40 C-terminal amino acids of Stat1α, fused to the Gal-4 DNA binding domain, are able to support transcription (55). The C-termini of other STAT proteins have been shown to serve a similar function (reviewed in (11)).

The transcriptional activation potential of the STATs is determined by multiple protein-protein interactions (Figure 1.1). The C-termini of Stat1 and Stat2 and the N-terminus of Stat1 have been shown to bind CBP/p300, histone acetyltransferases that play a role in gene activation (56, 57). STATs also interact with a number of transcription factors including p48, c-Jun, glucocorticoid receptor and SP-1 (reviewed in (9, 13)). STAT dimers have also been shown to interact with each other (58, 59). In cases of adjacent STAT binding sites in a promoter (as with the IFN-γ gene), the N-termini of Stat1 and Stat4 have been shown to play a role in STAT tetramerization (two connected dimers). This tetramerization leads to increased gene transcription through a more stable DNA binding complex.

In the case of Stat1, Stat3, Stat4 and Stat5, the transcriptional function of the C-terminus is further regulated by serine phosphorylation (reviewed in (12)). For example, Stat1α is phosphorylated on a single serine residue (60). When this residue is mutated to alanine, transcriptional induction drops to 25% compared to wild-type (61). It is not clear which serine kinases are involved in this phosphorylation. Recently, a protein (MCM5) that preferentially binds the serine phosphorylated C-terminus of Stat1 has been

identified and may explain some of the function of serine phosphorylation in transcriptional activation (55).

Protein-protein interactions may also play a role in inhibiting STAT DNA binding. Members of the PIAS (protein inhibitor of activated STATs) family can interact with phosphorylated STATs (62, 63). PIAS1 and PIAS3 bind to and affect the function of Stat1 and Stat3 respectively. These proteins block *in vitro* STAT DNA binding, and overexpression of PIAS in transiently transfected cells inhibits STAT induced transcription. How the balance of positive and negative acting factors control the extent of STAT activated gene expression remains to be determined.

1.5 The JAKs

As work was proceeding on the purification of ISGF-3, George Stark and Ian Kerr were using a different approach to investigate IFN-inducible gene expression (reviewed in (8)). By using somatic cell mutagenesis, cell lines were created that lacked components of the IFN-α and IFN-γ signaling pathways (Table 1.3). Some of these cells were shown to lack STAT proteins (54, 64). Others, however, lost individual members of the JAK family of tyrosine kinases (65-67). It was hypothesized and eventually demonstrated that these kinases were responsible for phosphorylation of the STATs (reviewed in (9)).

There are 4 members of the JAK family: Jak1, Jak2, Jak3 and Tyk2 (reviewed in (13)). They are all found associated with cytokine

receptors ((Table 1.2), reviewed in (12, 68)) For example, Jak1 and Tyk2 associate with the IFN–α receptor while Jak1 and Jak2 associate with the IFN–γ receptor. As might be expected, loss of Jak2 and Tyk2 results in loss of IFN–α and IFN–γ signaling respectively, while loss of Jak1 results in a defect in both Type I and Type II IFN signal transduction (67, 69, 70). It is believed that when ligand binds to the receptor, the JAKs are phosphorylated causing activation of the JAK kinase domain. The JAKs then phosphorylate both the receptor and the STATs on tyrosine (reviewed in (7, 13, 17)).

The JAKs are not required in all instances of STAT phosphorylation. For example, in the case of the epidermal growth factor (EGF) receptor, the intrinsic kinase activity of the receptor appears sufficient to activate the STATs (71). In addition, overexpression of certain kinases (e.g., c or v-src) leads to phosphorylation of STATs (reviewed in (53)). It is not clear in these cases, however, whether activation of the JAKs is also required.

1.6 IFN–γ Induced Signal Transduction--A Model of JAK-STAT Pathway Activation

IFN–γ treatment of cells serves as a paradigm for cytokine mediated JAK-STAT signaling from cytoplasm to nucleus ((Figure 1.2), reviewed in (17, 72)). The IFN–γ receptor consists of both α and β chains. IFN–γ binds and causes the dimerization of the receptor's α chains. This dimerization causes the recruitment of the receptor's β chains to the complex. Jak1 and Jak2, associated with the α and β chains respectively, are then activated through tyrosine

phosphorylation. Through studies with JAK deficient cell lines, it appears that JAK2 is the initiator of the phosphorylation events (73).

Following JAK activation, the receptor's α chain is phosphorylated on tyrosine 440, providing a docking site for Stat1 (74). Stat1 then interacts with the receptor through its SH2 domain and becomes phosphorylated on tyrosine 701 (75). Since the avidity of STAT-STAT interactions is higher than that of STAT-receptor interactions, the Stat1 dissociates from the receptor and dimerizes with another Stat1 through the previously described SH2-phosphotyrosine interactions (76). The dimerization allows for translocation to the nucleus, DNA binding and transcriptional activation (38, 75).

Typically, most Stat1 is present in the cytoplasm until cytokine-mediated activation leads to nuclear import (31). Classic nuclear localization signals (NLSs) contain strings of basic amino acids (77). Stat1 does not have a classic NLS and it is unclear what allows translocation into the nucleus. In immunoprecipitation studies, tyrosine phosphorylated Stat1 has been shown to interact with NPI-1, a component of the nuclear import machinery (78). Injection of anti-NPI-1 antibody into HeLa cells prevents Stat1 nuclear localization upon IFN–γ treatment. The region on the Stat1 or any other STAT dimer that binds to NPI-1 has not been determined.

The SH2 domain of the STAT, in concert with the STAT binding domain on the receptor, appears to determine how different receptors activate different STATs. Swapping SH2 domains between Stat1 and 2 alters receptor recognition (79). Fusion of the Stat3 docking site on gp130 (a component of a number of cytokine

receptors) to the erythropoietin receptor allows erythropoietin activation of Stat3 (80). In contrast, the JAKs do not appear to play a significant role in specificity (reviewed in (13)). Changing the particular JAKs associated with a receptor does not lead to activation of different STATs.

Other receptor-JAK-STAT pathways are believed to follow the IFN-γ activation paradigm. One partial exception involves the IFN-α activation of Stat1 and Stat2 (64). Stat1 is not activated by IFN-α in cells lacking Stat2. It appears that Stat2 serves as the docking site for Stat1. Another exception is that Stat5 can dock at the IL-6 receptor through an interaction with JAK2 (81).

1.7 The Transiency of Cytokine-Induced Gene Transcription

Early studies of cytokine-induced gene expression revealed not only its rapid activation but also its transient nature (1-4). Transcription rates of certain IFN-α stimulated genes, measured through nuclear run-on analysis, declined to almost baseline after only 5 or 6 hours of IFN treatment (2).

With the discovery of ISGF-3 and GAF, correlations were made with the decline in transcription and the disappearance of DNA binding activity (22, 24). ISGF-3 and GAF DNA binding was shown to only last 5 or 6 hours coincident with maximal transcription rates of a number of IFN-induced genes. With the purification of STAT proteins, the decrease in DNA binding was shown to correlate with the disappearance of phosphorylated STATs from the nucleus (31)

This disappearance of phosphorylated STAT occurs in two steps. First, the receptor-JAK complex must be downregulated in order to prevent the generation of any newly activated STATs. Second, the already existing phosphorylated STAT protein must be inactivated.

1.8 Downregulation of the Receptor-JAK Complex--The Role of the Ubiquitin-Proteasome Pathway

The classic mechanism for receptor downregulation involves endocytosis and targeting of the receptor plus ligand to the endosome (reviewed in (5, 82, 83)). In the endosome, the ligand is dissociated from the receptor, allowing the receptor to be transported back to the cytoplasm, while the ligand is transported to the lysosome for degradation. In some cases, both the receptor and ligand are degraded. Both "tyrosine-based" and "dileucine based" signals have been implicated in constitutive endocytosis of receptors. These motifs are recognized by components of the internalization machinery. The endocytosis rates of certain receptors, including many cytokine receptors, are increased upon ligand binding. Although the classic motifs may play some role in this process, the exact mechanisms behind ligand activated endocytosis have not been worked out.

In recent years, the ubiquitin-proteasome pathway has been show to play a role in endocytosis and inactivation of receptors (reviewed in (84)). This pathway is involved in the degradation of a wide variety of proteins (reviewed in (85, 86)). Ubiquitin is a small protein containing only 76 amino acids. Typically, lysines on target

proteins are joined through an amide bond to the C-terminal glycine of ubiquitin. The proteasome then recognizes and degrades the ubiquitin-target protein complex.

At least 10 cytokine and growth factor receptors have been shown to be ubiquitinated upon ligand stimulation, including a number known to activate the JAK-STAT pathway (e.g., the platelet derived growth factor (PDGF) and growth hormone receptors) ((87, 88), reviewed in (84)). A natural conclusion from these results is that upon ligand stimulation, receptors are bound to ubiquitin, thus targeting the intracellular domain of the receptor for downregulation through degradation by the proteasome. As support for this hypothesis, proteasome inhibitors do prevent some degradation of the PDGF receptor (89).

More recently, there has been evidence that ubiquitin may serve solely as a signal for receptor-mediated endocytosis and not degradation by the proteasome. In yeast, mono- or diubiquitinated receptors are selectively internalized and degraded (84). This destruction, however, occurs in the lysosome as yeast proteasome mutants show no defect in internalization and degradation. One group has provided evidence that the mammalian growth hormone receptor also uses ubiquitin as a signal for internalization (88, 90). Cells with a temperature sensitive defect in ubiquitin conjugation do not internalize or degrade this receptor at the non-permissive temperature. The relative contributions of the lysosome versus the proteasome in the destruction of the growth hormone receptor were not determined. In the final analysis, it is still not clear what role

the proteasome and ubiquitin play in the downregulation of mammalian receptors.

1.9 Downregulation of the Receptor-JAK Complex--The Role of Phosphatases

The activation of the receptors and JAKs involves tyrosine phosphorylation. This phosphorylation has been shown to decay over time even in the constant presence of ligand (74, 91). Two tyrosine phosphatases, SHP-1 and SHP-2, containing SH2 domains have been found to play a major role in cytokine signal transduction (reviewed in (92, 93)). Although there are some exceptions, SHP-1 plays a role in inactivation while SHP-2 plays a role in positive signaling.

Through immunoprecipitation experiments, SHP-1 has been found associated with both JAKs and receptors. For example, SHP-1 is constitutively associated with the IFN-α receptor-JAK complex (94). In the case of the erythropoietin receptor, ligand binding causes receptor phosphorylation and binding of SHP-1 to specific phosphotyrosines (91). Substitution with phenylalanine of two potential SHP-1 tyrosine binding sites in the erythropoietin receptor results in significantly prolonged tyrosine phosphorylation of Jak2.

Mice lacking functioning SHP-1 have proven useful in determining the role of SHP-1 in IFN receptor-JAK inactivation ((95, 96), reviewed in (97)). These "motheaten" mice have a number of hematopoietic defects and die 4 to 9 weeks post-partum. Stat1 DNA binding activity is increased in cells from motheaten mice in

response to both IFN–α and IFN–γ (94, 98). In the case of IFN–α, it appears that Jak1 but not Tyk2 phosphorylation is significantly increased in motheaten mice even though SHP-1 co-immunoprecipitates with both JAKs. In addition, while Stat1 dimer DNA binding increases, ISGF-3 binding does not. The mechanism for this apparent selectivity of SHP-1 remains unclear. Nevertheless, it appears that SHP-1 has some role in controlling IFN-induced signal transduction.

The recently discovered SOCS (Suppressors of Cytokine Signaling) family of proteins, also may play a role in JAK-receptor inactivation (99-102). The genes for many of these proteins are rapidly induced upon addition of a number of cytokines. When overexpressed, some of these proteins are able to bind the JAKs or receptors and suppress their activation. The precise mechanisms by which these proteins function have not been determined.

1.10 Inactivation of the STATs

Disappearance of phosphorylated Stat1 could theoretically occur by either proteolysis or dephosphorylation. Degradation by the proteasome has been implicated in the inactivation of a number of transcription factors including c-Jun, c-Fos and p53 (103-105). In fact, the oncogenic potential of v-Jun is due to its resistance to proteasome degradation leading to a longer half-life (104). Phosphorylated Stat1 also has been found conjugated to ubiquitin (106). In that study, however, no quantification was carried out

making it unclear what fraction of Stat1 might be inactivated by the proteasome.

Vanadate, an inhibitor of tyrosine phosphatases, has been shown to prolong IFN-α and γ signaling (107, 108). The authors of these studies concluded that a tyrosine phosphatase inactivates the STAT proteins. Vanadate, however, can activate the JAK-STAT pathway on its own and as discussed above, tyrosine phosphatases play a role in downregulation of receptor-JAK complexes (109). It is possible, therefore, that continued activation of STAT proteins as opposed to a block in STAT inactivation may enable prolonged IFN signaling in the presence of vanadate. A specific Stat1 phosphatase has not been identified, although SHP-1 has been shown to co-immunoprecipitate with Stat1 and Stat5 (98, 110). Since phosphorylation on serine increases the transcriptional activity of some STATs, dephosphorylation of these residues could also be a mechanism of STAT inactivation. Neither the kinetics of this process nor the identity of a serine phosphatase has been determined.

Other studies have identified regions in the STAT molecules that may promote their inactivation (Figure 1.1). In the case of Stat3 and Stat5, removal of 40 to 50 amino acids from the C-terminus results in proteins that remain tyrosine phosphorylated long after their full-length counterparts have become inactivated (111-114). The mechanism behind this phenomenon is unclear. In contrast, it appears that N-terminal alterations in Stat1 cause an inactivation defect (115). Truncation of only 62 amino acids from the N-terminus of Stat1 leads to a molecule that is constitutively active and has prolonged IFN-γ induced DNA-binding activity compared to wild-

type. It has also been reported that substitution of the first 130 amino acids of Stat1 with the N-terminus of Stat5 also results in longer-lived tyrosine phosphorylated molecules (116). In addition, the kinetics of Stat1β and Stat1α inactivation are essentially the same (117). These results suggest that the roles of the C and N-termini differ in Stat1 vs Stat3 and Stat5 inactivation.

One group has reported a correlation between the prolonged activation of Stat1 N-terminal mutants and their apparent inability to translocate to the nucleus (116). From these results, the authors argued that a nuclear phosphatase inactivates Stat1 This study, however, only showed a defect in nuclear transport in immunofluorescence experiments. Other standard measures of nuclear protein (e.g., Western blot) indicated that the N-terminal Stat1 mutants were able to enter the nucleus. The intracellular compartment of STAT inactivation remains uncertain.

1.11 The Effects of Aberrant JAK-STAT Pathway Activation

There is growing evidence that aberrant activation of the JAK-STAT pathway can lead to cancer (reviewed in (53)). In some cancer cell lines and human tumors, STATs (typically Stat3 or Stat5) as well as JAKs are constitutively activated. Transfection of cell lines with various oncogenic proteins (both kinases and receptors) also leads to constitutive activation of JAKs and STATs and transformation. As a demonstration of cause and effect, v-Src mediated transformation of fibroblasts can be blocked by a dominant negative form of Stat3

(118). The full role of JAKs and STATs in cancer progression is only beginning to be explored.

Aberrant activation of the JAK-STAT pathway may also lead to abnormal development (119). A specific point mutation in the fibroblast growth factor (FGF) receptor causes a lethal form of dwarfism. This receptor has a constitutive tyrosine kinase activity that phosphorylates Stat1. Since Stat1 has been shown in cell culture to play a role in growth arrest, it has been proposed that increased Stat1 activity leads to the retarded bone growth in this form of dwarfism.

1.12 Guide to the Thesis

The association of JAK-STAT pathway dysregulation with cancer and abnormal development highlights the importance of understanding how tight control of activation and inactivation is normally achieved. Proteases, phosphatases and inducible inhibitors have all been implicated in downregulation. The significance, however, of each of these components has not been ascertained.

This thesis describes experiments undertaken in order to better understand JAK-STAT pathway inactivation. IFN-γ was used as a model system for its relative simplicity in that only Stat1 is activated. In addition, Stat1 activation by IFN-γ is perhaps the best understood of all the receptor-JAK-STAT pathways. Studies on the kinetics of Stat1 inactivation are described in chapter 2. In chapter 3, we explore the mechanisms of JAK-STAT pathway inactivation

through the use of various inhibitors and ^{35}S labeling. In chapter 4, we describe our attempts to localize the intracellular compartment of STAT inactivation. Chapter 5 summarizes the work presented in this thesis and its implications for understanding the regulation of the JAK-STAT pathway.

Table 1.1 Phenotype of Mice with Targeted Disruptions of Mouse STAT Genes

Targeted Gene	Phenotype
Stat1	Defective Type I and Type II IFN signaling; defects in innate immunity
Stat2	Impaired resistance to infection? See note below.
Stat3	Embryonic lethal
Stat4	Defective T helper1 cell development
Stat5a	Defective breast development; defects related to impairment of GM-CSF and IL-2 signaling
Stat5b	Defects related to impairment of growth hormone signaling
Stat6	Defective T helper2 cell development

Recent work from Dr. Chris Schindler indicates the Stat2 knockout mouse have no obvious defects when grown in strictly controlled non-contaminated conditions. They are under tests for tolerance to specific infections (120).
This table is based on similar lists published elsewhere (9, 12).
Abbreviations: IFN--interferon, IL--interleukin, GM-CSF--granulocyte, macrophage-colony stimulating factor

Table 1.2 JAKs and STATs Activated by Various Growth Factors and Cytokines

Cytokine	JAKs	STATs
IL-2, IL-7, IL-9	Jak1, Jak3	Stat5a, Stat5b, Stat3
IL-4	Jak1, Jak3	Stat6
IL-3, IL-5, GM-CSF	Jak2	Stat5a, Stat5b
IL-6, IL-11, OSM, LIF	Jak1, Jak2, Tyk2	Stat3
Leptin	NA	Stat3
IL-12	Jak2, Tyk2	Stat4
Prolactin, EPO	Jak2	Stat5a, Stat5b
Growth hormone	Jak2	Stat5a, Stat5b, Stat3
IFN-α, IFN-β	Jak1, Tyk2	Stat1, Stat2
IFN-γ	Jak1, Jak2	Stat1
EGF, PDGF	Jak1, Jak2	Stat3

This table is not meant to be complete and is based on similar lists published elsewhere (12, 15).
Abbreviations: IL-interleukin, EPO--erythropoietin, IFN--interferon, OSM--oncostatin-M, LIF--leukemia inhibitory factor, EGF--epidermal growth factor, PDGF--platelet derived growth factor, GM-CSF--granulocyte, macrophage-colony stimulating factor, NA--not available.

Table 1.3 Mutant Cell Lines Defective in Response to IFNs and the Complementing Proteins

Cell line	Complementing Protein
U1	Tyk2
U2	p48
U3	Stat1
U4	Jak1
U5	NA
U6	Stat2
γ1	IFN-γ receptor β chain
γ2	Jak2

This table is based on similar lists published elsewhere (8, 13). Abbreviations: IFN-interferon, NA-not available.

Figure 1.1 Properties of STAT Molecules

Arrows point to well-defined and potential protein-protein interactions. Amino acid numbers refer to those for human Stat1α as determined by the crystal structure (42). They are similar for other members of the STAT family (41). Abbreviations: TAD--transcriptional activation domain. See introduction for more details. This figure is based on similar figures published elsewhere (9, 12, 13).

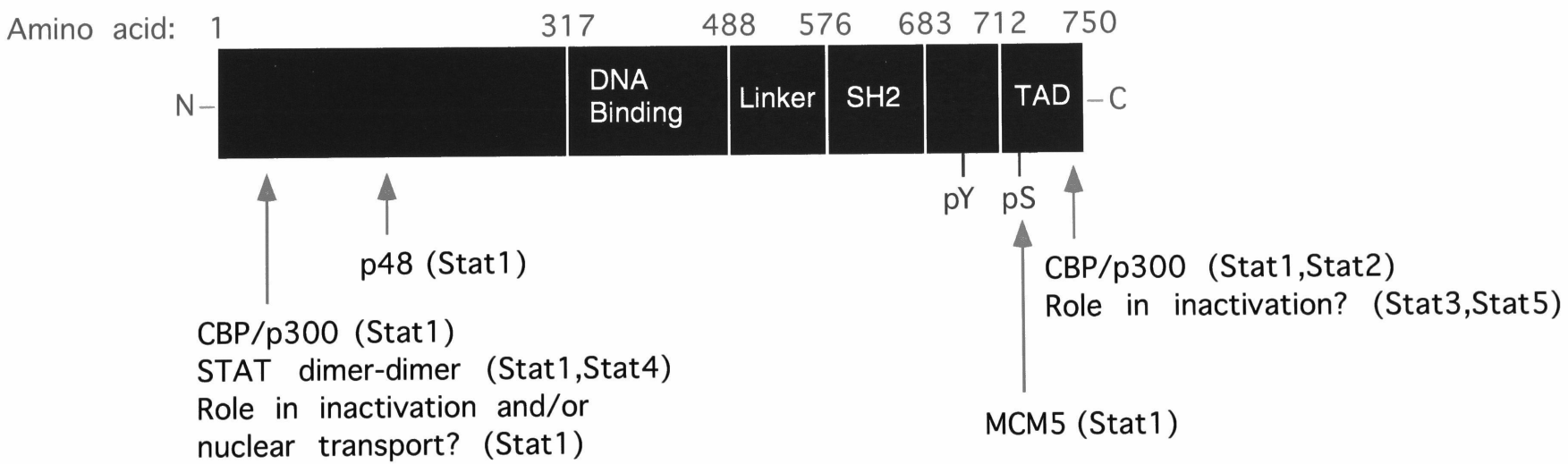
Amino acid: 1
317
488
576
683
712
750
N–
DNA Binding
Linker
SH2
TAD
–C
pY
pS
p48 (Stat1)
CBP/p300 (Stat1,Stat2)
Role in inactivation? (Stat3,Stat5)
CBP/p300 (Stat1)
STAT dimer-dimer (Stat1,Stat4)
Role in inactivation and/or
nuclear transport? (Stat1)
MCM5 (Stat1)

Figure 1.2 A Model for IFN-γ Induced Signal Transduction

Two α and two β chains of the IFN-γ receptor (A) are brought together by the addition of IFN-γ, leading to tyrosine phosphorylation and activation of the JAKs followed by tyrosine phosphorylation of the receptor α chains (B). Stat1 is then recruited to the receptor-JAK complex and phosphorylated on tyrosine 701 (C). The activated Stat1 is then able to dimerize with another phosphorylated Stat1 molecule (D) leading to the translocation of Stat1 dimers into the nucleus (E). The Stat1α dimers, but not the Stat1β dimers, are able to activate transcription by binding to GAS elements.
See introduction for more details. This figure is based on similar figures published elsewhere (17, 72).

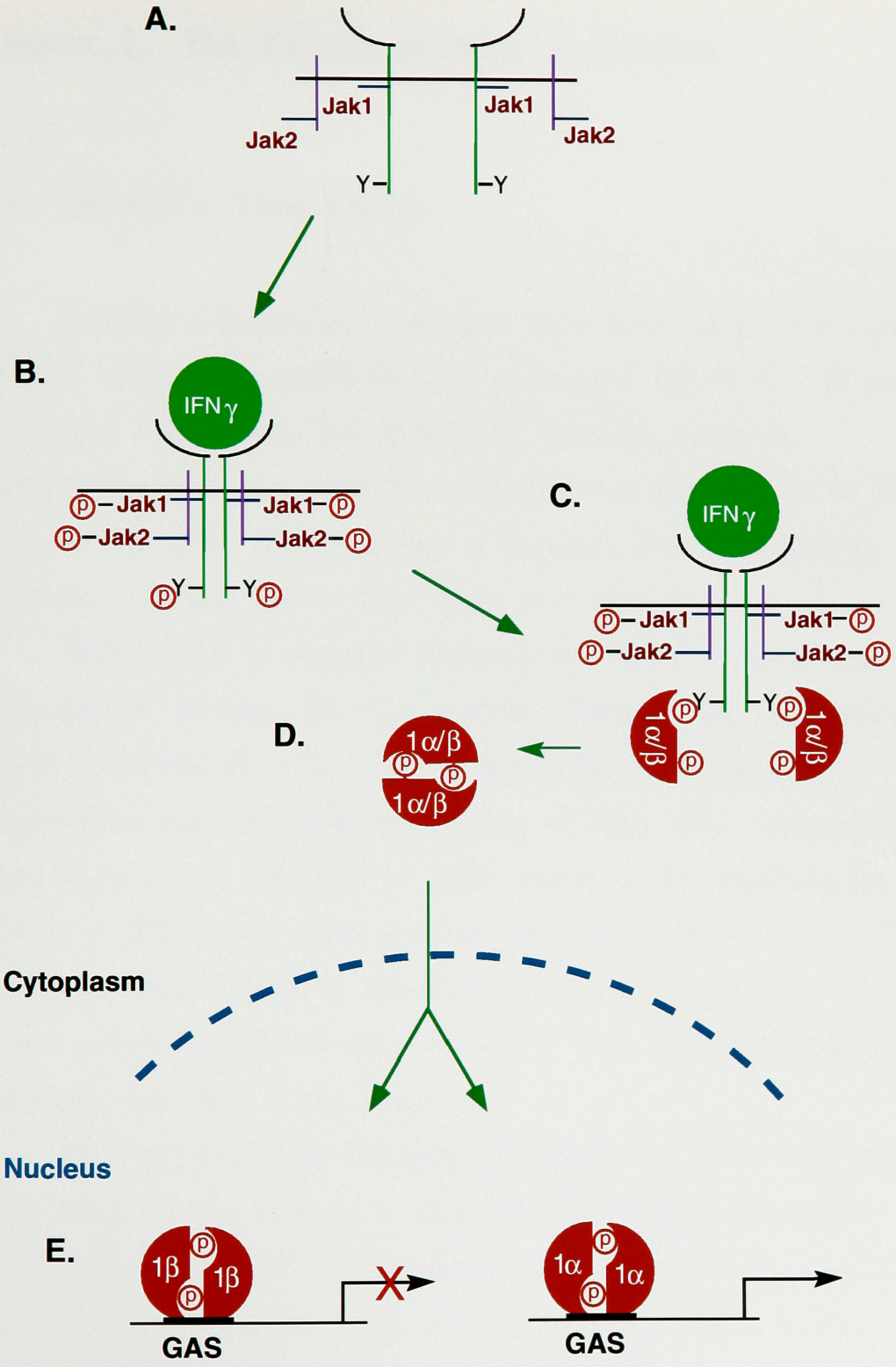
A.
Jak1
Jak1
Jak2
Jak2
Y
Y
B.
IFNγ
Jak1
Jak1
Jak2
Jak2
C.
IFNγ
Jak1
Jak1
Jak2
Jak2
1α/β
1α/β
D.
1α/β
1α/β
Cytoplasm
Nucleus
E.
1β
1β
GAS
1α
1α
GAS

Chapter 2 The Kinetics of Stat1 Inactivation

2.1 The IFN-γ Time Course

Cellular activation by cytokines often leads to a rapid increase in gene transcription followed by a subsequent fall (1-4). In the case of ligands that activate the JAK-STAT pathway, peaks in transcription rates can often be correlated with the activity of STAT proteins (22, 24). STAT activity is transient with DNA-binding generally spanning one to four hours (31, 121, 122).

With regard to receptor signaling that leads to novel gene transcription, perhaps the best studied cytokines are the interferons (IFNs) (reviewed in (17)). IFN-γ causes the phosphorylation, dimerization and entry into the nucleus of Stat1 (31). Activation of Stat1 leads to the induction of genes known to be important for the effects of IFN-γ (e.g. those involved in viral-resistance) (123). It has previously been shown in fibroblasts that Stat1 is rapidly activated within minutes of IFN-γ treatment (31). This binding activity is short lived and lasts only a few hours.

We examined more carefully the kinetics of IFN-γ induced Stat1 DNA binding activity in Bud-8 normal human fibroblasts. Cells were treated with IFN-γ and nuclear extracts prepared at intervals up to 4 hours. Activated Stat1 was detected by a DNA binding assay (electrophoretic mobility shift assay, EMSA) using a labeled oligonucleotide probe that binds Stat1 dimers (M67). The peak of

the induced Stat1 DNA binding activity occurred at approximately 30 minutes (Figure 2.1A, lane 2) followed by a gradual decay, with only 5-10% of the DNA binding activity remaining after 4 hours (lane 5 and Figure 2.1C).

The DNA-binding activity correlated well with the amount of phosphorylated Stat1 protein in the nucleus as determined by Western blot (Figure 2.2A). Using Stat1 C- terminal antiserum, nuclear extracts from untreated cells showed a single reactive band at 91 kD (Figure 2.2A lane 1) but extracts from cells treated for 30 minutes with IFN-γ also show a second slower moving band that contains tyrosine phosphorylated Stat1. With constant IFN-γ treatment, the upper band gradually disappeared over 4 hr. The results in Figures 2.1 and 2.2 demonstrating the transient nature of the IFN-γ time course agree with those obtained previously using similar cells (31).

2.2 The Half-Life of Activated Stat1

The decay in Stat1 DNA binding activity during an IFN-γ time course must be first due to the attenuation of signaling from the IFN-γ receptor and second, the removal of activated Stat1. In order to distinguish between these two events, we developed a variation of a pulse-chase experiment (Figure 2.3). IFN-γ was added to cells in order to build up a pool of activated Stat1 in the nucleus. Staurosporine, a kinase inhibitor known to prevent JAK activity (30, 124), was then added to the cells (in the continuing presence of IFN)

to block the generation of additional phosphorylated Stat1. The decay of the already phosphorylated Stat1 could then be followed over time.

The results of this type of experiment are shown in Figures 2.1B and 2.1C. Cells were treated with IFN-γ for 30 minutes, and then signaling from the receptor was halted by adding staurosporine. Nuclear extracts were prepared at the indicated time points and DNA-binding activity determined by EMSA. In several experiments, the amount of nuclear DNA binding activity was approximately the same for the first 15 minutes after staurosporine treatment. This result most likely reflected the time necessary for the pool of phosphorylated Stat1 in the cytoplasm to transfer to the nucleus (discussed in chapter 4). After an additional 15 minutes, the nuclear DNA binding activity decreased by at least one-half and the signal disappeared almost completely after 1 hour of staurosporine treatment. Western blotting with antiserum to the C-terminus of Stat1 correlated with the EMSA analysis (Figure 2.2B). Due to the nature of this assay, it was difficult to make precise quantitative assessments. Nevertheless, upon treatment with staurosporine, there was a consistent, rapid decline in the amount of phosphorylated Stat1 with almost no phosphorylated Stat1 remaining in the nucleus 60 minutes after addition of kinase inhibitor. Treatment with staurosporine shortens the IFN-γ time course and reveals the half-life of nuclear activated Stat1 to be no more than 15 minutes.

2.3 The Effect of Staurosporine Treatment on Inactivation Defective Stat1 Mutants.

Staurosporine is a powerful kinase inhibitor with pleiotropic effects on cells (125, 126). One of our concerns was that staurosporine might activate a non-specific phosphatase or protease and that this might account for the rapid inactivation of Stat1. Shuai et al. have demonstrated that certain mutations in the N-terminus of Stat1 lead to molecules that can be phosphorylated and bind DNA but are inactivated at a slower rate than wild-type Stat1 (115). The possibility that staurosporine leads to non-specific removal of STAT proteins would be less likely if these mutants were still not inactivated upon staurosporine addition.

Various Stat1 expression constructs were introduced into U3A cells that contain no endogenous Stat1 and cell lines were selected that expressed the different Stat1 proteins. (Figure 2.4) The constructs used in these experiments included both murine and human full-length Stat1 (p91), a deletion mutant lacking the first 154 amino acids (Δ154), the naturally occurring splice variant lacking the last 38 amino acids (p84), and an arginine to alanine mutant at amino acid 31 (U3R). The U3A cells complemented with these different Stat1 proteins were treated with IFN-γ over a four hour time course. At the indicated times, whole cell extracts were prepared and subjected to EMSA analysis with the M67 probe (Figure 2.5). Both p91 and p84 had DNA binding activity in whole cell extracts that peaked at approximately 30 minutes and then rapidly declined by 60 minutes to approximately 45% of maximum

where it remained (p91) or continued to drop gradually (p84) over the next three hours. (Mouse p91 behaved similarly to human p91 (data not shown)). Perturbations in the N-terminus of Stat1, however, led to a prolonged time course. Both U3R, which had previously shown to be inactivation defective, and Δ154 had DNA binding activity that peaked at approximately 120 minutes and remained high through 240 minutes.

Wild-type Stat1 and the N-terminal mutants also differed in their kinetics upon staurosporine treatment (Figure 2.6). As previously described for the Bud-8 cells, the U3 lines were treated with IFN-γ for 30 minutes followed by addition of staurosporine. The DNA-binding activity of wild-type Stat1 in whole cell extracts declined to almost zero after only 30 minutes of treatment with staurosporine. The activity of the N-terminal mutants, however, remained at approximately 80% of the maximal level after 30 minutes of staurosporine treatment. Clearly, the N-terminal Stat1 mutants are resistant to inactivation even in the presence of kinase inhibitor. These results indicate that the rapid decline in wild-type Stat1 DNA binding activity upon staurosporine treatment is not due to non-specific removal but most likely reflects the actual half-life of activated Stat1.

2.4 N-terminal Stat1 Mutants Translocate to the Nucleus

A recent report investigated hybrid Stat1 molecules containing the N-terminal 140 amino acids of Stat2 or 129 amino acids of Stat5

fused to Stat1 at amino acid 130 (116). These molecules were inactivated at a slower rate than wild-type Stat1 and no nuclear transport of these hybrid molecules could be detected by immunofluorescence. By Western Blot, gel shift and transcription assays, however, it appeared that the molecules were entering the nucleus. The authors suggested that the detection of hybrid Stat1 molecules in the nucleus in certain assays was due to interactions with endogenous wild-type Stat1. The authors concluded that a nuclear phosphatase is required for Stat1 inactivation and that the hybrid molecules were inactivated at a slower rate due to their deficiency in nuclear import.

To further explore the role of the N-terminus in Stat1 nuclear import, we examined the ability of the Δ154 N-terminal mutant to translocate to the nucleus. Since this construct was in U3A cells, there was no possibility of nuclear transport solely due to interactions with endogenous Stat1. As shown in Figure 2.7, EMSA analysis demonstrated the presence of activated p91 and Δ154 proteins in the cytoplasm and nucleus upon IFN-γ stimulation.

Western blotting also revealed the translocation of N-terminal Stat1 mutants to the nucleus. For unknown reasons, phosphorylated p91 in U3A cells does not appear as a slower migrating band (as compared to unphosphorylated Stat1) when blotting with anti-Stat1 serum; therefore, in order to detect activated molecules, we blotted with an antiserum that specifically recognizes Stat1 phosphorylated on tyrosine 701. As shown in Figure 2.7C, there was no phosphorylated p91 or Δ154 molecules in the cytoplasmic or nuclear extracts from untreated cells. Thirty minutes after addition of IFN-γ,

phosphorylated p91 and the faster migrating phosphorylated Δ154 were detected in both the cytoplasm and the nucleus. The same extracts (in the same amounts) as in Figure 2.7C were run on a separate gel and blotted with antiserum to the SH2 region of Stat1, demonstrating that all extracts contain Stat1 molecules (Figure 2.7D). Clearly, the defect in inactivation of Stat1 N-terminal mutants is not simply due to a lack of nuclear import.

2.5 Discussion

In this chapter, we explored the kinetics of Stat1 inactivation. Treatment of Bud-8 cells with IFN–γ caused a rapid increase in DNA binding activity that peaked at approximately 30 minutes and declined to almost zero by four hours. U3 cells complemented with wild-type Stat1 (p91) also showed a rapid rise and decline in DNA-binding activity over time. The decay kinetics of U3A cells, a well-studied tumor cell line, and Bud-8 euploid fibroblasts differed slightly but the similarity suggests Stat1 is generally rapidly inactivated.

The decline in Stat1 DNA-binding during an IFN–γ time course is dependent upon first, JAK and receptor inactivation and second, Stat1 inactivation. The use of staurosporine enables the disassociation of these two events and indicated a half-life of activated Stat1 of fifteen minutes or less. Staurosporine addition to cells containing N-terminal mutants of Stat1, however, did not lead to a rapid decay in DNA binding activity. This "staurosporine

resistance" was not due to an inability of these mutants to enter the nucleus. The possible role of the Stat1 N-terminus in inactivation and nuclear transport will be discussed in chapter 5.

Other groups have used kinase inhibitors to determine the half-life of phosphorylated STAT molecules (113, 127, 128). Both Stat3 and Stat5 appear to be rapidly inactivated. The experiments with Stat3 are particularly interesting because of the use of a specific inhibitor of the epidermal growth factor (EGF) receptor kinase. Even with this inhibitor, the half-life of Stat3 was determined to be 10 minutes, further demonstrating that it is not a unique property of staurosporine that leads to the rapid decay of activated STAT proteins. Clearly, kinase inhibitors are very useful in exploring the kinetics of JAK-STAT pathway inactivation and may prove useful in dissecting other signaling pathways.

The disappearance of nuclear EMSA activity could be due to actual removal of the Stat1 from the nucleus or a modification to the Stat1 or appearance of another molecule that disrupts DNA-binding. For example, using EMSA analysis, purified PIAS1 (Protein Inhibitor of Activated Stat1) has been shown to block Stat1 DNA-binding activity. In addition, overexpression of PIAS1 in 293 cells blocks IFN-γ mediated gene transcription (63). Although we did not specifically examine PIAS proteins, our Western blot analysis of Stat1 demonstrated that the decay shown by EMSA was due to the removal of activated Stat1 from the nucleus and not simply a decrease in DNA-binding activity.

The overall time-course of IFN-γ induced Stat1 activation and inactivation is several hours while the half-life of the phosphorylated

molecules is under 15 minutes. This suggests that the activity of the receptor-JAK complex determines the time of the overall activation-inactivation cycle. A recent study particularly illustrates this point (129). Daudi cells, when treated with IFN–α, have an exceptionally long STAT DNA binding activity lasting 24 hours. Lee et al. demonstrated that the prolonged signal was not due to an increase in the lifetime of phosphorylated STAT proteins but to continued activation of the JAKs (through endogenous IFN–α production). Whenever there is prolonged STAT activity in response to cytokine, both the inactivation rates of the STAT proteins and the receptors must be investigated in order to determine the basis for the extended signaling.

Figure 2.1 Effect of Staurosporine Treatment on Pre-Induced IFN-γ DNA Binding Activity

(A) EMSA analysis with an M67 probe. Nuclear extracts were prepared from Bud-8 normal human fibroblasts treated with IFN-γ for the indicated times.

(B) Same as (A) except after 30 minutes of IFN-γ treatment, staurosporine (500 nM) was added to the cells and nuclear extracts prepared every 15 minutes over the next 60 minutes.

(C) Plot of the PhosphorImager analysis of Stat1 DNA binding complexes at various times after IFN-γ and IFN-γ plus staurosporine treatment.

A.

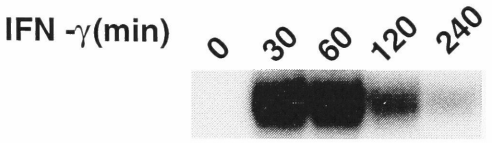
IFN -γ(min)
0
30
60
120
240

B.

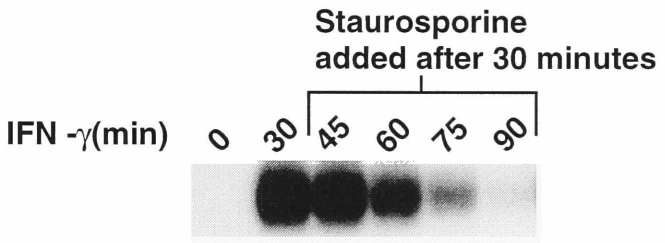
Staurosporine
added after 30 minutes
IFN -γ(min)
0
30
45
60
75
90

C.

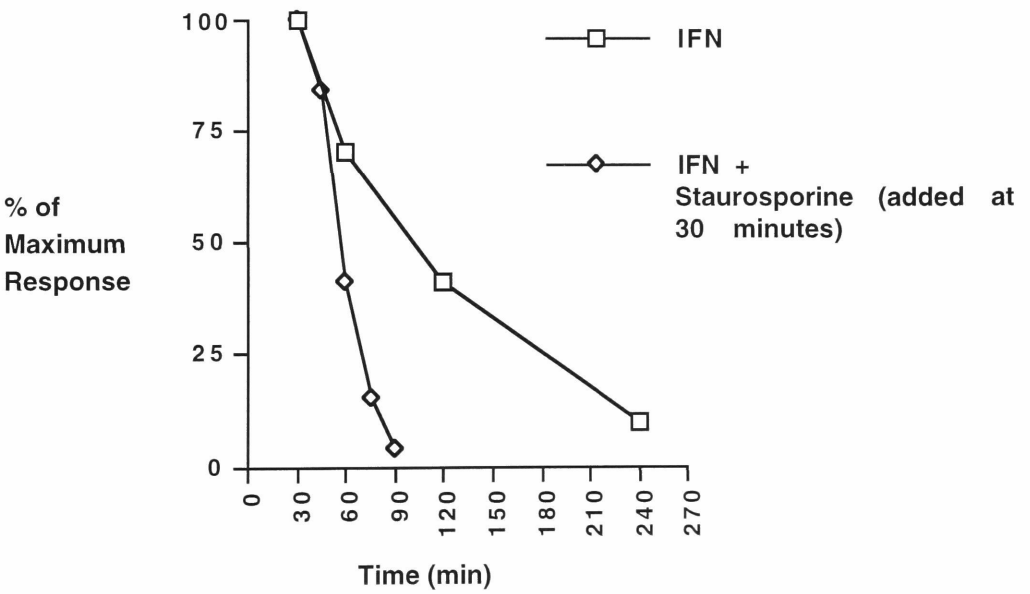
100
75
50
25
0
% of
Maximum
Response
0
30
60
90
120
150
180
210
240
270
Time (min)
IFN
IFN +
Staurosporine (added at
30 minutes)

Figure 2.2 Western Blots of Stat1 in IFN–γ Treated Cells with and without Staurosporine

(A) Western Blot Analysis. Nuclear extracts were prepared from Bud-8 fibroblasts treated with IFN–γ for the indicated times. These extracts were then subjected to SDS-PAGE and blotted with anti-Stat1 C-terminal serum.

(B) Same as (A) except after 30 minutes of IFN–γ treatment, staurosporine (500 nM) was added to the cells and nuclear extracts prepared every 15 minutes for the next 60 minutes.

A.

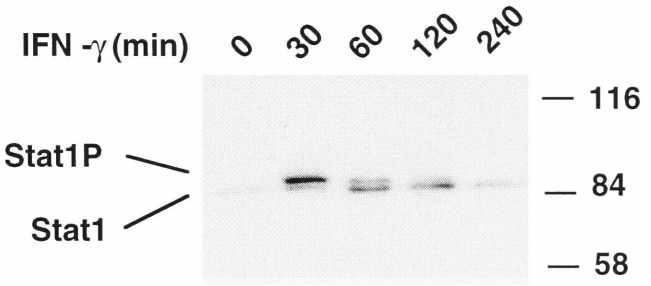
IFN -γ (min)
0
30
60
120
240
Stat1P
Stat1
116
84
58

B.

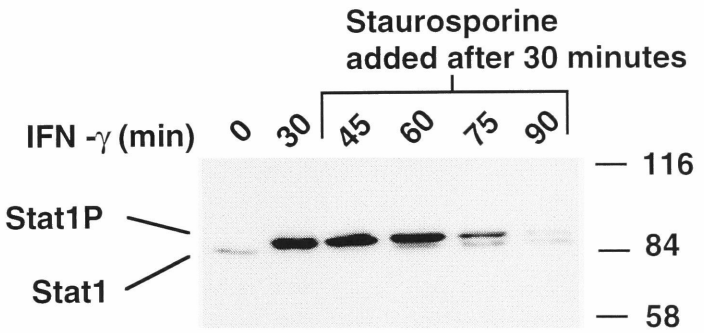
Staurosporine
added after 30 minutes
IFN -γ (min)
0
30
45
60
75
90
Stat1P
Stat1
116
84
58

Figure 2.3 The Staurosporine Pulse-Chase Experiment

(A) Cells were treated with IFN-γ to build up a pool of activated Stat1 in the nucleus.

(B) Cells were then treated with staurosporine to block the generation of additional phosphorylated Stat1. The decay of the already phosphorylated Stat1 could then be followed over time.

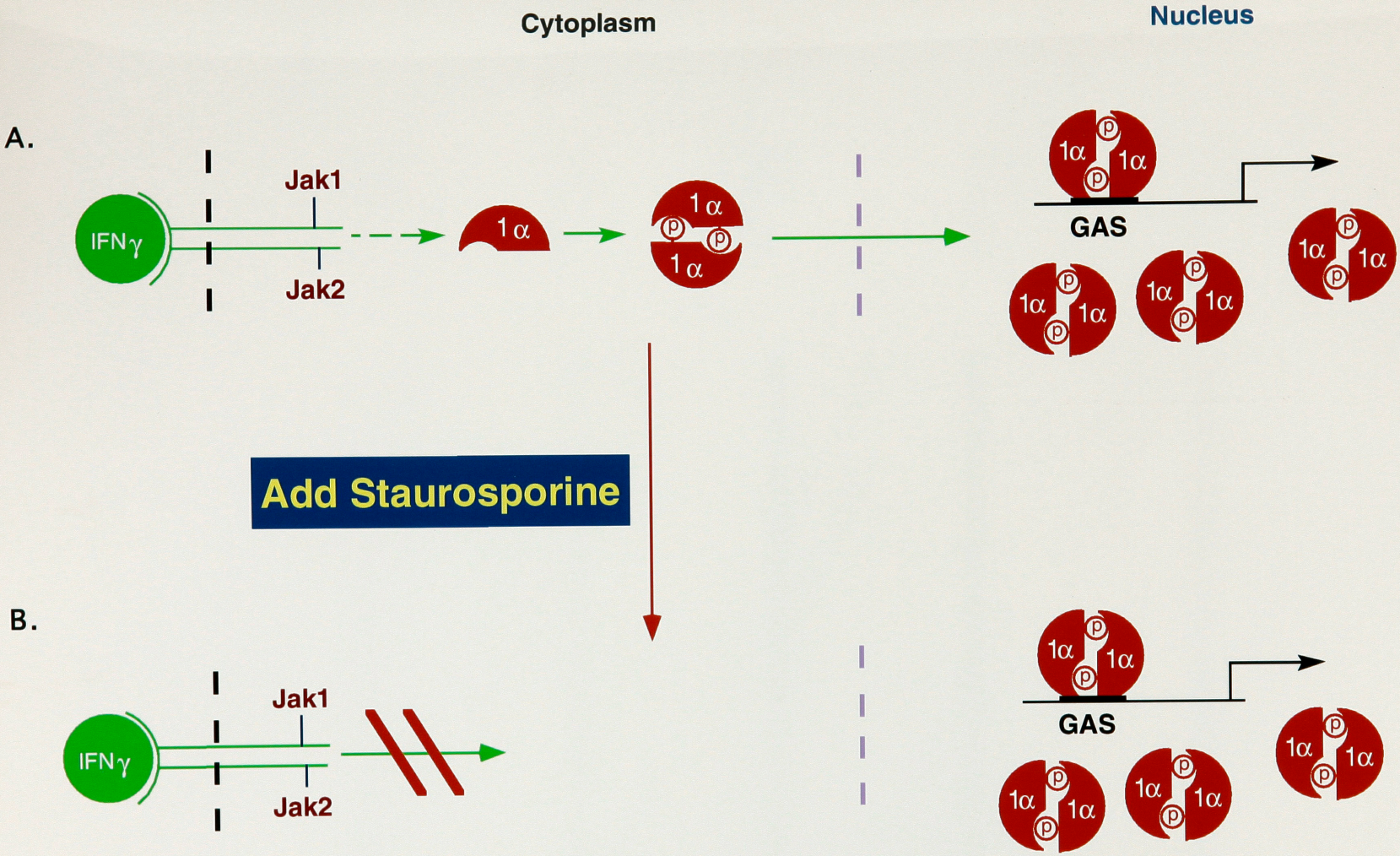
Cytoplasm
Nucleus
A.
IFNγ
Jak1
Jak2
1α
GAS
Add Staurosporine
B.
IFNγ
Jak1
Jak2
GAS

Figure 2.4 Stat1 Constructs Stably Transfected into U3A Cells

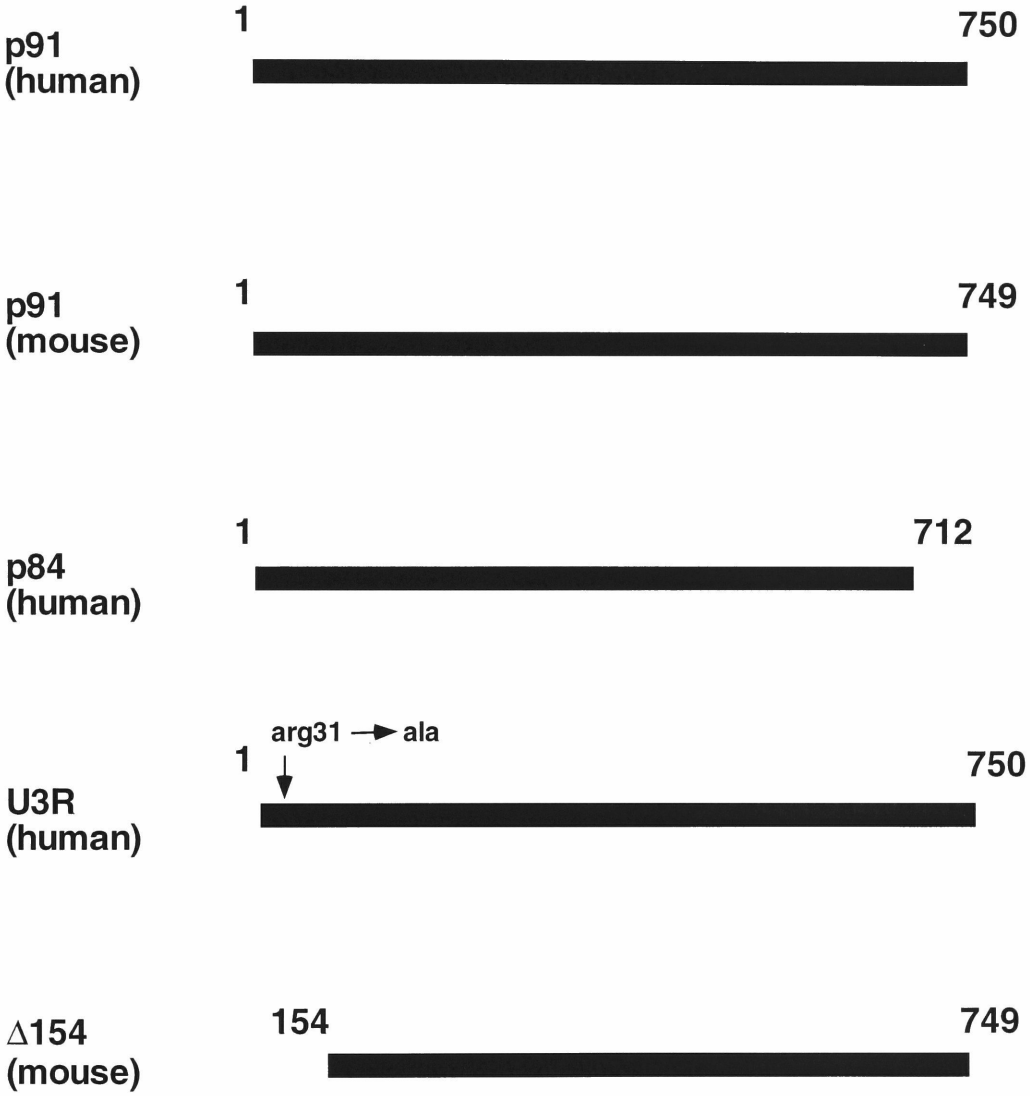
p91
(human)
1
750
p91
(mouse)
1
749
p84
(human)
1
712
arg31 → ala
1
U3R
(human)
750
Δ154
(mouse)
154
749

Figure 2.5 The IFN–γ Time Course in U3A Cells Complemented with Wild-type and N-terminal Mutants of Stat1

(A) EMSA analysis with an M67 probe. Whole cell extracts were prepared from U3A cells complemented with wild-type human Stat1 (p91) treated with IFN–γ for the indicated times.

(B) Same as (A) except U3A cells complemented with Stat1 containing a mutation in arginine 31 to alanine (U3R).

(C) Plot of the PhosphorImager analysis of Stat1 DNA binding complexes in U3A cells complemented with different Stat1 constructs (p91, p84, U3R and Δ154) at various times after IFN–γ treatment. The results shown are the average of two experiments with error bars representing the standard error of the mean.

A. p91

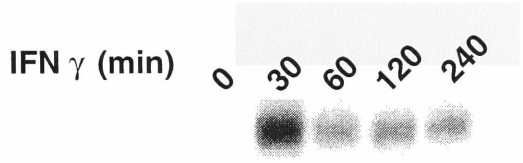
IFN γ (min)
0
30
60
120
240

B. U3R

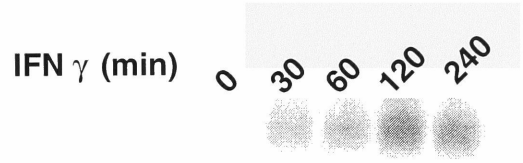
IFN γ (min)
0
30
60
120
240

C.

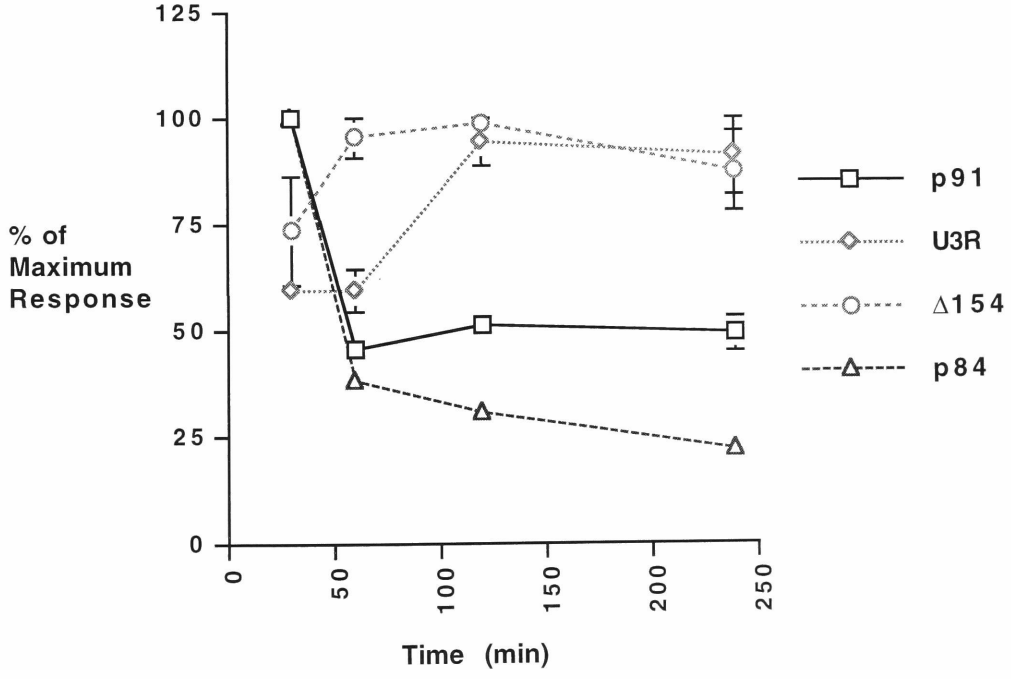
125
100
75
50
25
0
% of Maximum Response
0
50
100
150
200
250
Time (min)
p91
U3R
Δ154
p84

Figure 2.6 Effect of Staurosporine Treatment on U3A Cells Complemented with Wild-type and N-terminal Mutants of Stat1

(A) EMSA analysis with an M67 probe. Whole cell extracts were prepared from U3A cells complemented with wild-type human Stat1 (p91) treated with IFN-γ for 30 minutes followed by staurosporine (500 nM) for the indicated times.

(B) Same as (A) except U3A cells complemented with Stat1 containing a mutation in arginine 31 to alanine (U3R).

(C) Plot of the PhosphorImager analysis of Stat1 DNA binding complexes in U3A cells complemented with different Stat1 constructs (p91, p84, U3R and Δ154) at various times after IFN-γ and staurosporine treatment. The results shown are the average of two experiments with error bars representing the standard error of the mean.

A. p91

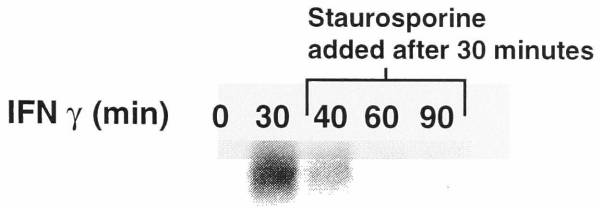
Staurosporine
added after 30 minutes
IFN γ (min)
0 30 40 60 90

B. U3R

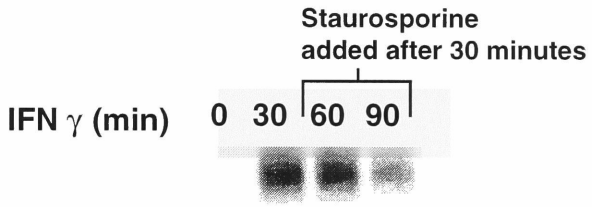
Staurosporine
added after 30 minutes
IFN γ (min)
0 30 60 90

C.

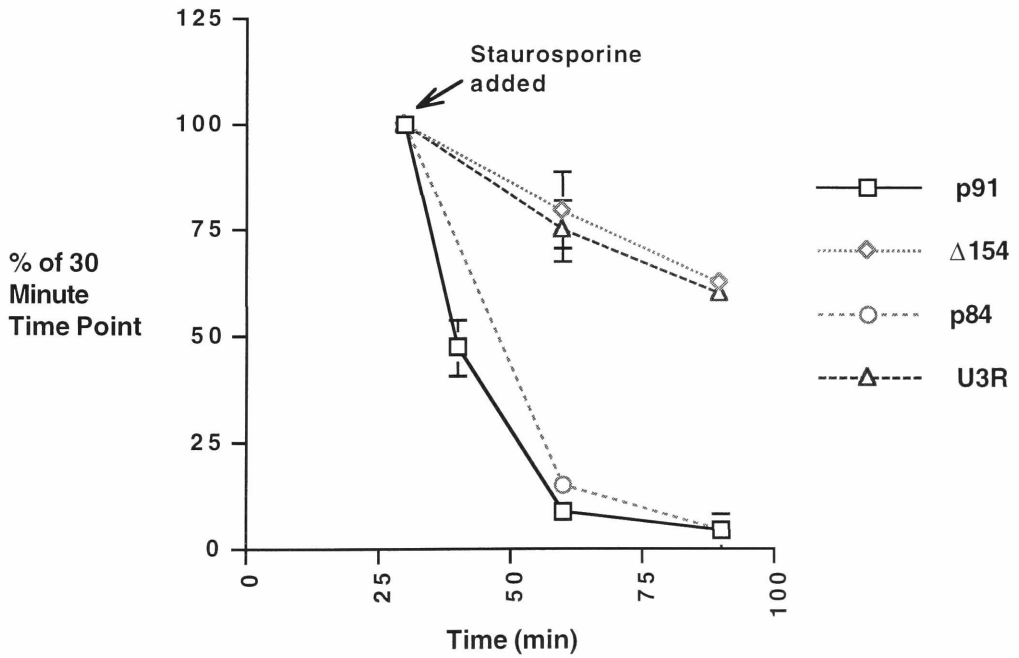
125
100
75
50
25
0
% of 30
Minute
Time Point
Staurosporine
added
0
25
50
75
100
Time (min)
p91
Δ154
p84
U3R

Fig 2.7 EMSA and Western Blot Analysis of Cytoplasmic and Nuclear Extracts from U3A Cells Complemented with p91 and Δ154

(A) EMSA analysis with an M67 probe. Cytoplasmic (C) and nuclear (N) extracts were prepared from U3A cells complemented with wild-type Stat1 (p91) and treated with IFN-γ for the indicated times.

(B) Same as (A) except U3A cells complemented with Stat1 lacking the first 154 amino acids (Δ154).

(C) Western blot analysis. The same extracts in (A) and (B) were subjected to SDS-PAGE and blotted with antiserum that recognizes Stat1 phosphorylated on tyrosine 701.

(D) Same as (C) except blotting with anti-Stat1 SH2 region serum.

A. p91

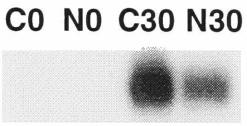

B. **Δ154**

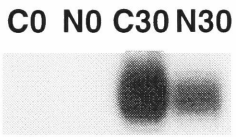

C. Anti-Tyrosine Phosphorylated Stat1

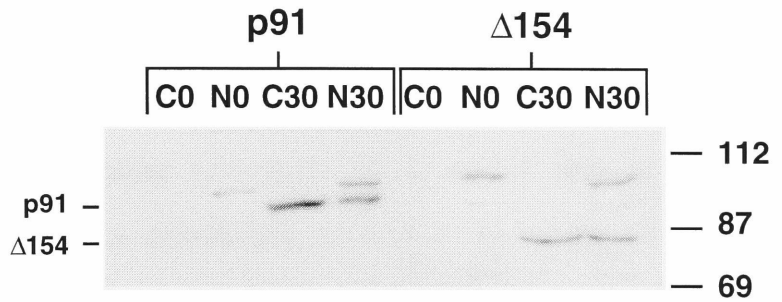

D. Anti-Stat1 SH2 Region

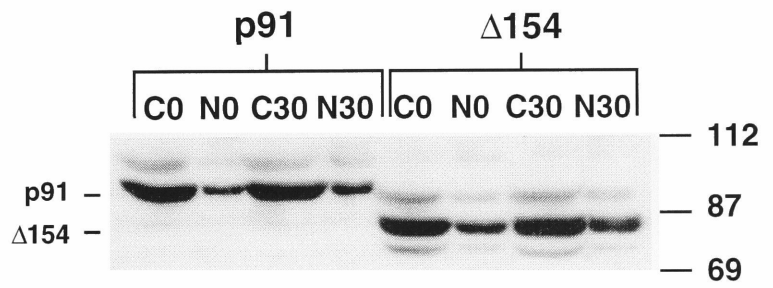

Chapter 3 Mechanisms of JAK-STAT Pathway Inactivation

The results in the previous chapter beg the question of what causes the rapid inactivation of Stat1. This chapter will address this question as we explore whether IFN-γ induced RNA and protein synthesis is required for Stat1 inactivation and whether Stat1 is inactivated by proteolysis or dephosphorylation. In our experiments, we utilize a number of different inhibitors as well as ^{35}S labeling. Staurosporine proves to be a useful tool in determining whether an inhibitor is a producing an effect by acting at the receptor-JAK complex or at the level of the STAT molecule.

3.1 Inhibitors of Transcription Prolong IFN-γ Signaling

Early work on IFN-γ induced gene expression determined that blockade of protein synthesis increased transcription rates after cytokine treatment (4). Protein synthesis might be necessary for inactivation of the receptor, JAKs, Stat1 or other components of the IFN-γ induced transcriptional machinery. In some studies, blockade of protein synthesis prevented full Stat1 DNA-binding while in others it had no effect or resulted in slightly prolonged Stat1 activity (22, 107, 108).

We, therefore, investigated more carefully the effects of RNA synthesis on Stat1 activation in Bud-8 fibroblasts. We utilized actinomycin D, which inhibits transcription by binding tightly to

double-stranded DNA (5). Cells were treated for 1 hour with actinomycin D followed by IFN-γ. Nuclear extracts were prepared at the indicated time points and DNA-binding activity was determined by EMSA. As shown in Figure 3.1, actinomycin D prolonged the time course of IFN-γ induced Stat1 activation. While at 30 minutes there was little difference in DNA-binding activity between actinomycin D treated and untreated cells, by 4 hours there was still strong nuclear DNA-binding activity in the actinomycin D treated lane while it had almost dropped to zero in the control lane. In addition, actinomycin D did not activate Stat1 on its own (Figure 3.1, lane 1 and data not shown). Actinomycin D prolongs the presence of activated Stat1 and may explain the increase in IFN-γ induced transcription rates seen in the absence of protein synthesis.

3.2 RNA and Protein Synthesis is Not Required For Stat1 Inactivation

The actinomycin D may be blocking synthesis of a protein required for the inactivation of the receptor-JAK complex or for the inactivation (or more specifically decrease in DNA-binding activity) of Stat1. In order to distinguish between these two possibilities, IFN-γ was added to actinomycin D treated cells for 4 hours followed by staurosporine addition for one hour. If RNA synthesis was required for inactivation of the Stat1 molecules, then actinomycin D treatment should still prolong DNA-binding activity even in the absence of constantly generated phosphorylated Stat1. As shown in

Figure 3.1, lane 5, the DNA binding activity was almost completely abolished after an hour with staurosporine treatment while in the control lane there was still strong DNA-binding activity. Similar results were obtained with the translation inhibitor cycloheximide (data not shown). The effect of staurosporine in these experiments suggests that RNA and protein synthesis is not required for Stat1 inactivation but for inactivation of the receptor-JAK complex.

3.3 Proteasome Inhibitors Prolong IFN-γ Signaling

We next sought to determine the mechanism of Stat1 inactivation. The disappearance of phosphorylated Stat1 protein from the nucleus might be due either to proteolytic destruction and/or dephosphorylation of that protein. The proteasome is a multi-subunit protease that degrades molecules conjugated to ubiquitin and is known to inactivate a number of transcription factors including c-Fos and c-Jun and may play a role in the inactivation of certain receptors (84-86, 89, 104, 105). We decided to determine whether the proteasome plays a role in JAK-STAT pathway inactivation.

In the early 90's, a group of small peptide analogs as well as a structurally unrelated fungal compound (lactacystin) were shown to be potent inhibitors of the proteasome (130-132). We treated Bud-8 cells for 1 hour with one of these peptide analogs (MG132), lactacystin or carrier (DMSO). These cells were then treated with IFN-γ (Figure 3.2) and nuclear extracts prepared and subjected to

EMSA analysis. After 30 minutes, all nuclear extracts had strong DNA binding activity with the activity in the extracts from cells pretreated with the proteasome inhibitors being slightly stronger (compare lanes 2, 3 and 4). In extracts from cells without pretreatment with proteasome inhibitor, the great majority of the DNA binding activity had disappeared after 4.5 hours (lane 5). However, the nuclear extracts from the cells treated with proteasome inhibitor still had at least half as much DNA binding activity as at 30 minutes (compare lanes 3 and 4 with lanes 6 and 7). When cells were treated with only the proteasome inhibitors for 4.5 hours, there was no detectable Stat1 DNA binding activity (lanes 8 and 9). Thus, the proteasome inhibitors MG132 and lactacystin do not independently generate a signal but prolong the presence of activated Stat1.

3.4 The Effect of the Proteasome Inhibitor MG132 is Upstream From the Stat1 Molecules

We next sought to determine at what point in the IFN-γ signaling cascade the proteasome inhibitors exerted their effect. Staurosporine was once again used to block signaling at the receptor after a pool of phosphorylated Stat1 had been accumulated. Bud-8 cells were pretreated with MG132 or carrier and IFN-γ was added for 30 minutes or for 3.5 hours. At each time point cell samples were treated with staurosporine. Even in the presence of MG132, whether early or late in the IFN-γ treatment course, the DNA binding

activity still disappeared 1 hr after addition of the staurosporine (Figure 3.3, lanes 5 and 10). We concluded that the proteasome inhibitor does not spare the DNA binding protein from removal but must exert its effect upstream by sustaining the signal that causes activation of Stat1 at the cell surface.

3.5 MG132 Prolongs Activation of the IFN-γ Cell Surface Receptor

The human IFN-γ receptor is composed of both α and β chains (133-135). The activation of Stat1 after IFN-γ treatment is preceded by ligand dependent activation of JAKs associated with the α and β chains and subsequent phosphorylation of a number of tyrosines on the α chains (reviewed in (72)). We tested activation of the α chain of the receptor by treating cells with IFN-γ, making cell extracts, precipitating with an antiserum to the α chain, separating on SDS-PAGE and using antiphosphotyrosine antibody to determine the phosphorylation state of the receptor. For these experiments, WI-38 cells were used which are identical to Bud-8 fibroblasts in their responses to IFN-γ, staurosporine and MG132 (data not shown).

As shown in Figure 3.4A, the receptor was not phosphorylated until IFN-γ treatment and was maximally phosphorylated within 10 minutes (lanes 1 and 2). By 4 hours, very little phosphorylated receptor remained (lane 3) even though all lanes contained approximately equivalent amounts of the α chain of the IFN-γ receptor (Figure 3.4B). In the presence of MG132, the receptor

remained heavily phosphorylated even 5 hours after the beginning of IFN–γ treatment (Figure 3.4A, lane 6). Thus prolonged signaling from the receptor in the presence of MG132 could account for the sustained activation of Stat1 in the presence of the proteasome inhibitors.

3.6 The Effect of Proteasome Inhibitor on Stat5 Activation

We next sought to extend our findings with IFN–γ to another cytokine that activates the JAK-STAT pathway. In response to IL-2 treatment, Stat5 has been shown to become phosphorylated, dimerize and activate transcription (136-140). HT-2 cells, which require IL-2 for growth, have been used as a model system for Stat5 activation (139, 141). These cells, when starved of IL-2, activate Stat5 upon readdition of cytokine.

In our experiments, we cultured HT-2 cells for 4 hours in IL-2 deficient media, added back IL-2 and then prepared nuclear extracts at various time points. These extracts were then used in EMSA analysis with a probe that binds activated Stat5 dimers (a portion of the β-casein promoter). By 10 minutes, there was already substantial Stat5 DNA binding activity that peaked at approximately 30 minutes and then declined over the next four hours to below 60% of maximum (Figure 3.5A and C). The shift complexes appearing in Figure 3.5 were determined to be Stat5 by supershift analysis (data not shown). In addition, very little Stat1 or Stat3 is activated by IL-2 in HT-2 cells as determined by running similar extracts with an

M67 probe (data not shown). IL-2 activation of Stat5 is similar to IFN-γ activation of Stat1 in that DNA-binding occurs rapidly and then gradually declines over the next several hours.

We were interested in knowing whether treatment with proteasome inhibitor would prolong the IL-2 time course. Cells were pretreated with MG132 for 1 hour before the readdition of IL-2, generation of nuclear extracts and EMSA analysis (Figure 3.5B and C). As with IFN-γ, the proteasome inhibitor treatment prolonged IL-2 signaling. In contrast to control cells, the peak of Stat5 DNA activity was approximately 120 minutes and decayed little over the next two hours. In multiple experiments, DNA binding activity was always prolonged in the presence of MG132.

3.7 The Effect of the Proteasome Inhibitor MG132 is Upstream From the Stat5 Molecules

We were next interested in determining whether the proteasome played a role in inactivation of Stat5 or inactivation of the IL-2 receptor. We treated HT-2 cells with MG132 or carrier (DMSO) 1 hour prior to the readdition of IL-2. Staurosporine was then added at the point of maximal Stat5 DNA-binding activity as determined by time course experiments (30 minutes for DMSO treated and 120 minutes for MG132 treated cells). As shown in Figure 3.6, Stat5 DNA binding activity declined rapidly even in the presence of MG132 with almost no signal remaining after only 20

minutes. The proteasome, in the case of both IL-2 and IFN–γ, appears to act upstream of the STAT molecules.

3.8 Vanadate Prolongs the Stat1 Signal In the Presence of Staurosporine

At this point we could invoke a possible role for proteolysis in decreasing receptor signaling for both IL-2 and IFN–γ, but not in the disappearance of the phosphorylated nuclear STAT proteins. We returned to the IFN-γ system to explore the possibility that the removal of active STAT proteins required a tyrosine phosphatase. We used Na vanadate, a compound well known to be a phosphatase inhibitor (142). Bud-8 cells were treated with IFN–γ to establish a pool of active molecules and were then treated with either staurosporine or staurosporine plus Na vanadate. As expected from the experiments in chapter 2, treatment of the IFN–γ induced cells with staurosporine for 60 additional minutes caused almost complete disappearance of the Stat1 signal. (Figure 3.7, lane 3). If vanadate was added together with the staurosporine, the disappearance of active Stat1 was partially prevented (lane 4). Thus we conclude that at least part of the removal of Stat1 is due to phosphatase action. Two other samples were included in this experiment. IFN–γ treated cells by 90 minutes had somewhat less active Stat1 than at 30 minutes, as expected (lane 6). This decline did not occur in the presence of vanadate (lane 5). From these results it is clear that vanadate, even in the presence of staurosporine, affects the removal

of activated Stat1 consistent with a role for a phosphatase in deactivation.

3.9 Direct Evidence For Cytoplasmic-Nuclear Cycling of Stat1 Involving a Tyrosine Phosphatase

To test directly the fate of Stat1 molecules after activation, a quantitative recovery experiment with ^{35}S-labeled-cells was carried out. Cells were labeled for 2.5 hr with ^{35}S methionine, washed and medium containing non-radioactive methionine was added. IFN-γ was then used to activate Stat1 and samples were taken at frequent intervals thereafter. Anti-Stat1 antiserum was used to precipitate the protein from nuclear and cytoplasmic extracts; subsequently gel electrophoresis, autoradiography and quantitation of both the non-phosphorylated and the more slowly migrating tyrosine phosphorylated form was carried out.

The experimental results were clear cut (Figure 3.8A, B, C and D). Prior to treatment the great majority of ^{35}S labeled Stat1 was cytoplasmic; after treatment the ^{35}S labeled, phosphorylated Stat1 was evident at a maximal level in the cytoplasm by 10 minutes at which time there was already a strong phosphorylated Stat1 signal in the nucleus. (The X-ray film exposures in Figure 3.8A and B are not equal but quantitation of data from two experiments is presented in 3.8C and D.) By 30-45 minutes the amount of phosphorylated Stat1 had increased to a maximum in the nucleus and equaled about 20-25% of the total labeled Stat1 in the cell. The nuclear phosphorylated

Stat1 started to slowly decline at this point, remaining at about one-third of the peak for 3 hr. Coincident with the fall in nuclear phosphorylated Stat1 there was a rise in cytoplasmic Stat1 to initial levels.

It was possibly significant that in these experiments the total ^{35}S recovery was higher at the beginning and end of these experiments than at intermediate periods after IFN-γ treatment when the maximal nuclear phosphorylated Stat1 was evident. It is possible therefore that the nuclear phosphoprotein may not be quantitatively extracted. If this were true then even more Stat1 molecules could be present in the nucleus as phosphorylated Stat1 in the period from ~30 to 120 minutes after IFN-γ treatment. The relative preservation of STAT protein through an IFN-γ time course makes dephosphorylation and not proteolysis the likely mechanism of inactivation of Stat1.

3.10 Treatment with Staurosporine Also Reveals the Presence of a Stat1 Phosphatase

In many experiments we have used staurosporine as a tool for dissecting Stat1 inactivation. The question of whether staurosporine activates non-specific proteases and/or phosphatases was addressed by determining the "staurosporine resistance" of N-terminal Stat1 mutants (see chapter 2). To test directly the fate of Stat1 molecules in the presence of staurosporine, we labeled Bud-8 fibroblasts with ^{35}S methionine for 2.5 hours, washed away the label, and treated cells with IFN-γ and staurosporine as indicated in Figure 3.9.

Cytoplasmic and nuclear extracts were immunoprecipitated with a monoclonal antibody to the C-terminus of Stat1, run on an SDS-PAGE gel and quantitated using a PhosphorImager.

The results of a typical experiment are shown in Figure 3.9A and B (Figure 3.9A and B are equal exposures but A represents only a quarter of the total cytoplasmic extracts. Quantitation is shown in Figure 3.9C and D.) At time 0, most of the Stat1 was cytoplasmic. After 30 minutes of IFN-γ treatment, the amount of Stat1 in the cytoplasm dropped as phosphorylated molecules were transferred to the nucleus. After the addition of staurosporine, the tyrosine phosphorylated Stat1 disappeared rapidly from the nucleus and reappeared in the cytoplasm in a dephosphorylated state. In several experiments, between 80 and 90% of the total labeled Stat1 in the cell was recovered in the cytoplasm after 60 minutes of staurosporine treatment. This result provides further evidence for dephosphorylation and not proteolysis being the major mode of Stat1 inactivation.

3.11 Discussion

Decade-old experiments demonstrated that inhibition of protein synthesis prolonged IFN–γ (as well as other cytokine) induced transcription (2, 4). In this chapter, we described experiments indicating that prolongation of STAT signaling may account for the increase in transcription rates. Treatment with either actinomycin or cycloheximide followed by IFN–γ prolonged Stat1 DNA-binding

growth hormone receptor. In regard to IFN-α, STAT activation was slightly prolonged after inhibiting protein synthesis in fibroblasts but not in Daudi cells (107, 129). It appears that the assay, cell type and cytokine used all determine the effect of protein synthesis blockade on STAT signal transduction.

We next turned our attention to the actual mechanism of STAT inactivation. Some investigators have used vanadate to prolong an IFN-γ induced Stat1 signal and argue that tyrosine dephosphorylation of Stat1 occurs (107, 108). These experiments, however, cannot discriminate between phosphatase inactivation of an IFN-γ surface signal or phosphatase inactivation of Stat1. We show, however, that even in the absence of a continuing IFN-γ induced cell surface signal (staurosporine treatment) vanadate did delay the decrease in the Stat1 signal. The fact that Na vanadate by itself can lead to accumulation of active Stat1 and the possibility that this activity may not be suppressible by staurosporine complicates the interpretation of this result (144).

The studies with vanadate are compatible but do not prove phosphatase inactivation of Stat1. To test directly for the existence of a phosphatase, we metabolically labeled cells and followed the fate of Stat1 molecules following IFN-γ treatment. By 30 minutes, approximately 25% of the total Stat1 was activated and translocated to the nucleus. The level of Stat1 remained high in nucleus for another 90 minutes before declining by 4 hours. With a half-life of activated Stat1 of only 15 minutes (see chapter 2) but an elevated level of activated Stat1 for two hours, the majority of Stat1 molecules must be activated, cycle through the nucleus and reappear in the

cytoplasm in a dephosphorylated state. In spite of this conclusion, the total amount of labeled Stat1 (within the limits of experimental error) was the same at the end of the 4 hour IFN-γ treatment as at the beginning.

We also used metabolic labeling to follow the fate of Stat1 throughout a staurosporine-chase experiment. The results corroborated our experiments with EMSA and Western Blot analysis showing the rapid disappearance of nuclear phosphorylated Stat1 after only 60 minutes of staurosporine treatment. More importantly, the majority of Stat1 was quantitatively recovered in the cytoplasm in a dephosphorylated state. It appears that staurosporine treatment does not induce non-physiological mechanisms of Stat1 inactivation and is a valid method for dissecting the JAK-STAT pathway.

Kim and Maniatis have detected phosphorylated Stat1 associated with ubiquitin indicating some protein turnover by the proteasome (106). In their experiments, however, it was not possible to estimate the fraction of Stat1 molecules bound to ubiquitin. Our near-quantitative recovery of labeled Stat1 throughout a IFN-γ time course or after staurosporine treatment argues against removal of a major fraction of Stat1 by proteolysis. In addition to our results, Lee et al. have also demonstrated through metabolic labeling the preservation of Stat1 and Stat2 during IFN-α treatment (129). The possible nature and localization of the Stat1 phosphatase will be discussed in the next two chapters.

Even though our major conclusion is that the removal of nuclear activated Stat1 must require phosphatase action, the experiments with proteasome inhibitors do indicate an important

role for proteolysis in the overall receptor-JAK-STAT activation and deactivation pathway. The proteasome inhibitor, MG132, (and lactacystin, a chemically different proteasome inhibitor) supported the presence of nuclear phosphorylated Stat1 long after it would have disappeared in an untreated cell. However, the MG132 supported signal could still be eliminated in an hour or less by staurosporine, implying that continued signaling from the cell surface was required to keep up the level of active Stat1 in the presence of MG132. This continued signaling in the presence of MG132 obviously could originate at the receptor-JAK complex. We therefore tested for phosphotyrosine on the receptor and found that MG132 prevented loss of tyrosine phosphorylation from the receptor as it normally occurs without proteasome inhibitor. We conclude that inactivation of the ligand, receptor, or JAK involves a proteasome-regulated step. The possible role of the proteasome in receptor downregulation will be discussed further in chapter 5.

Although most of our experiments are with IFN–γ and Stat1, we have confirmed that the basic principles apply to the IL-2 and Stat5 system as well. IL-2 induced Stat5 DNA-binding also decayed over time with a short half-life of phosphorylated molecules, determined through "staurosporine chase", of less than 10 minutes. As with IFN–γ, proteasome inhibitor prolonged IL-2 signaling. This effect, however, was abolished upon the addition of staurosporine indicating that the proteasome acts upstream of the Stat5 molecules. Other groups have determined that proteasome inhibitor actually prolongs the activation of the JAKs involved in IL-2 signaling (analogous to our finding that MG132 prevents the loss of tyrosine

phosphorylation from the IFN–γ receptor) (127, 128). The similarities uncovered in our experiments involving the IFN–γ and IL-2 JAK-STAT pathways make it likely that both are inactivated through cognate mechanisms.

Figure 3.1 Actinomycin D Prolongs IFN–γ Signaling but not in the Presence of Staurosporine.

EMSA analysis with an M67 probe. Bud-8 fibroblasts were pretreated with actinomycin D (2.5 μg/ml) for 1 hr. IFN–γ was then added and nuclear extracts prepared at the indicated time points. Where noted, staurosporine (500 nM) was added for 60 minutes.

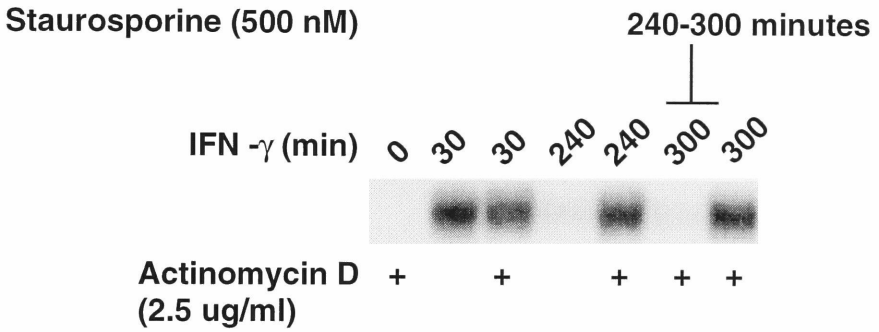
Staurosporine (500 nM)
240-300 minutes
IFN -γ (min)
0
30
30
240
240
300
300
Actinomycin D
(2.5 ug/ml)
+
+
+
+
+

Figure 3.2 Proteasome Inhibitors Prolong IFN–γ Signaling

EMSA analysis with an M67 probe. Bud-8 fibroblasts were pretreated with lactacystin (10 μM) or MG132 (20 μM) or an equivalent volume of DMSO (carrier used to dissolve compounds) for 1 hr. IFN–γ was then added (except in lanes 8 and 9) and nuclear extracts prepared at the indicated time points.

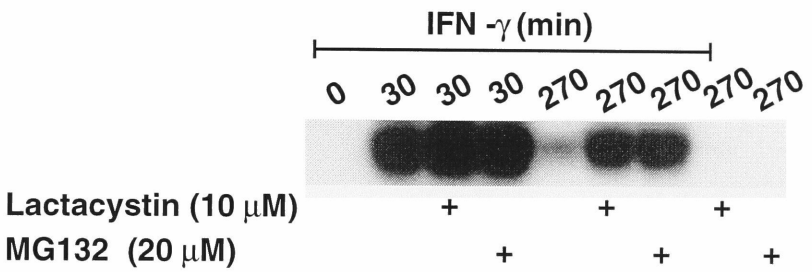
IFN -γ (min)
0
30
30
30
270
270
270
270
270
Lactacystin (10 μM)
+
+
+
MG132 (20 μM)
+
+
+

Figure 3.3 MG132 Does Not Prolong Signaling in the Presence of Staurosporine

EMSA analysis with an M67 probe. Bud-8 fibroblasts were pretreated with MG132 (20 μM) or DMSO for 1 hr. IFN-γ was then added to the cells and nuclear extracts prepared at the indicated time points. Where noted, staurosporine (500 nM) was added to the cells for 60 min.

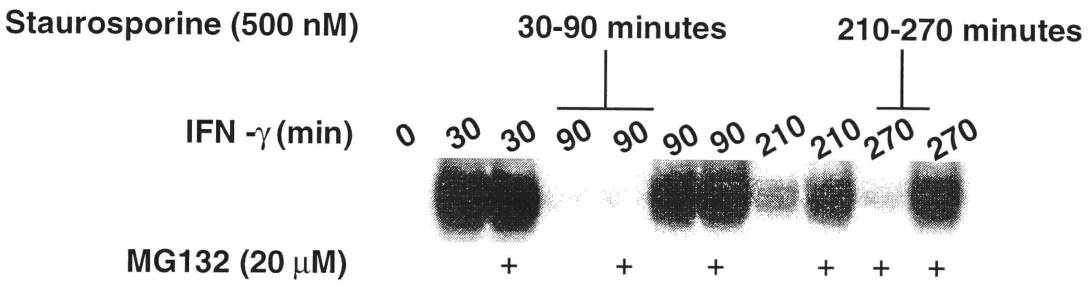
Staurosporine (500 nM)
30-90 minutes
210-270 minutes
IFN -γ (min)
0 30 30 90 90 90 90 210 210 270 270
MG132 (20 μM)
+ + + + + +

Figure 3.4 MG132 Prolongs Phosphorylation of the IFN–γ Receptor α Chain

(A) Protein immunoblot of precipitated α chain of IFN–γ receptor with anti-phosphotyrosine antibody. WI-38 cells were pretreated with MG132 (20 μM) or DMSO for 1 hr. IFN–γ was then added to the cells and whole cell extracts were prepared at the indicated time points. The IFN–γ receptor α chain was then precipitated, PAGE and transfer to filters was carried out and filters were then blotted with anti-phosphotyrosine antibody.

(B) The blot in (A) was stripped and reprobed with the antibody to the IFN–γ receptor α chain.

A. Anti-phosphotyrosine

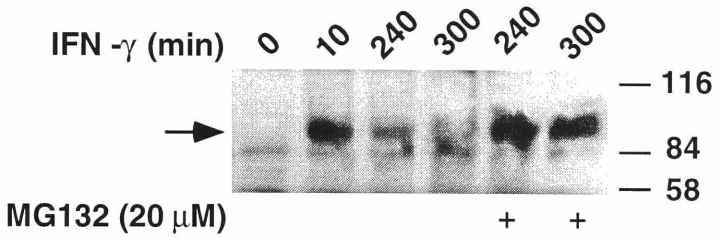

B. Anti-IFN-γ receptor α chain

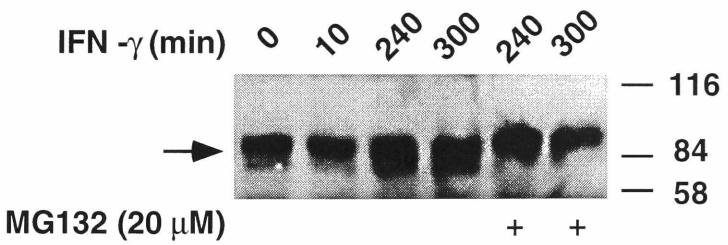

Figure 3.5 MG132 Prolongs IL-2 Signaling

(A) EMSA analysis with a β-casein probe. IL-2 starved HT-2 cells were pretreated with carrier (DMSO) for 1 hour. IL-2 was then added back to the cells and nuclear extracts prepared at the indicated time points.

(B) Same a (A) except cells were pretreated with MG132 (20 μM) for 1 hour prior to the readdition of IL-2

(C) Plot of the PhosphorImager analysis of Stat5 DNA binding complexes shown in (A) and (B) averaged with two other experiments. Error bars represent the standard error of the mean.

A. DMSO

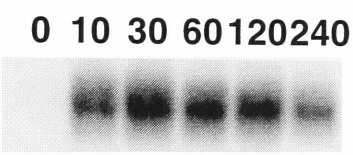

B. MG132

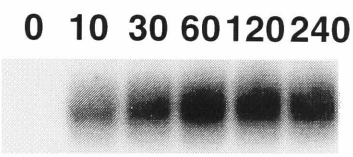

C.

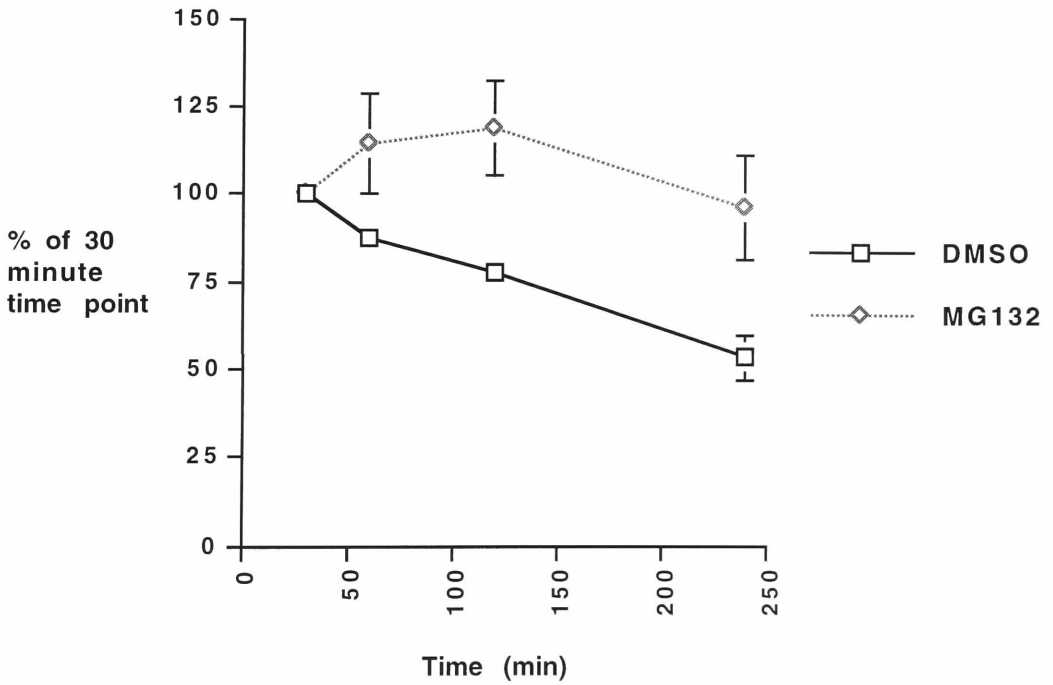

Figure 3.6 MG132 Does Not Prolong IL-2 Signaling in the Presence of Staurosporine

(A) EMSA analysis with a β-casein probe. IL-2 starved HT-2 cells were pretreated with carrier (DMSO) for 1 hr followed by readdition of IL-2. After 30 minutes of IL-2 treatment, staurosporine (500 nM) was added to the cells and nuclear extracts prepared at the indicated times.

(B) Same as (A) except cells were pretreated with MG132 (20 μM) for 1 hour followed by readdition of IL-2. After 120 minutes of IL-2 treatment, staurosporine (500 nM) was added to the cells and nuclear extracts prepared at the indicated times.

(C) Plot of the PhosphorImager analysis of Stat5 DNA binding complexes shown in (A) averaged with one other experiment and (B) averaged with two other experiments. Error bars represent the standard error of the mean.

A. DMSO

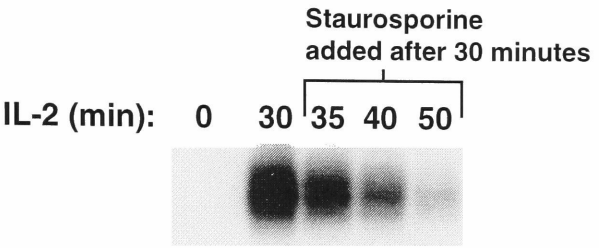

B. MG132

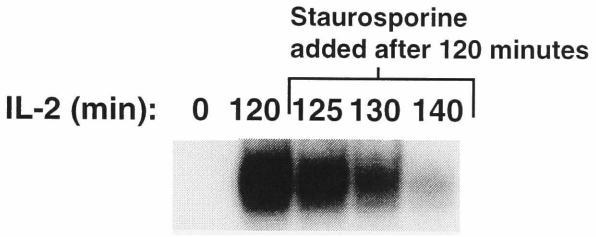

C.

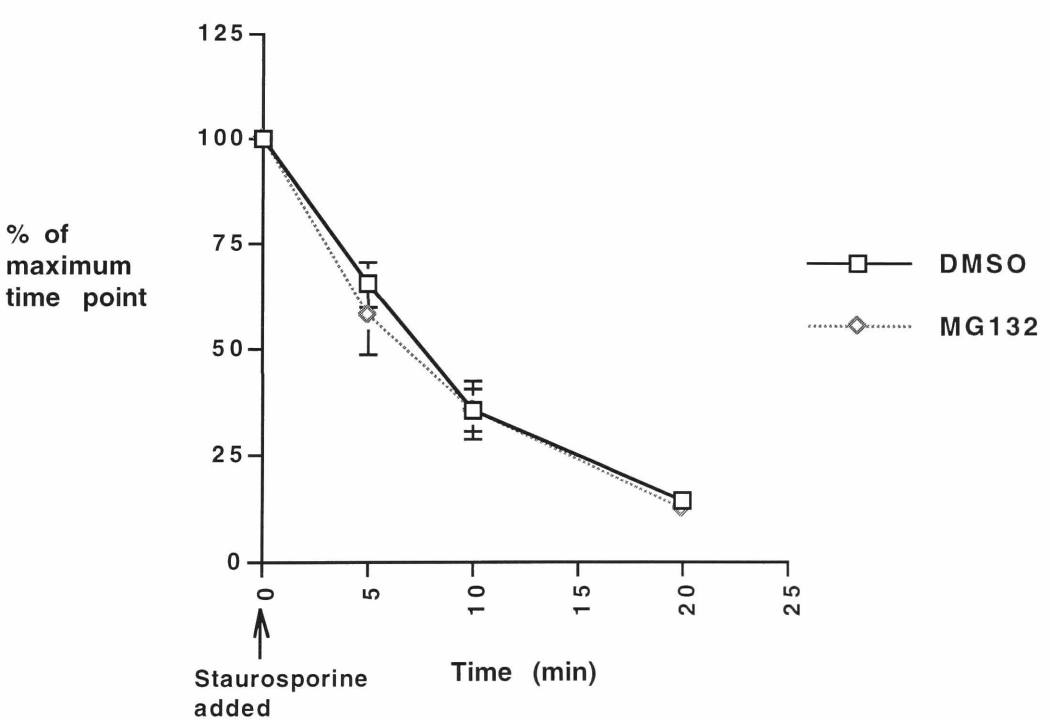

Figure 3.7 Vanadate Prolongs IFN–γ Signaling Even in the Presence of Staurosporine

EMSA analysis with a M67 probe. Bud-8 fibroblasts were treated with IFN–γ for 30 min. Staurosporine or carrier (DMSO) was then added to the cells. In lanes 4 and 5 vanadate (1 mM) was also added and the incubation continued for an additional 60 min. Nuclear extracts were prepared at the indicated time points.

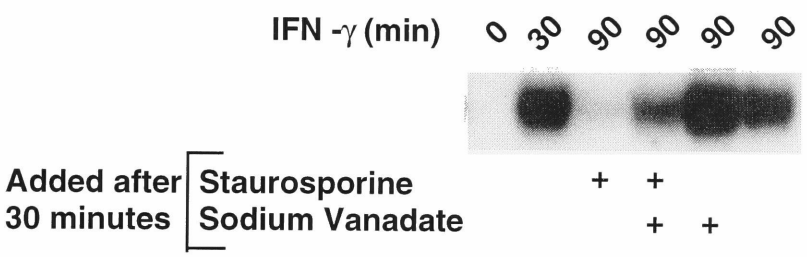
IFN -γ (min)
0
30
90
90
90
90
Added after 30 minutes
Staurosporine
Sodium Vanadate
+
+
+
+

Figure 3.8 The Stat1 Activation/Inactivation Cycle Analyzed by ^{35}S Labeling

(A) ^{35}S labeling followed by immunoprecipitation with anti-Stat1 antiserum. Bud-8 fibroblasts were labeled with ^{35}S for 2.5 hr as described in Experimental Procedures. Label was removed, cells washed in normal medium and IFN-γ was added. At the indicated time points, cytoplasmic and nuclear extracts were prepared. The cytoplasmic extracts were then subjected to SDS-PAGE and autoradiography.

(B) Same as (A) except SDS-PAGE and autoradiography of nuclear extracts.

(C) Plot of the PhosphorImager analysis of the Stat1 bands (both phosphorylated and unphosphorylated) shown in (A) (Experiment 1) and a separate experiment (Experiment 2). Data is expressed as percent of baseline (the value in the no treatment lane of the cytoplasmic extracts).

(D) Plot of the PhosphorImager analysis of the phosphorylated Stat1 band shown in (B) (Experiment 1) and a separate experiment (Experiment 2). Data is expressed as percent of baseline (the value in the no treatment lane of the cytoplasmic extracts).

A. Cytoplasmic

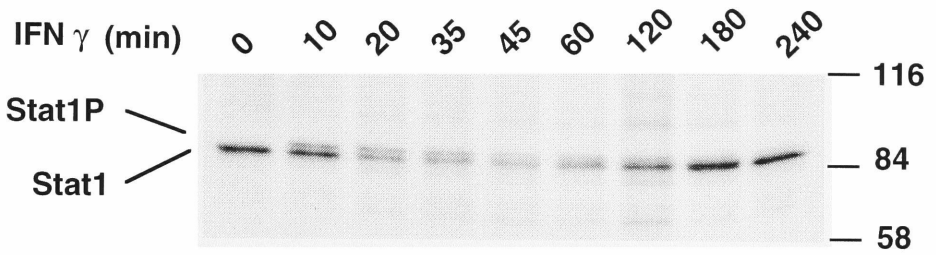

B. Nuclear

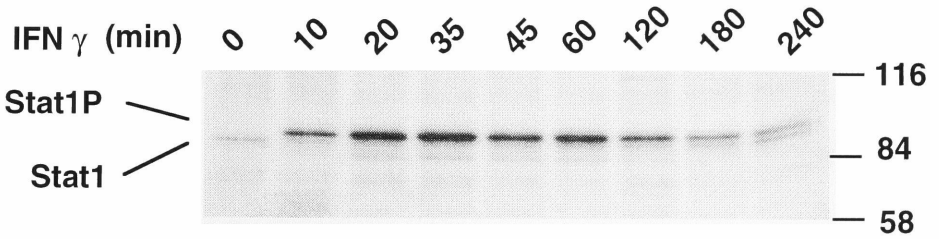

C. Cytoplasmic

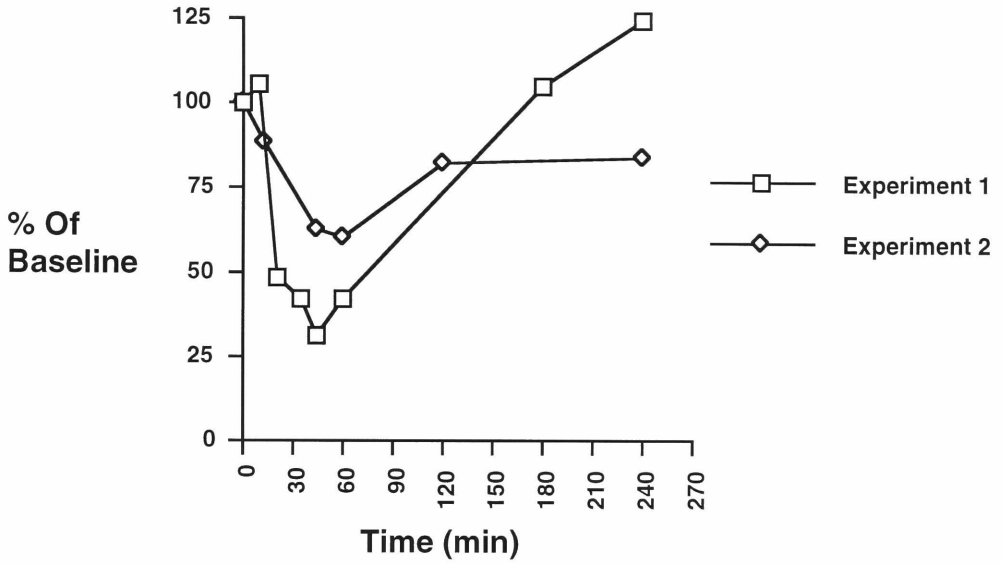

D. Nuclear

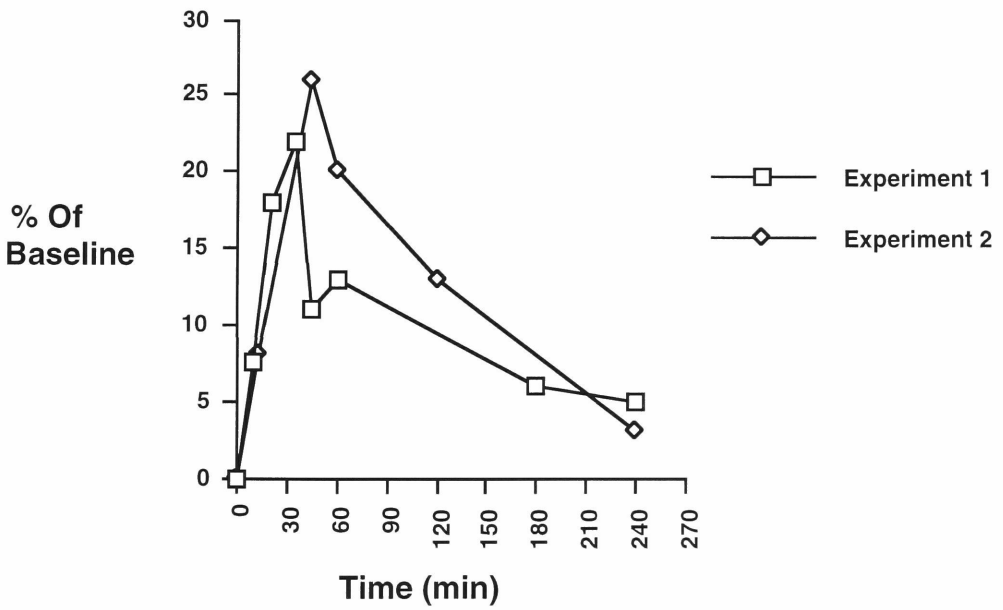

Figure 3.9 The Effect of Staurosporine on the Stat1 Activation-Inactivation Cycle Analyzed by ^{35}S Labeling

(A) ^{35}S labeling followed by immunoprecipitation with an anti-Stat1 monoclonal antibody. Bud-8 fibroblasts were labeled with ^{35}S for 2.5 hr as described in Experimental Procedures. Label was removed, cells washed in normal medium, IFN-γ and staurosporine were added at the indicated time points and cytoplasmic and nuclear extracts were prepared. The cytoplasmic extracts were then subjected to SDS-PAGE and autoradiography.

(B) Same as (A) except SDS-PAGE and autoradiography of nuclear extracts.

(C) Plot of the PhosphorImager analysis of the Stat1 bands (both phosphorylated and unphosphorylated) shown in (A). Data is expressed as percent of baseline (the value in the no treatment lane of the cytoplasmic extracts).

(D) Plot of the PhosphorImager analysis of the Stat1 bands (both phosphorylated and unphosphorylated) shown in (B). Data is expressed as percent of baseline (the value in the no treatment lane of the cytoplasmic extracts).

A.

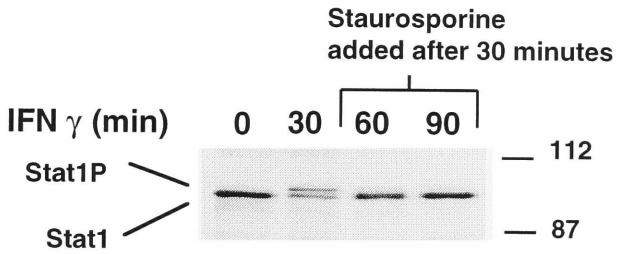
Staurosporine
added after 30 minutes
IFN γ (min)
0
30
60
90
Stat1P
Stat1
112
87

B.

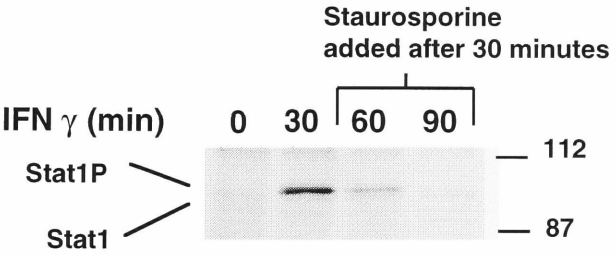
Staurosporine
added after 30 minutes
IFN γ (min)
0
30
60
90
Stat1P
Stat1
112
87

C. Cytoplasmic

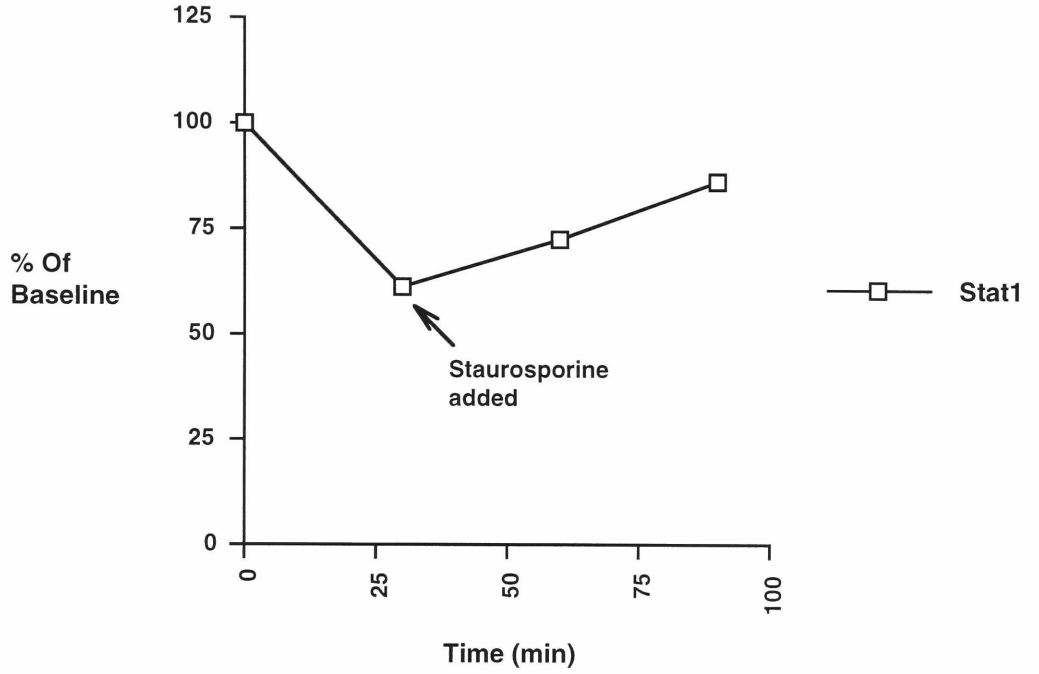

D. Nuclear

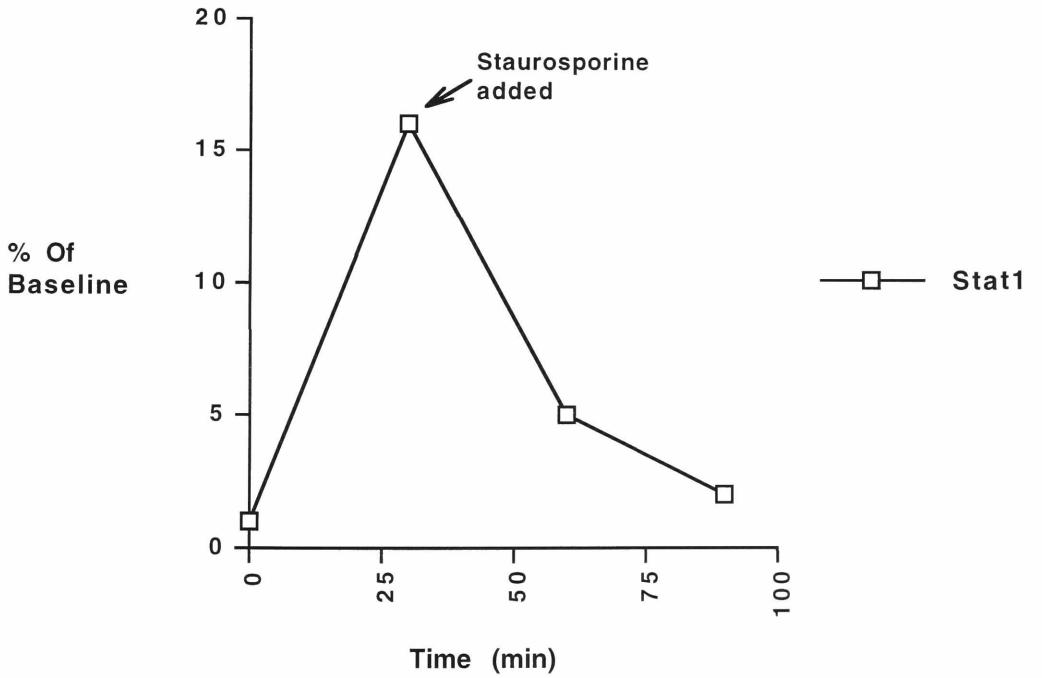

Chapter 4 Localizing the Stat1 Phosphatase

A major conclusion from the previous two chapters is that a protein tyrosine phosphatase has an important direct effect on Stat1 inactivation. In this chapter, experiments are presented that strongly imply the major subcellular location of Stat1 dephosphorylation is the nucleus.

4.1 Cells Lacking SHP-1 Have a Prolonged IFN-γ Time Course

The cytoplasmic tyrosine phosphatase SHP-1 (PTP-1C) is believed to play a role in the cessation of cytokine signaling (92, 93). Most evidence suggests that inactivation of JAKs and receptors is the major function of SHP-1. Some studies, however, indicate that STAT proteins co-immunoprecipitate with this phosphatase (98, 110). In fact, SHP-1 is the only phosphatase known to have any association with STAT molecules. These results prompted us to explore a possible role for SHP-1 in Stat1 dephosphorylation.

A naturally occurring mouse mutation in the SHP-1 gene leads to animals with no functioning SHP-1 ((95, 96), reviewed in (97)). These "motheaten" mice have a variety of hematopoietic defects and die at an age of 3 to 9 weeks. We obtained immortalized macrophages from these mice as well as cells from normal littermates. The cells were immortalized through infection with a retrovirus containing the v-Raf and v-Myc oncogenes (145). The

motheaten macrophages had no detectable SHP-1 by Western blot analysis of whole cell extracts probed with an antibody to the N-terminus of SHP-1 (Figure 4.1).

We treated the motheaten and control macrophages with IFN-γ. Whole cell extracts were prepared at various time points and subjected to EMSA analysis. As shown in Figure 4.2, the peak in Stat1 DNA-binding activity in response to IFN-γ was later in the motheaten macrophages and remained higher over a 4 hour time course when compared to the control macrophages. Although there was more variability in the response of the motheaten macrophages to IFN-γ, in every experiment the DNA binding activity of the motheaten macrophages was prolonged when compared to control cells. These results agree with previous experiments demonstrating an increase in IFN-γ induced Stat1 DNA-binding in astrocytes from motheaten mice (98).

4.2 The Effect of SHP-1 On IFN-γ Signaling is Upstream of Stat1

The prolonged IFN-γ time course in cells lacking SHP-1 could be due to SHP-1 having an effect on the receptor-JAK complex or on the dephosphorylation of Stat1. To distinguish between these possibilities we treated cells for 30 minutes with IFN-γ followed by treatment with staurosporine. At the indicated time points, whole cell extracts were prepared and used in EMSA analysis (Figure 4.3). The decay rate of activated Stat1 was virtually indistinguishable in

motheaten and control macrophages with approximately 50% of the DNA-binding activity disappearing after only 10 minutes of staurosporine treatment and almost all the activity disappearing after 60 minutes. Clearly, lack of SHP-1 does not significantly affect the decay of Stat1 in the presence of staurosporine; therefore, the increase in IFN-γ induced Stat1 activity in the motheaten macrophages is most likely due to SHP-1 mediated inactivation of the IFN–γ receptor or JAKs. Our experiments suggest that SHP-1, the only phosphatase reported to have an interaction with STAT proteins, does not play a major direct role in Stat1 dephosphorylation.

4.3 The IFN–γ Time Course in Cytoplasts

Enucleated cells can be prepared by treatment with cytochalasin B followed by centrifugation in a ficoll gradient (146-149). The cytochalasin disrupts the cytoskeleton, enabling the dense nucleus to be expelled from the cytoplasm during centrifugation. The remaining "cytoplasts" reseal and remain viable for at least 24 hours. In the late 1980's, cytoplasts were used to determine that STAT signaling originates in the cytoplasm (22, 23).

We prepared cytoplasts in an attempt to determine the cellular location of the Stat1 phosphatase. If the nucleus plays an important role in JAK-STAT pathway inactivation, extracts from cytoplasts should not show the typical decay in Stat1 DNA binding activity during a 4 hour IFN–γ time course. Bud-8 cells were treated with

cytochalasin B and then spun in a ficoll gradient. Control cells were treated with cytochalasin B but not centrifuged. In Figure 4.4, control cells and cytoplasts were stained with Hoescht dye which binds to nucleic acids. In the control cells, the nuclei were clearly visible in every cell. In the cytoplasts, there were very few intact nuclei and the majority of cells contained no nuclei at all (approximately 80 to 90%).

Cytoplasts and control cells were treated with IFN-γ and cytoplasmic extracts were prepared; these extracts were analyzed by EMSA (Figure 4.5A, B, and D). In control cells, there was a rapid increase in Stat1 DNA-binding activity that decayed gradually with only 11% of the initial activity remaining after 270 minutes. This result indicates that cytochalasin B by itself does not affect Stat1 inactivation. IFN-γ treatment of cytoplasts also induced rapid activation of Stat1 but the DNA-binding activity remained high through 270 minutes.

Extracts were then run on a SDS-PAGE gel and Western blotted with antiserum to the C-terminus of Stat1 (Figure 4.5C). The lower band is non-phosphorylated Stat1. After 30 minutes of IFN-γ treatment, the slower migrating phosphorylated Stat1 band appeared. This upper band disappeared in control cells but remained in the cytoplasts even at the 270 minute time point. The Western blot data correlates well with the EMSA analysis indicating the IFN-γ time course is prolonged in cytoplasts

4.4 The Effect of Staurosporine on the IFN-γ Time Course in Cytoplasts

To detect whether any decay at all of tyrosine phosphorylated Stat1 occurred in cytoplasts, we used staurosporine to suppress receptor-JAK signaling. Control cells and cytoplasts were prepared as described above and treated with IFN-γ. At the 30 minute time point, staurosporine was added and cytoplasmic extracts were prepared and analyzed by EMSA (Figure 4.6). A decay in DNA binding activity upon staurosporine treatment still occurred in cytoplasts but was significantly slower than in the control cells. In three experiments, 30 minutes after staurosporine treatment, there was a consistent 25% difference in DNA binding activity in the control cells compared to the cytoplasts (Figure 4.6C). There was also a difference, although less pronounced, 60 minutes after kinase inhibitor treatment. Unfortunately, due to the large numbers of cells required for these experiments, only two time points after staurosporine treatment were examined. Although it is difficult to make precise kinetic measurements with only two time points, the reproducibility of these experiments suggest a half-life of Stat1 DNA binding activity in cytoplasts of approximately 30 minutes as compared to 15 minutes for nuclear DNA binding activity (see chapter 2).

The same extracts were run on an SDS-PAGE gel and Western blotted with antiserum to the C-terminus of Stat1 (Figure 4.7). The phosphorylated Stat1 band disappeared 60 minutes after staurosporine treatment in both control cells and cytoplasts. The

Western blot data correlates with the EMSA analysis although due to the decreased sensitivity of this assay the difference in inactivation between cytoplasts and cells was not as apparent. As will be expanded upon in the discussion section, the slower decay in DNA binding upon staurosporine treatment in cytoplasts suggests the nucleus is required for the normal inactivation of Stat1.

4.5 The Flow of Activated Stat1 Upon Receptor-JAK Inactivation is from Cytoplasm to Nucleus

To further determine the location of Stat1 dephosphorylation, we examined intracellular inactivation kinetics by comparing cytoplasmic versus nuclear extracts. At points of maximal JAK-receptor activation, phosphorylated Stat1 flows to the nucleus (see chapter 3). As receptor signaling is downregulated, the flow of activated Stat1 molecules should be to the site of their dephosphorylation. In other words, the final compartment in which phosphorylated Stat1 is detected is arguably the subcellular location of Stat1 inactivation.

Bud-8 fibroblasts were treated with IFN-γ and cytoplasmic and nuclear extracts were prepared and analyzed by EMSA. As shown in Figure 4.8, the Stat1 DNA-binding kinetics in the nucleus resembled that previously shown and gradually decayed over the four hour time course (see chapter 2). At the time points between 30 and 240 minutes, the level of Stat1 DNA-binding activity in the cytoplasm was always lower than that in the nucleus (Figure 4.8C). It appears that as the receptor is shutdown, the remaining cytoplasmic

phosphorylated Stat1 is translocated to the nucleus where it is ultimately inactivated.

4.6 Flow of Activated Stat1 Upon Staurosporine Addition

The difference between the cytoplasmic and nuclear decay in Figure 4.8 is the result of a gradual inactivation of the IFN–γ receptor. If the receptor was shut-off abruptly, as with the addition of kinase inhibitor, the flow of activated molecules from the cytoplasm to the nucleus should be more pronounced. To test this hypothesis, staurosporine was added to Bud-8 fibroblasts after 30 minutes of IFN–γ treatment. Nuclear and cytoplasmic extracts were prepared and analyzed by EMSA (Figure 4.9). The pattern of decay of nuclear Stat1 DNA-binding closely resembled that shown previously (see chapter 2). After 15 minutes of staurosporine treatment the amount of DNA-binding was maintained at the maximal level and only after an additional 15 minutes was there a detectable drop in activity. In contrast, the cytoplasm showed a decline of more than 50% within the first 15 minutes of staurosporine treatment (Figure 4.9C). Without replenishment from the receptor, continued nuclear import of activated Stat1 apparently caused a reduction in cytoplasmic phosphorylated Stat1 leading to a decrease in cytoplasmic DNA binding in the first 15 minutes. There was no change, however, in the nuclear DNA-binding activity due to the continued translocation of Stat1 into the nucleus. Fifteen minutes later, the flow of activated Stat1 from the cytoplasm had decreased to a low enough level for

dephosphorylation in the nucleus to be detectable. These experiments with staurosporine provide further evidence that the nucleus is the site of Stat1 inactivation.

4.7 Vanadate Prolongs Stat1 DNA Binding Activity in the Nucleus As It Decreases in the Cytoplasm

We next sought to determine the effect of phosphatase inhibition on the flow of activated Stat1. We reasoned that phosphatase inhibition might lead to accumulation of phosphorylated Stat1 in the nucleus, the presumed compartment of inactivation, as it decreased in the cytoplasm. We treated Bud-8 fibroblasts with vanadate, an inhibitor of tyrosine phosphatases, and with IFN-γ. Nuclear and cytoplasmic extracts were prepared and analyzed by EMSA. As shown in Figure 4.10, Stat1 DNA-binding decreased in the cytoplasmic extracts to below 40% of maximum by 240 minutes. The decay is not as pronounced as shown in the absence of phosphatase inhibitor probably due to the continuous generation of some phosphorylated Stat1 in the presence of vanadate (144). In contrast to the cytoplasmic activity, nuclear DNA-binding remained high and even increased past the 30 minute time point. With cytoplasmic activity decreasing to such a low level, the high-level of nuclear DNA-binding could only be maintained if there was a block of Stat1 inactivation and if phosphorylated molecules were not able to exit the nucleus.

4.8 ^{35}S Labeling Reveals Nuclear Trapping of Phosphorylated Stat1

We have previously shown with metabolic labeling that Stat1 goes through an activation-inactivation cycle in which the protein becomes phosphorylated, enters the nucleus and then returns to the cytoplasm in a dephosphorylated state (see chapter 3). That experiment, however, was unable to distinguish between dephosphorylation in the nucleus with rapid export or dephosphorylation in the cytoplasm. In order to determine the compartment where Stat1 inactivation occurs, we metabolically labeled cells and followed the fate of Stat1 in extracts treated with both IFN-γ and vanadate. Cells were incubated in the presence of ^{35}S methionine for 2.5 hr, washed and medium containing non-radioactive methionine was added. IFN-γ or IFN-γ plus vanadate was then used to activate cells and samples were taken at the indicated time points. An anti-Stat1 monoclonal antibody was used to precipitate the protein from nuclear and cytoplasmic extracts; subsequently gel electrophoresis, autoradiography and quantitation of both the non-phosphorylated and the more slowly migrating tyrosine phosphorylated form was carried out.

The results of a typical experiment are shown in Figure 4.11A (cytoplasmic) and B (nuclear) (Figure 4.11A and B are equal exposures but A represents only a quarter of the total cytoplasmic extracts. Quantitation of two experiments is shown in C and D.) Before treatment, most of the Stat1 was in the cytoplasm. Upon IFN-γ addition, there was a decrease of total Stat1 in the cytoplasm as the

phosphorylated Stat1 was transported to the nucleus (left half of Figure 4.11A and B). At the end of the 4 hour cycle, the Stat1 had left the nucleus and the amount of Stat1 in the cytoplasm returned to close to initial levels (between 80 and 90%). The results were quite different when the cells were also treated with vanadate (right half of Figure 4.11A and B). We still observed the initial decrease of Stat1 in the cytoplasm with an increase in the nucleus seen at 30 minutes. At later time points, however, the amount of Stat1 in the nucleus rose to approximately 40% of the total labeled Stat1 in the cell while the amount of Stat1 in the cytoplasm decreased to about 15%.

As with our previous experiments, the total ^{35}S recovery was lower when the maximal nuclear phosphorylated Stat1 was evident. It is possible therefore that the nuclear phosphoprotein may not be quantitatively extracted. If this were true then even more phosphorylated Stat1 molecules could be present in the nucleus upon vanadate treatment. The results of these experiments argue strongly that the nucleus is the normal site of Stat1 dephosphorylation, and in the absence of dephosphorylation the activated Stat1 molecules are trapped in the nucleus.

4.9 Discussion

In this chapter, we attempted to determine the subcellular location of the Stat1 inactivating tyrosine phosphatase. As an initial approach, we used cytoplasts to examine the effect of enucleation on

the IFN-γ activation-inactivation cycle. The cytoplasts clearly had a prolonged IFN–γ time course, indicating a possible role for the nucleus in Stat1 inactivation. It must be remembered, however, that cells treated with actinomycin D had a prolonged time course due to a defect in receptor inactivation, and that cytoplasts do not synthesize RNA. We used staurosporine to determine whether enucleation affected the receptor-JAK complex or the STAT molecules.

While the decrease in Stat1 DNA-binding activity upon staurosporine treatment was consistently slower in cytoplasts, in these experiments cytoplasmic extracts were prepared. Therefore, the decay in the control cells measured any inactivation in the cytoplasm in combination with nuclear translocation of Stat1 while the decay in the cytoplasts measured only inactivation. Metabolic labeling experiments demonstrated rapid nuclear transport of activated Stat1 within 10 minutes after IFN-γ treatment (see chapter 3). Comparison of cytoplasts and control cells also reveals the rapid nature of Stat1 nuclear import.

Assuming the protocol to prepare cytoplasts did not activate non-physiological proteases or phosphatases, our results indicate that inactivation of Stat1 can occur in the cytoplasm with a half-life of phosphorylated Stat1 of approximately 30 minutes. Even if this inactivation was physiological, the transit time of activated Stat1 is rapid enough to insure nuclear accumulation of phosphorylated molecules. The prolonged signaling observed in cytoplasts, however, most likely resulted from the same cause as that seen upon

actinomycin D treatment; that is, new RNA and protein synthesis is required to block continued signaling from the liganded receptor.

As the receptor-JAK complex is downregulated, the flow of phosphorylated Stat1 molecules should be to the site of their inactivation. During an IFN-γ time course, the Stat1 DNA-binding activity in the cytoplasm decayed at a faster rate than the activity in the nucleus. This result suggests that the flow of phosphorylated Stat1 upon receptor-JAK inactivation is from cytoplasm to nucleus.

The use of staurosporine made this flow more evident due to the abrupt cessation in receptor signaling. Most striking was the difference 15 minutes after staurosporine addition as the nuclear DNA binding activity remained constant while the cytoplasmic DNA binding dropped to less than half of its pretreatment level. The flow of Stat1 to the nucleus could still be consistent with cytoplasmic inactivation if nuclear phosphorylated Stat1 molecules were dephosphorylated almost immediately upon re-emergence in the cytoplasm. The half-lives of nuclear Stat1 DNA binding activity (15 minutes) and of cytoplasmic Stat1 DNA binding activity (30 minutes in cytoplasts) argue against rapid cytoplasmic dephosphorylation, and in favor of nuclear inactivation of Stat1.

Our experiments with vanadate support this hypothesis. Other groups have also observed with IFN-γ treatment a prolonged nuclear Stat1 signal in agreement with our evidence of nuclear tyrosine phosphatase inactivation of Stat1 (107). The earlier experiments, however, did not examine the amount of cytoplasmic phosphorylated Stat1 and could not discriminate between phosphatase inactivation of a continuing IFN-γ receptor signal and phosphatase inactivation of

Stat1. We treated cells with staurosporine and vanadate to demonstrate that in the absence of continued signaling from the IFN-γ receptor, Stat1 DNA-binding in the nucleus could be maintained by phosphatase inhibition (see chapter 2). Surprisingly, the use of staurosporine was not necessary to reach this conclusion. Treatment of cells with vanadate and IFN-γ caused prolonged Stat1 DNA binding activity in the nucleus as it declined to low levels in the cytoplasm.

Our metabolic labeling experiment corroborated the EMSA analysis. After a four hour treatment with IFN-γ and vanadate, only 15% of the initially labeled Stat1 in the cell remained in the cytoplasm while over 40% of the initially labeled Stat1 could be recovered as phosphorylated Stat1 in the nucleus. As with previous labeling experiments, the total ^{35}S recovery was lower when maximal nuclear phosphorylated Stat1 was evident. It is possible that the nuclear phosphoprotein is not quantitatively extracted and even more Stat1 is present in the nucleus than we were able to detect. It is also possible that vanadate might promote some proteolysis of STAT molecules. Nevertheless, our experiments with vanadate showing a dramatic shift of labeled Stat1 from the cytoplasm to the nucleus strongly argue for the importance of the nucleus in Stat1 inactivation and for the inability of phosphorylated molecules to reenter the cytoplasm.

While it is possible that vanadate acts to block dephosphorylation and nuclear export through different processes, it is reasonable to hypothesize that Stat1 molecules can be exported only after dephosphorylation. It has recently been shown that a blockade of nuclear export is required for the accumulation of M

phase promoting factor (MPF) in the nucleus (150). Without this blockade, export is faster than import and the majority of the molecules are detected in the cytoplasm. A similar phenomenon is observed with the proteins MAPK kinase and MAPKAP kinase 2 (151, 152). The requirement of dephosphorylation for export of Stat1 may allow phosphorylated Stat1 molecules to increase to high levels in the nucleus. Rapid export may also explain our inability to detect significant amounts of dephosphorylated Stat1 in the nucleus in Bud-8 cells. The implications of this model will be discussed in chapter 5. It should be noted that in other cell lines significant amounts of non-phosphorylated Stat1 are found in the nucleus, indicating that dephosphorylation and nuclear export are not always as tightly coupled as they appear to be in Bud-8 euploid fibroblasts (data not shown).

Our major conclusion is that the majority of Stat1 is dephosphorylated in the nucleus. Cytoplasmic phosphatases, however, do play a significant role in the JAK-STAT pathway. In our experiments with motheaten macrophages, the IFN-γ induced DNA binding activity was consistently prolonged. This extended signal was abolished upon staurosporine treatment, revealing that SHP-1, consistent with its usual role in cytokine signaling, was dephosphorylating the receptor-JAK complex and not the Stat1 protein (92, 93). The significance of a possible interaction between SHP-1 with STAT proteins remains uncertain (98, 110). We did not explore the role of SHP-2, the other member of the SH2-containing tyrosine phosphatase family, in IFN-γ signaling. Although we cannot completely rule out the role of SHP-2 in Stat1 inactivation, this

phosphatase has never been found associated with the IFN-γ receptor and usually plays a role in positive signaling (92, 93). While cytoplasmic phosphatases play an important role in modulating the function of the receptor-JAK complex, the results of our experiments implicate a nuclear protein tyrosine phosphatase in Stat1 inactivation.

Figure 4.1 Western Blots of SHP-1 Macrophages from Motheaten Mice and Littermate Controls

Western Blot Analysis. Whole cell extracts were prepared from immortalized motheaten (Me) and littermate control (Con) macrophages. These extracts were then subjected to SDS-PAGE and blotted with anti-SHP-1 N-terminal antiserum.

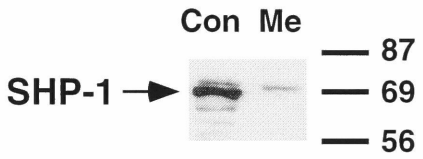
Con
Me
SHP-1
87
69
56

Figure 4.2 IFN–γ Time Course In Macrophages from Motheaten Mice and Littermate Controls

(A) EMSA analysis with an M67 probe. Whole cell extracts were prepared from immortalized littermate control macrophages treated with IFN–γ for the indicated times.

(B) Same as (A) except immortalized macrophages from motheaten mice.

(C) Plot of the PhosphorImager analysis of Stat1 DNA binding complexes in motheaten and control macrophages at various times after IFN–γ treatment. The results shown are the average of two experiments with error bars representing the standard error of the mean.

A. Control

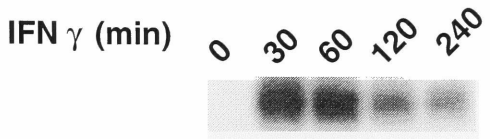

B. Motheaten

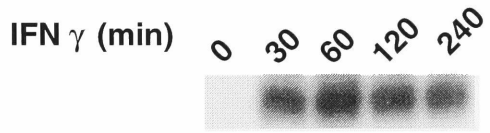

C.

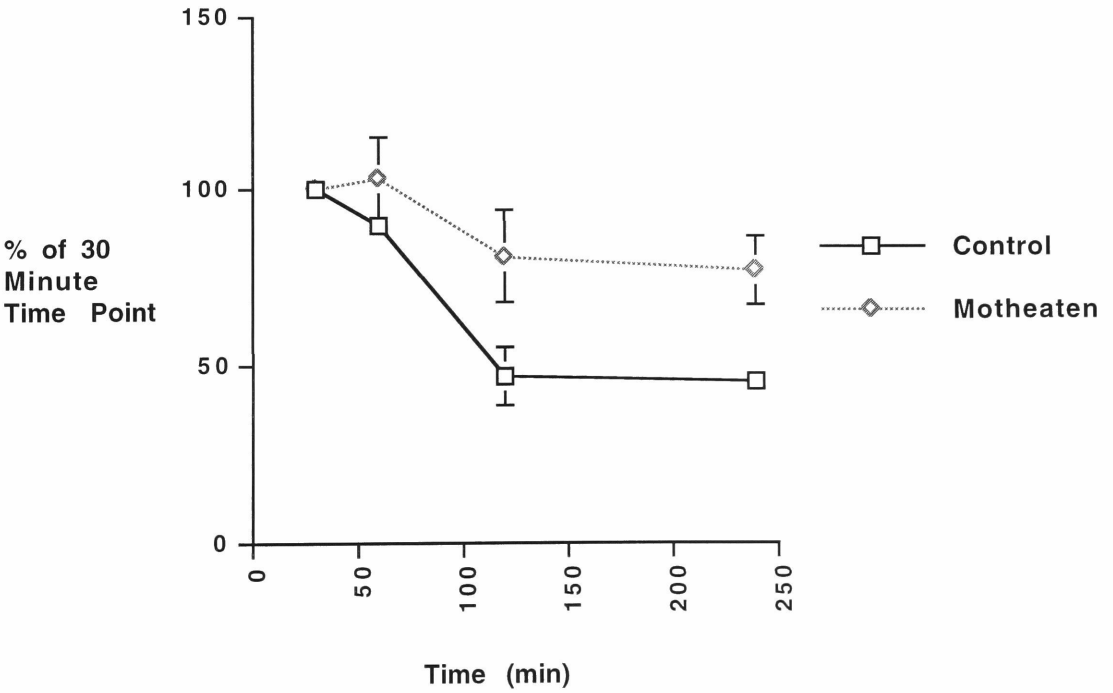

Figure 4.3 IFN-γ Signaling in Macrophages from Motheaten Mice is Not Prolonged in the Presence of Staurosporine

(A) EMSA analysis with a M67 probe. Whole cell extracts were prepared from immortalized littermate control macrophages treated with IFN-γ for 30 minutes followed by staurosporine (500 nM) for the indicated times.

(B) Same as (A) except immortalized macrophages from motheaten mice.

(C) Plot of the PhosphorImager analysis of Stat1 DNA binding complexes shown in (A) and (B).

A. Control

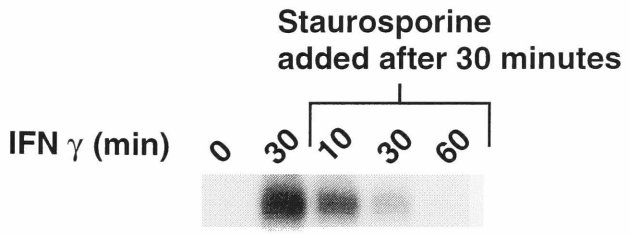

B. Motheaten

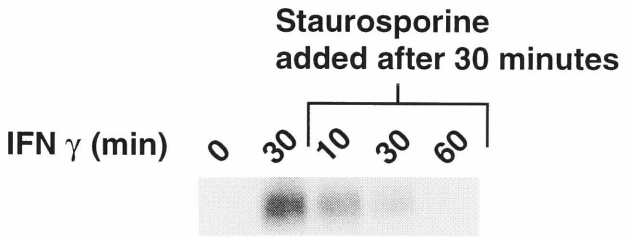

C.

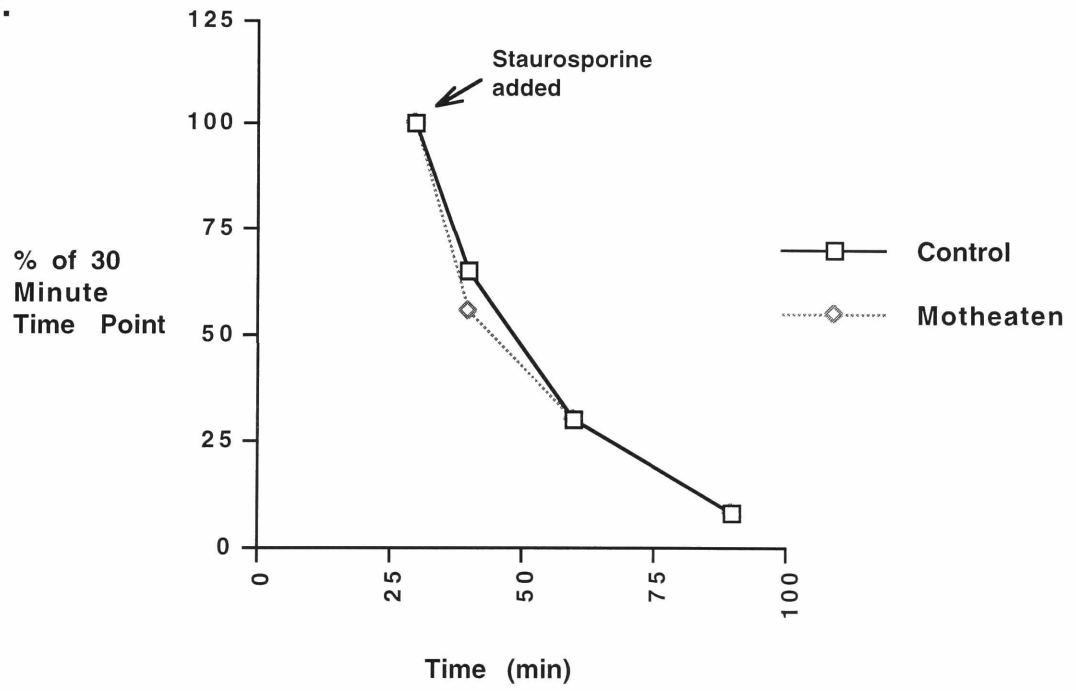

Figure 4.4 Preparation of Cytoplasts

(A) Control Bud-8 fibroblasts, treated with cytochalasin B but not centrifuged, were stained with Hoescht dye to indicate the presence of nuclei.

(B) Cytoplasts, prepared by cytochalasin B treatment and centrifugation of Bud-8 fibroblasts, were stained as in (A).

A. Control Cells

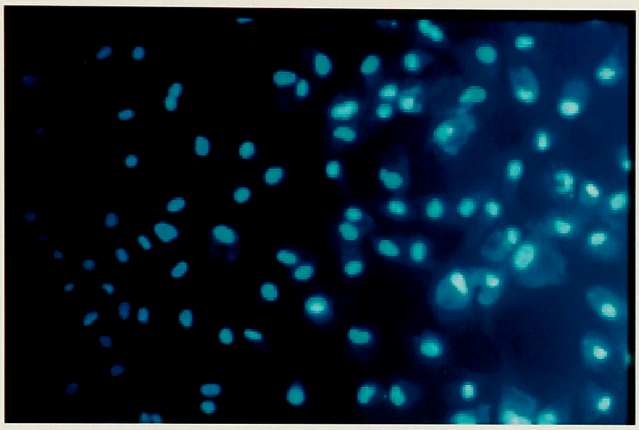

B. Cytoplasts

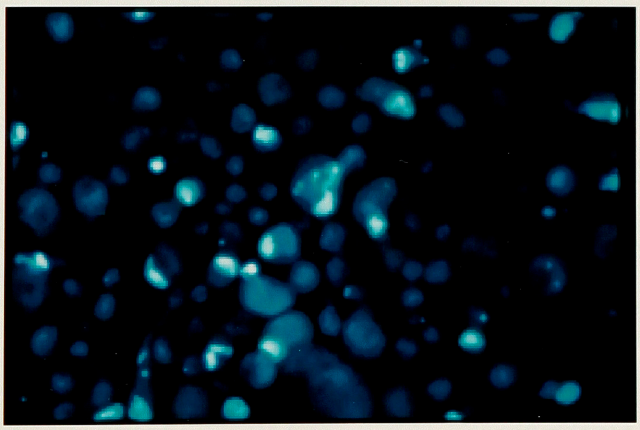

Figure 4.5 The IFN-γ Time Course in Cytoplasts and Control Cells

(A) EMSA analysis with an M67 probe. Cytoplasmic extracts were prepared from control cells treated with IFN-γ for the indicated times.

(B) Same as (A) except cytoplasts.

(C) Western Blot Analysis. The extracts shown in (A) and (B) were subjected to SDS-PAGE and blotted with an anti-Stat1 C-terminal serum.

(D) Plot of the PhosphorImager analysis of the Stat1 DNA binding in IFN-γ treated cytoplasts and control cells.

A. Cells

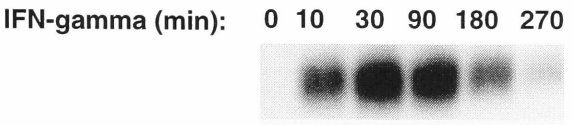

B. Cytoplasts

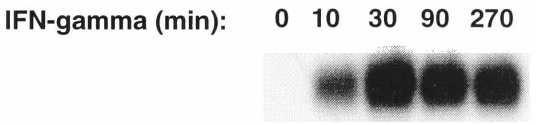

C.

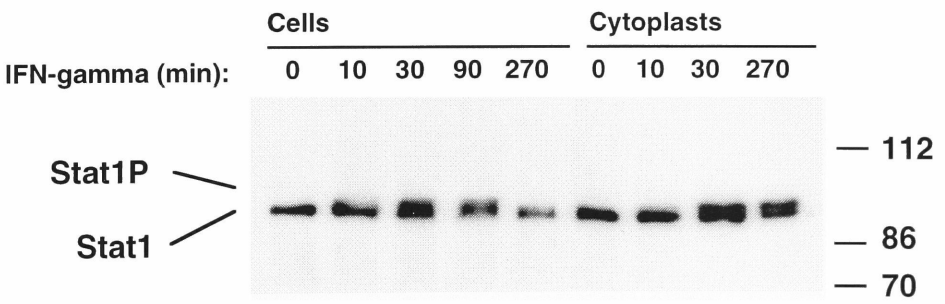

D.

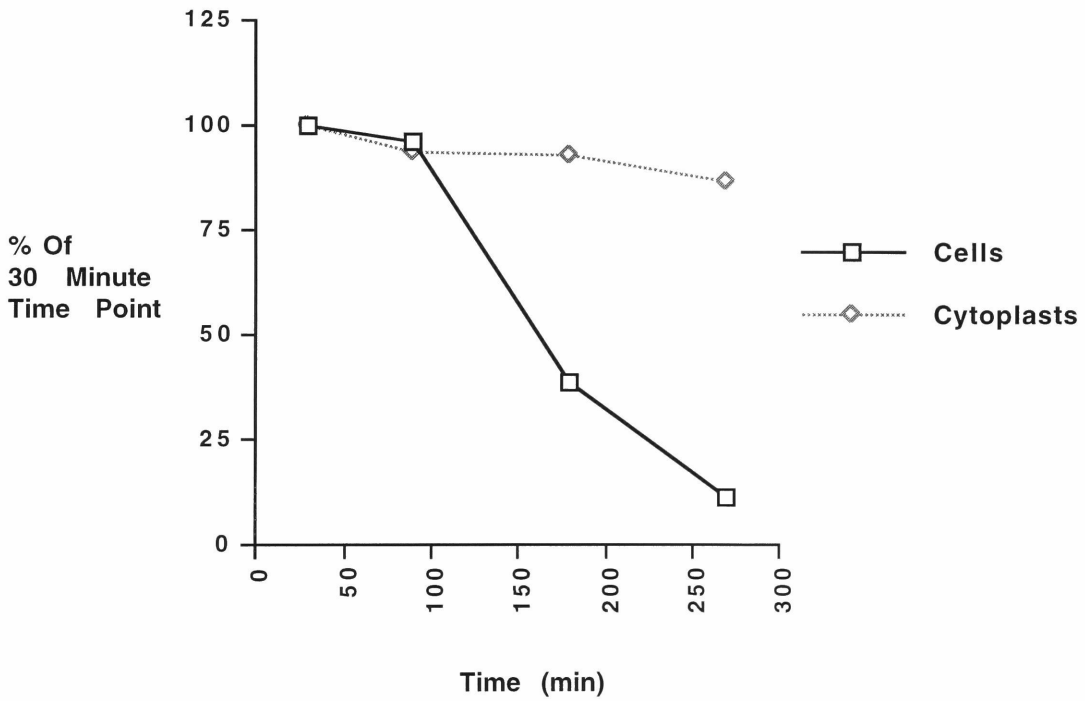
% Of
30 Minute
Time Point
125
100
75
50
25
0
0
50
100
150
200
250
300
Time (min)
Cells
Cytoplasts

Figure 4.6 The Effect of Staurosporine on the IFN–γ Time Course in Cytoplasts and Control Cells

(A) EMSA analysis with a M67 probe. Cytoplasmic extracts were prepared from control cells treated with IFN–γ for 30 minutes followed by staurosporine (500 nM) for the indicated times.

(B) Same as (A) except cytoplasts.

(C) Plot of the PhosphorImager analysis of the Stat1 DNA binding in cytoplasts and control cells at various times after IFN–γ and staurosporine treatment. The results shown are the average of three cytoplast experiments. In two of these experiments, control cells were also prepared. Error bars represent the standard error of the mean.

A. Cells

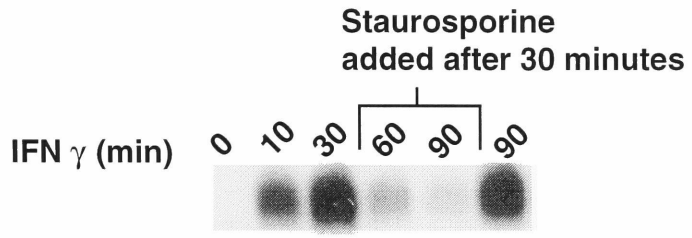

B. Cytoplasts

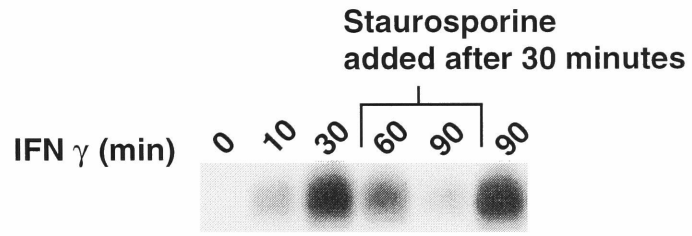

C.

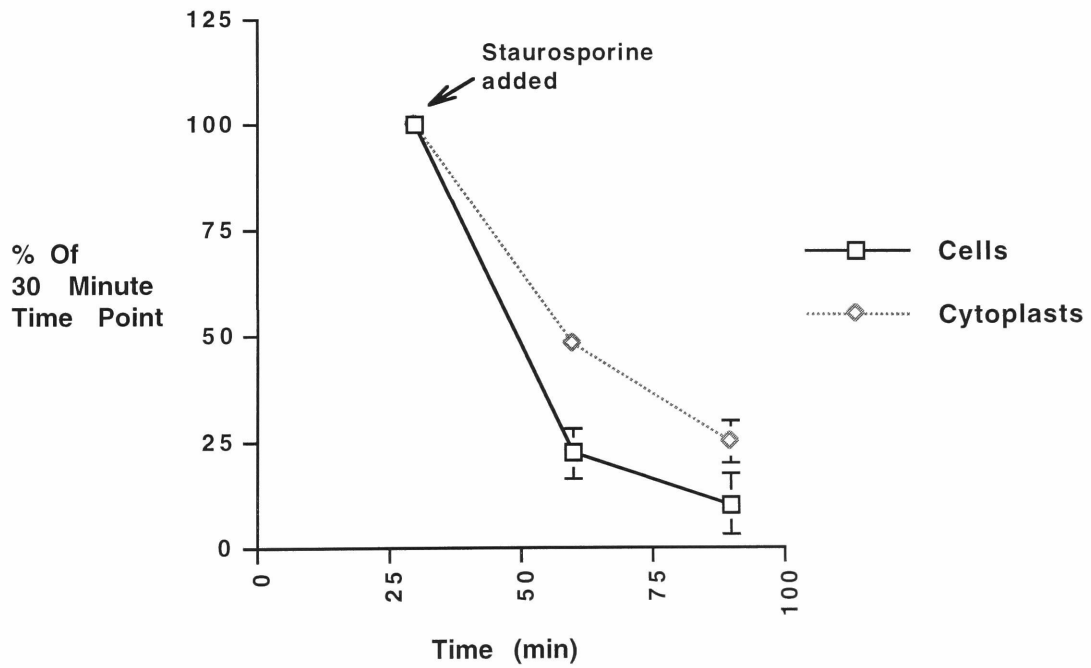

Figure 4.7 Western Blots of Stat1 in IFN–γ and Staurosporine Treated Cytoplasts and Control Cells.

(A) Western Blot Analysis. Cytoplasmic extracts were prepared from control cells treated with IFN–γ for 30 minutes followed by staurosporine (500 nM) for the indicated times. These extracts were then subjected to SDS-PAGE and blotted with anti-Stat1 C-terminal serum.

(B) Same as (A) except cytoplasts.

A. Cells

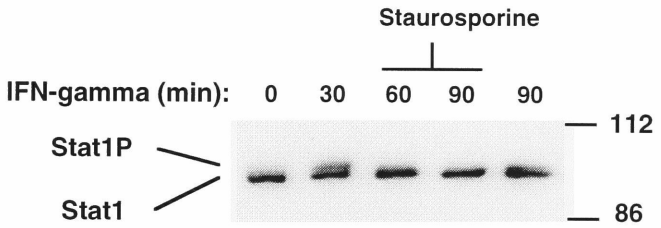

B. Cytoplasts

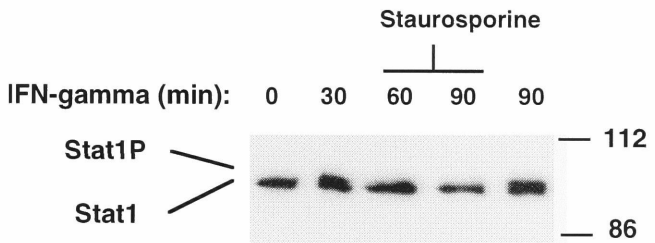

Figure 4.8 The Decay in Stat1 DNA Binding in Cytoplasmic and Nuclear Extracts During an IFN–γ Time Course.

(A,B) EMSA analysis with an M67 probe. Cytoplasmic (A) and nuclear (B) extracts were prepared from Bud-8 normal human fibroblasts treated with IFN–γ for the indicated times.

(C) Plot of the PhosphorImager analysis of Stat1 DNA binding complexes at various times after IFN–γ treatment.

A. Cytoplasmic

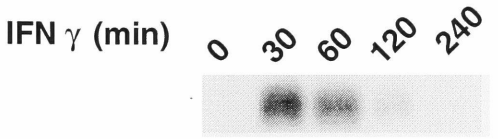

B. Nuclear

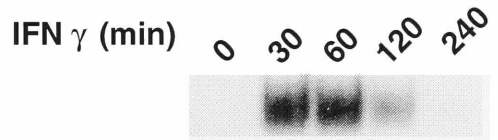

C.

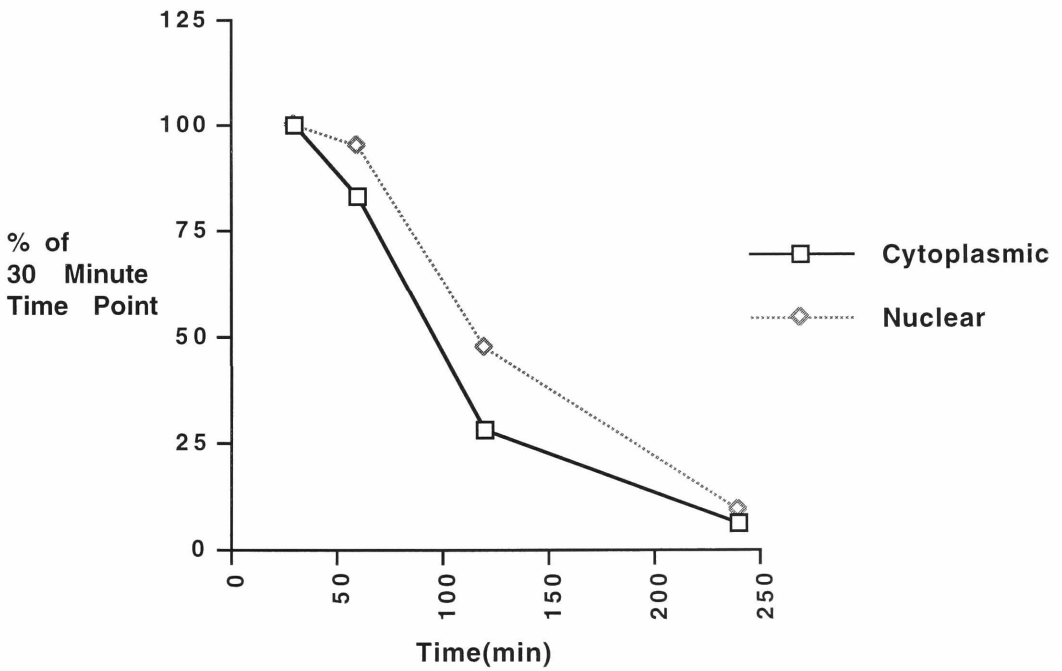

Figure 4.9 The Decay in Stat1 DNA Binding in Cytoplasmic and Nuclear Extracts Upon Staurosporine Addition

(A,B) EMSA analysis with an M67 probe. Cytoplasmic (A) and nuclear (B) extracts were prepared from Bud-8 normal human fibroblasts treated with IFN-γ for 30 minutes followed by staurosporine (500 nM) for the indicated times.

(C) Plot of the PhosphorImager analysis of Stat1 DNA binding complexes at various times after IFN-γ plus staurosporine treatment.

A. Cytoplasmic

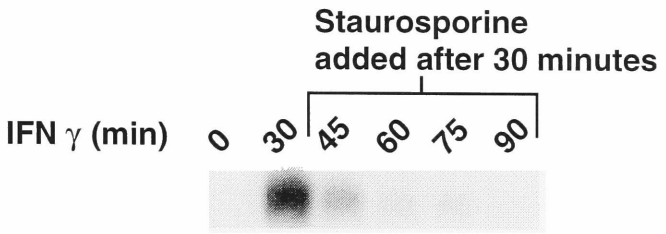

B. Nuclear

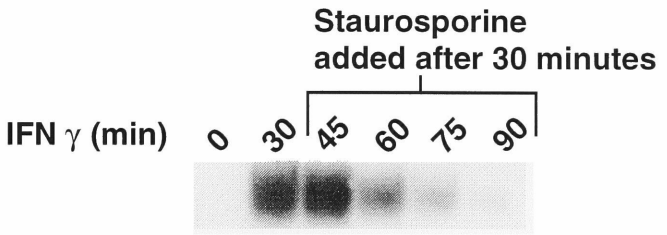

C.

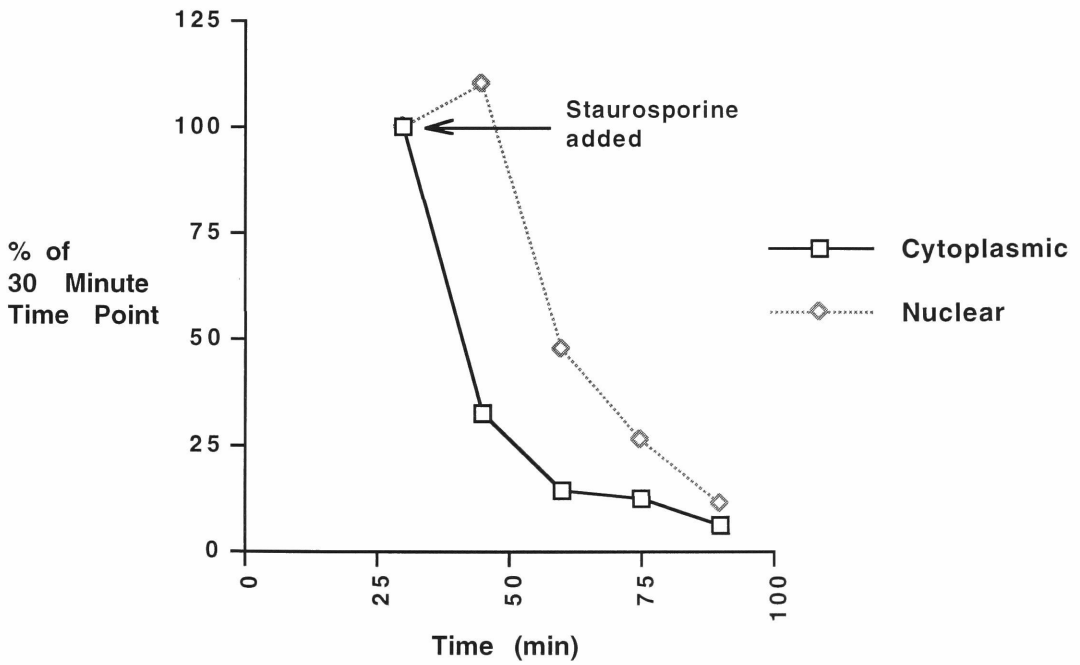

Figure 4.10 The Effect of Vanadate on Stat1 DNA Binding in Cytoplasmic and Nuclear Extracts

(A,B) EMSA analysis with an M67 probe. Cytoplasmic (A) and nuclear (B) extracts were prepared from Bud-8 normal human fibroblasts treated with IFN–γ plus vanadate for the indicated times. (C) Plot of the PhosphorImager analysis of Stat1 DNA binding complexes at various times after IFN–γ plus vanadate treatment.

A. Cytoplasmic

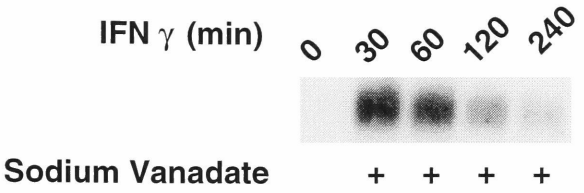

B. Nuclear

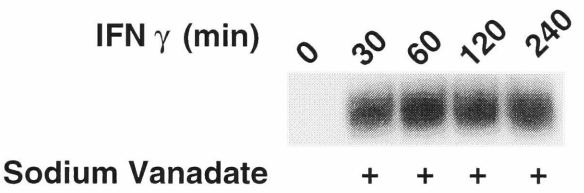

C.

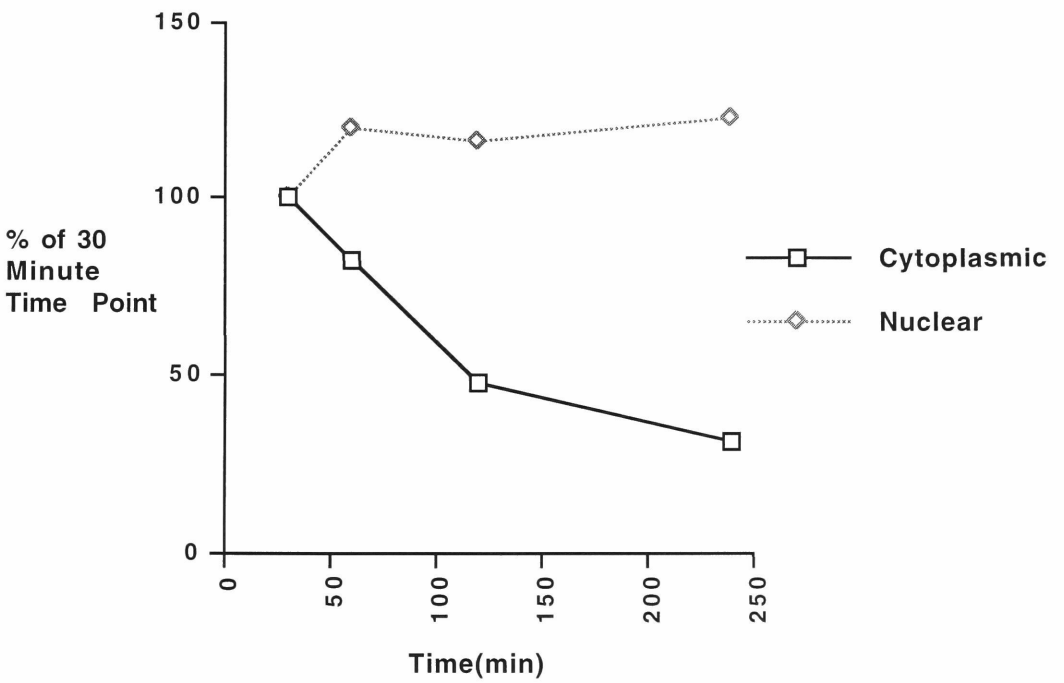

Figure 4.11 The Effect of Vanadate on the Stat1 Activation-Inactivation Cycle Analyzed by ^{35}S Labeling

(A) ^{35}S labeling followed by immunoprecipitation with an anti-Stat1 monoclonal antibody. Bud-8 fibroblasts were labeled with ^{35}S for 2.5 hr as described in Experimental Procedures. Label was removed, cells washed in normal medium and IFN-γ or IFN-γ plus vanadate was added. At the indicated time points, cytoplasmic and nuclear extracts were prepared. The cytoplasmic extracts were then subjected to SDS-PAGE and autoradiography.

(B) Same as (A) except SDS-PAGE and autoradiography of nuclear extracts.

(C) Plot of the PhosphorImager analysis of the Stat1 bands (both phosphorylated and unphosphorylated) in cytoplasmic extracts averaged from two separate experiments. Data is expressed as percent of baseline (the value in the no treatment lane of the cytoplasmic extracts). Error bars represent the standard error of the mean.

(D) Plot of the PhosphorImager analysis of the Stat1 bands (both phosphorylated and unphosphorylated) in nuclear extracts averaged from two separate experiments. Data is expressed as percent of baseline (the value in the no treatment lane of the cytoplasmic extracts). Error bars represent the standard error of the mean.

A. Cytoplasmic

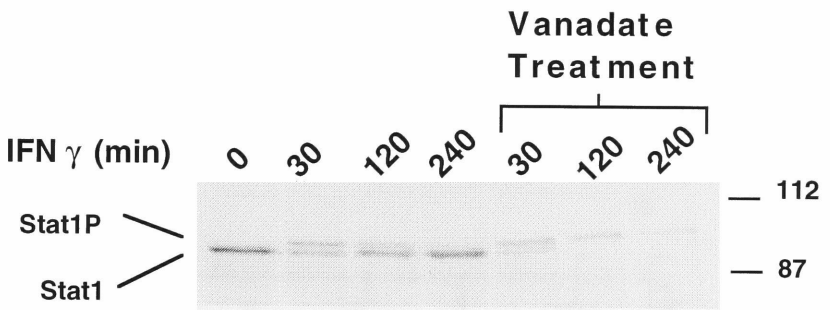

B. Nuclear

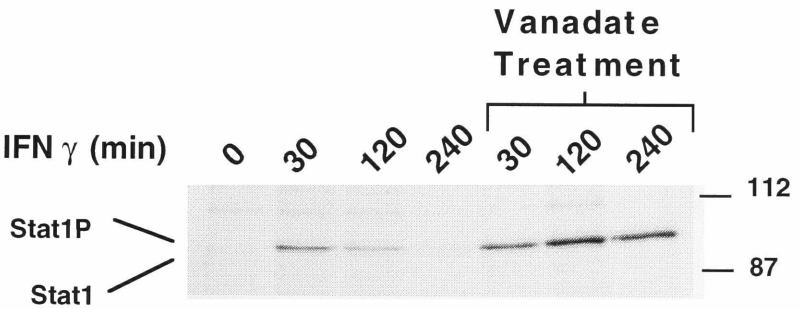

C. Cytoplasmic

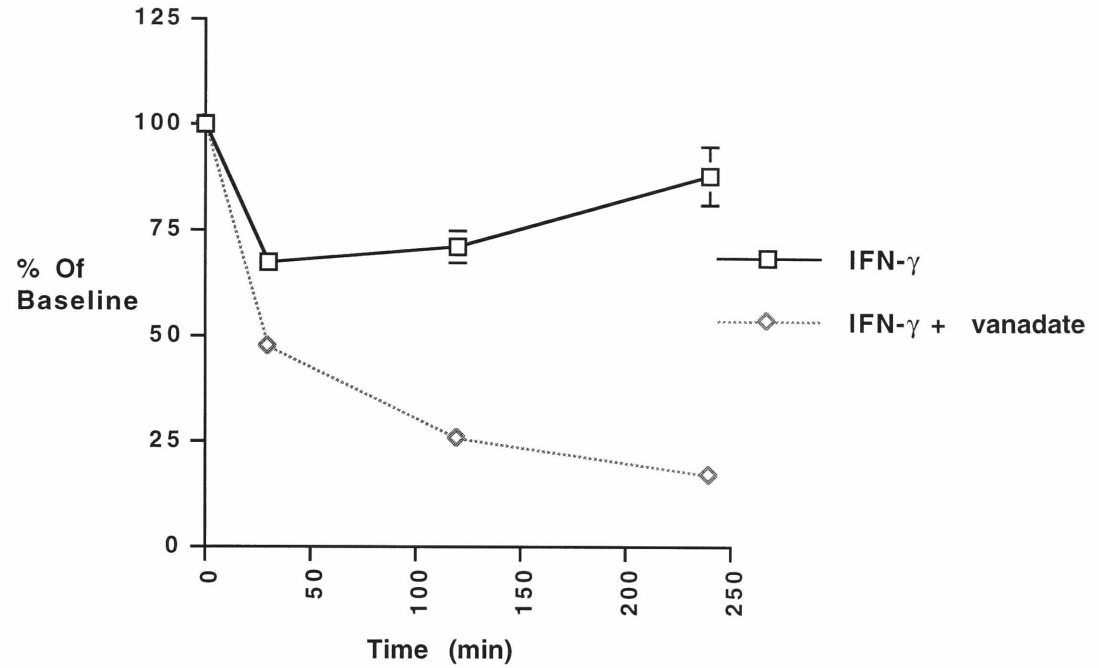

D. Nuclear

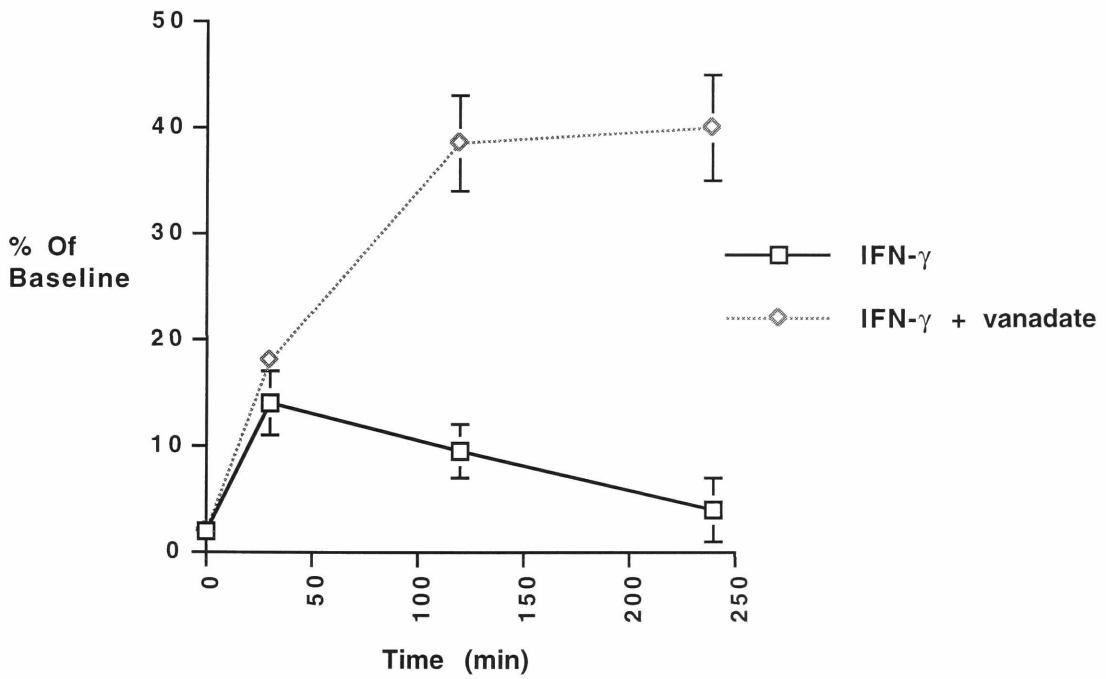

Chapter 5: Perspectives and Future Directions

The experiments in the previous three chapters demonstrate and characterize the Stat1 activation-inactivation cycle. Stat1 is phosphorylated in the cytoplasm, translocated to the nucleus and following dephosphorylation exported back to the cytoplasm. This chapter focuses on the implications of these results, proposes a model for IFN-γ receptor-JAK-STAT pathway inactivation and suggests future directions for experimentation.

5.1 What controls the duration of cytokine signaling?

The downregulation of cytokine-induced STAT activation is dependent on two factors. First, the receptor-JAK complex must be inactivated, and second, the STAT proteins must be inactivated. In order to determine the relative contributions of these two events to the duration of the IFN–γ and IL-2 induced signal transduction, we stimulated cells with cytokine to build up a pool of phosphorylated STAT in the nucleus. We then added the kinase inhibitor staurosporine to eliminate continued signaling from the receptor. This experimental design effectively creates a pulse of activated STAT protein that can then be followed throughout its life cycle. The half-lives of activated Stat1 and Stat5 were found to be approximately 15 and 10 minutes respectively.

In the continuous presence of IFN–γ or IL-2, a typical time course of STAT activation extended to at least 4 hours. Clearly, given

the short half-lives of activated Stat1 and Stat5, the cessation of signaling from the receptor, and not the rate of STAT inactivation, determines the length of IFN–γ and IL-2 induced STAT signaling. Lee et al. have obtained similar results with IFN–α (129). They determined through staurosporine addition that the half-life of ISGF-3 was 2 hours. In one cell line, however, ISGF-3 DNA binding activity was still present 24 hours after IFN–α addition. This prolonged signaling was shown to be a result of continued receptor activation through endogenous IFN–α production.

While it is difficult to completely determine whether staurosporine leads to non-physiological inactivation of Stat1, the results from several lines of investigation make this an unlikely possibility. The DNA-binding activity of inactivation-defective Stat1 mutants was still prolonged compared to wild-type Stat1 in the presence of staurosporine. Staurosporine, therefore, does not appear to activate general phosphatases or proteases. In addition, metabolic labeling experiments demonstrated Stat1 is inactivated by a similar mechanism (to be discussed below) in the presence or absence of staurosporine.

5.2 How is the IFN-γ receptor-JAK complex inactivated?

The use of staurosporine also enabled us to distinguish whether a particular inhibitor was having an effect on the receptor-JAK complex or on the STAT molecules. Previous experiments demonstrated that cycloheximide prolonged IFN–γ induced

transcription (4). Our results with actinomycin D and cycloheximide showed that the prevention of IFN-γ induced protein synthesis led to prolonged Stat1 activation. This prolonged signaling was not maintained in the presence of staurosporine; therefore, sustained activation of the IFN–γ receptor-JAK complex most likely accounts for the prolonged Stat1 DNA binding activity and gene induction in the absence of protein and RNA synthesis.

Similar results have been obtained with Stat5 activation by growth hormone (143). This study showed that cycloheximide treatment prolonged growth hormone induced Stat5 DNA binding activity and prolonged the phosphorylation state of the JAKs associated with the growth hormone receptor. Endocytosis of the growth hormone and IFN-γ receptors is not inhibited by cycloheximide; therefore, other mechanisms besides blockade of receptor internalization must account for the observed delay in receptor-JAK inactivation in the absence of protein synthesis (153, 154). The genes for the recently described SOCS family of JAK and receptor inhibitors are rapidly induced upon cytokine treatment (99-102). Our results implicate factors such as these, and not simply endocytosis, in the cessation of cell surface signaling.

Ubiquitination has recently been implicated as an internalization signal for receptor-mediated endocytosis (reviewed in (84)). Whether or not the proteasome is also important for the downregulation of receptors has been a controversial issue. We and others have found that proteasome inhibitors prolonged the presence of phosphorylated Stat1 in the nucleus (106). This extended DNA-binding activity of Stat1 in the presence of proteasome inhibitor.

however, was abolished after blockade of receptor signaling by staurosporine. Proteasome inhibitor also maintained the tyrosine phosphorylation of the IFN-γ receptor. These results suggest the proteasome acts upstream of the STAT molecules and that the proteasome is required to stop receptor signaling.

Our experiments with IL-2 and Stat5 support this hypothesis. While proteasome inhibitor was able to prolong Stat5 DNA binding, it did not do so after staurosporine was added to prevent receptor-JAK signaling. More recent studies have confirmed our results and have shown that proteasome inhibitors maintain the tyrosine phosphorylation of the receptor associated JAKs after IL-2 or IL-3 treatment (127, 128). While these experiments did not determine how or on what molecules the proteasome acts, they clearly show that the proteasome is required for the inactivation of the JAKs and/or receptors.

It is, of course, possible that the proteasome simply degrades ubiquitinated receptors; however, proteasome inhibitors and the blockade of protein synthesis have such similar prolonging effects on signaling. It is possible that they act on the same pathway for receptor-JAK inactivation. A case in point is the protein CIS, a member of the SOCS family, that is mainly found in 37 and 32 kD forms (100). Upon ligand stimulation, the larger form gradually disappears and the smaller form becomes predominant. The 37 kD form has recently been found conjugated to ubiquitin (155). Perhaps the proteasome is required for the inhibitory effects of CIS and other SOCS proteins.

In our studies, SH2-containing protein tyrosine phosphatases were also shown to play a role in IFN–γ receptor inactivation. Previously, experiments with astrocytes from mice lacking SHP-1 (motheaten mice) demonstrated increases in IFN–γ signaling (98). We obtained similar results using macrophages from these mice. Addition of staurosporine to block receptor signaling demonstrated that the likely target of SHP-1 is not Stat1, but the receptor-JAK complex. How this phosphatase interacts with proteases and induced inhibitory proteins to downregulate receptor signaling remains to be determined.

One classic pathway of receptor inactivation involves endocytosis with the degradation of ligand in the lysosome followed by recycling of the receptor to the cell surface (reviewed in (82, 83)). IFN–γ and its receptor have been shown to follow this classic paradigm (reviewed in (72)). In fact, there is evidence that multiple rounds of receptor occupancy are necessary for full IFN-γ biological response induction (153). Mechanisms may be required to inactivate the intracellular portions of the receptors in order to limit continuous recycling and restimulation with extracellular IFN-γ. Dephosphorylation and/or proteolysis of the interior domains of the receptor and/or the induction of proteins to inhibit receptor function may all serve to inactivate receptors and lead to the downregulation of IFN–γ mediated signal transduction.

5.3 What controls STAT inactivation?

Previous studies have claimed to implicate both phosphatases and proteases in the inactivation of STAT proteins (106-108). Both tyrosine phosphatase and proteasome inhibitors can prolong the presence of phosphorylated Stat1 in the nucleus and Stat1 has been found conjugated to ubiquitin. None of these studies, however, determined whether these inhibitors caused a continued cell-surface signal or actually prevented the inactivation of phosphorylated Stat1. As noted above, proteasome inhibitors were not able to maintain Stat1 DNA binding activity in the presence of staurosporine, suggesting that the proteasome does not play a major role in Stat1 inactivation. In contrast, we determined the phosphatase inhibitor vanadate was able to prolong Stat1 DNA binding activity even in the presence of staurosporine, indicating that dephosphorylation is the major mechanism of Stat1 inactivation.

The previous studies using proteasome or phosphatase inhibitors also did not determine the amount of activated Stat1 that may be proteolytically degraded or dephosphorylated. We measured the stability of Stat1 by ^{35}S metabolic labeling of Bud-8 fibroblasts. Thirty minutes after IFN-γ treatment, phosphorylated Stat1 in both the cytoplasm and nucleus ranged between 30 and 45% of the total ^{35}S-labeled Stat1 in the cell. The 15 minute half-life of activated Stat1 and the 4 hour duration of the IFN-γ time course make it likely that even more of the total Stat1 becomes phosphorylated and enters the nucleus during the entire time course. Even so, between 80 and 90% of the Stat1 was typically recovered in the cytoplasm in a dephosphorylated state following 4 hours of IFN-γ treatment. While

a small amount of activated Stat1 may be ubiquitinated and proteolytically degraded, most activated Stat1 is dephosphorylated.

The short half-lives of Stat1, Stat3 and Stat5 as determined by us and others through kinase inhibitor treatment suggest a similar inactivation mechanism (113, 127, 128). Lee et al demonstrated through ^{35}S labeling that very little Stat1 and Stat2 were degraded during an IFN-α time course (129). These studies all converge on the conclusion that a phosphatase controls STAT inactivation.

5.4 What is the nature of the Stat1 phosphatase?

Our experiments in chapter 3 provide strong evidence that the nucleus is the major site of Stat1 dephosphorylation. The flow of activated Stat1 upon receptor-JAK complex inactivation was from cytoplasm to nucleus. In addition, blockade of phosphatase action through vanadate treatment led to an accumulation of phosphorylated Stat1 in the nucleus as it dropped to low levels in the cytoplasm. Our results with enucleated cells are consistent with this hypothesis. The experiments with cytoplasts demonstrated the rapid nature of Stat1 nuclear import and relatively slow nature of cytoplasmic inactivation. While the cytoplasm may play a small role, the nucleus appears to be the major site of Stat1 dephosphorylation.

The identity of the Stat1 phosphatase remains a mystery. SHP-1 has been found associated with Stat1 and Stat3 and initially appeared to be a good candidate for the Stat1 phosphatase (98, 110).

However, the half life of Stat1 DNA binding activity, as determined by staurosporine addition, was essentially the same in immortalized macrophages from motheaten mice and littermate controls demonstrating that SHP-1 is not crucial for Stat1 inactivation. It is possible that either the severe cellular abnormalities of motheaten mice or the method of immortalization might have led to non-physiological mechanisms of STAT inactivation ((97, 145)). Nevertheless, SHP-1 is primarily a cytoplasmic phosphatase and our results indicate that the Stat1 phosphatase is nuclear (156).

So far, the only criteria for a potential Stat1 phosphatase is that it must be nuclear and, as determined by our experiments with actinomycin D and cycloheximide, it does not require new protein or RNA synthesis to function. A number of nuclear protein tyrosine phosphatases (PTPs) have been identified but none have been shown to play a role in STAT inactivation (157, 158). Fewer than 100 PTPs have been characterized. Genome sequencing, however, predicts the existence of approximately 500 human PTPs, raising the possibility that the Stat1 phosphatase has not yet been isolated (92).

Many phosphatases lack substrate specificity *in vitro*, making purification of a phosphatase based on its substrate a difficult endeavor (159, 160). In many cases, relevant substrates have been identified *in vivo* by making mutations in the catalytic site of an already isolated phosphatase. These mutations prevent dissociation of the substrate-phosphatase complex and immunoprecipitation of the mutant phosphatase allows determination of its relevant substrates ((160), reviewed in (92)). As more PTPs are isolated, this method of "substrate trapping" may identify the Stat1 phosphatase.

5.5 How is Stat1 exported from the nucleus?

The lack of unphosphorylated Stat1 in the nuclei of Bud-8 fibroblasts after a 4 hour IFN-γ time course and the entrapment of phosphorylated Stat1 in the nucleus upon vanadate treatment argue that dephosphorylation and nuclear export are tightly coupled. In a number of studies, nuclear export has been shown to be very rapid and only blockade of this export allows accumulation of certain proteins in the nucleus (150-152). Perhaps the inability of phosphorylated Stat1 to be exported leads to the large amounts of phosphorylated Stat1 observed in the nucleus upon IFN-γ treatment and is responsible for efficient gene induction. In some cancer cells, unphosphorylated Stat1 is sometimes present in the nucleus and may still function as a transcriptional activator (161). In normal fibroblasts, rapid export may prevent unphosphorylated molecules from accumulating in the nucleus.

The nuclear export mechanism used by Stat1 remains a mystery. Many proteins use a nuclear export signal (NES) containing strings of hydrophobic amino acids (reviewed in (162)). NES binding to the protein exportin 1 (CRM1) allows for export; a process than can be blocked *in vivo* by the addition of leptomycin B ((163, 164), reviewed in (165)). Leptomycin B did not lead to accumulation of Stat1 in the nucleus in the presence of IFN-γ (data not shown). It is possible, therefore, that Stat1 may use a novel export mechanism.

5.6 What is the role of the N-terminus in Stat1 inactivation?

Our results confirm previous findings that deletions or mutations in the N-terminus of Stat1, but not deletions in the C-terminus, prevent normal inactivation (115, 116). What causes this effect remains uncertain. It is possible that the Stat1 phosphatase may interact with the N-terminus. The N-terminus might also bind to a factor that promotes separation of the Stat1 dimer, allowing better access to the phosphotyrosine.

One study recently postulated that the N-terminus allows nuclear import and that without this import Stat1 cannot be dephosphorylated (116). In this study, however, N-terminal Stat1 mutants only seemed to have a import defect using immunofluorescence. The authors noted that using traditional techniques of cell fractionation Stat1 mutants were still detectable in the nucleus. Indeed, in our experiments, N-terminal mutants are clearly transported into the nucleus.

Recent work with MPF, MAPK kinase and MAPKAP kinase 2 illustrate that a protein may be entering the nucleus but cannot be detected by immunofluorescence if export is more rapid than import (150-152). It is possible, therefore, that the N-terminus plays a role in Stat1 nuclear export. The N-terminus of a phosphorylated Stat1 molecule may normally block a nuclear export signal and dephosphorylation may alter the structure of the Stat1 so this signal is then revealed. Taking this hypothesis a step further, perhaps

mutations in the N-terminus uncouple the normally tight association between Stat1 dephosphorylation and export; Stat1 N-terminal mutants may be able to be exported without first being dephosphorylated. While cytoplast experiments indicate some inactivation in the cytoplasm, accumulation in the nucleus might be required for efficient dephosphorylation of Stat1.

5.7 A model and future directions

From our results a model of the Stat1 activation-inactivation cycle emerges (Figure 5.1). The proteasome, SHP-1, and inducible inhibitors all play a role in IFN-γ receptor-JAK complex downregulation. It is possible that the proteasome and the induced proteins lie in the same pathway of receptor-JAK inactivation. The inactivation of Stat1 is primarily controlled by a nuclear tyrosine phosphatase and Stat1 molecules can normally only exit the nucleus once dephosphorylated.

In the future, the fine details of receptor-JAK-STAT inactivation need to be explored. How do the proteasome and SOCS family members inactivate the JAK-receptor complex? What are the binding sites for SHP-1 on the IFN–γ receptor-JAK complex and what is the effect of removal of these sites on STAT activation? What are the signals for Stat1 nuclear import and export and how is the N-terminus involved in these processes and dephosphorylation? Whereas the C-terminus plays a role in the inactivation of Stat3 and

Stat5, why is this not the case for Stat1? And lastly, what is the identity of the Stat1 phosphatase?

There is growing evidence that aberrant activation of the JAK-STAT pathway leads to abnormal development and cellular transformation (53, 119). Further studies of inactivation mechanisms will allow a better understanding of these disease processes.

Figure 5.1 The Stat1 Activation-Inactivation Cycle

The Stat1 Activation-Inactivation Cycle

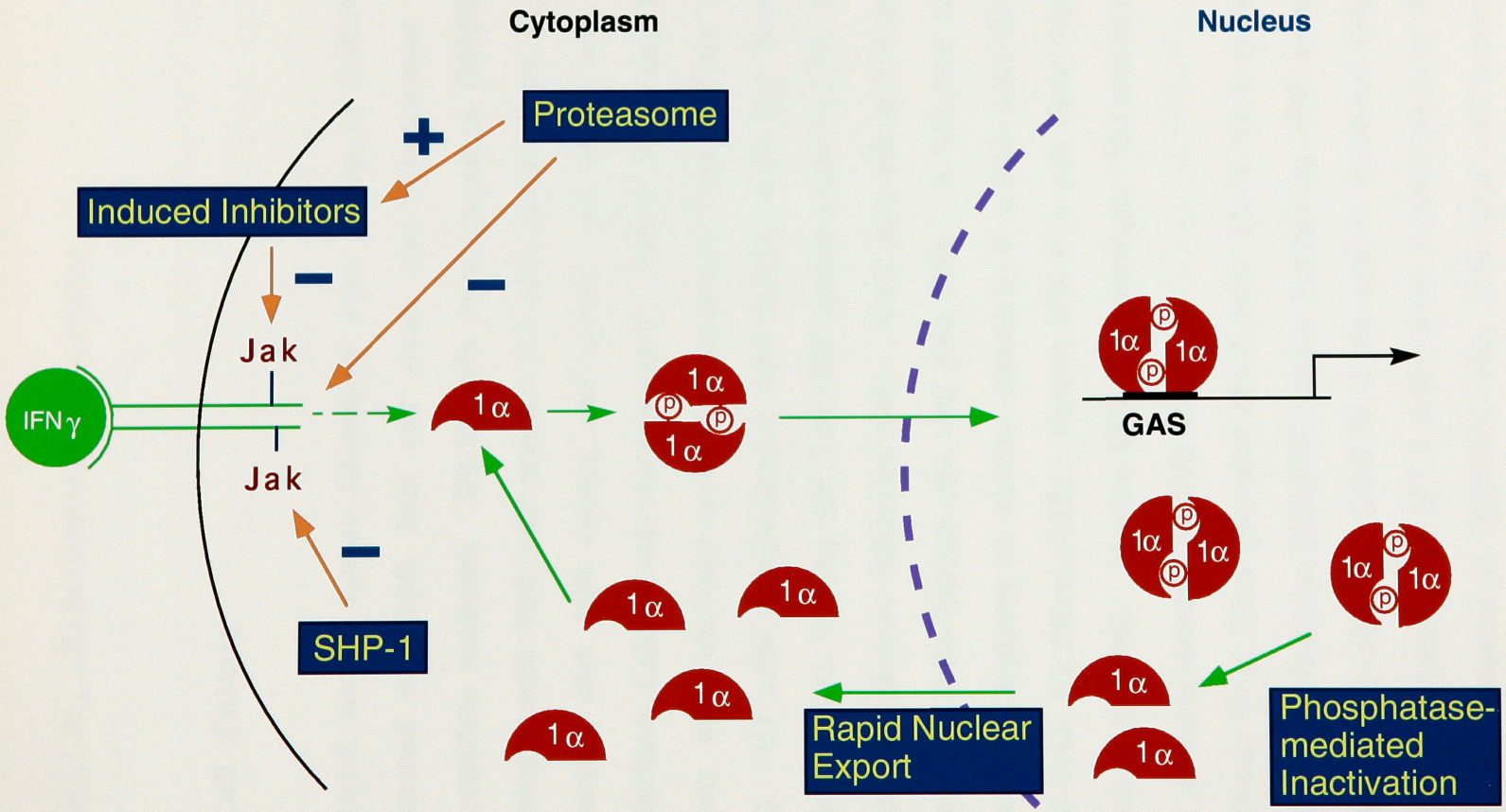

Appendix A Experimental Procedures

A.1 Cell Culture

Bud-8 normal human fibroblasts were grown in DMEM supplemented with 10% fetal calf serum and non-essential amino acids (complete medium). WI-38 cells were grown in DMEM supplemented with 10% calf serum. U3 cells were grown in DMEM supplemented with 10% cosmic calf serum. All serum was obtained from Hyclone Laboratories Incorporated. WI-38 cells and Bud-8 fibroblasts were obtained from the American Type Culture Collection (ATCC). U3 cells complemented with murine wild-type Stat1 (p91) and murine Stat1 lacking the first 154 amino acids (Δ154) were obtained from Robert Schreiber (49). Curt Horvath provided U3 lines complemented with human p91 and p84 (39). A U3 line containing Stat1 with an arginine to alanine mutation at amino acid 31 was obtained from Ke Shuai (115). Human IFN-γ (a gift from AMGEN) was used at 5 ng/ml. Murine IFN-γ (Boehringer Mannheim) was used at a concentration of 100 U/ml.

Young Won Choi provided HT-2 cells which were grown as previously described in MEM/TC media containing 10% fetal calf serum (Intergen) plus 2.5 U/ml IL-2 (R and D Systems) (166). Before an experiment, the HT-2 cells were washed once in MEM/TC and then resuspended in MEM/TC plus 10% fetal calf serum but without IL-2. Cells were then added to 24 well dishes at 1 to 2

million cells per well and incubated for 4 hours before addition of IL-2 at 25 U/ml.

Immortalized macrophages from motheaten mice and littermates were the kind gift of Katherine Siminovitch, Daniel Radzioch and Martin Olivier. They were immortalized through infection with a retrovirus (J2) containing v-Myc and v-Raf oncogenes as described previously (145).

A.2 Preparation of Cytoplasts

Cytoplasts were essentially prepared as described previously (146-149). Bud-8 fibroblasts were resuspended at 2 million cells/ml in complete medium containing 10 µg/ml cytochalasin B and placed in the incubator (37°C with 5% carbon dioxide) for 30 minutes. A quarter of the cell suspension was then removed into a 5 cm tissue culture dish and placed in the incubator (control cells). The rest of the cell suspension was layered upon a ficoll gradient prepared the previous evening. The gradient consisted of 25%, 17%, 16%, 15% and 12.5% ficoll dissolved in complete media containing 10 µg/ml cytochalasin B. The gradient was then equilibrated overnight in the incubator. After layering the cells, the gradients were spun at 31°C for 60 minutes at 25,000 RPM in an SW-41 rotor.

The cytoplasts were removed from the 15-17% Ficoll interfaces. Both control cells and cytoplasts were washed twice in complete medium and plated in 6 well plates at 1 to 2.5 million cells per well. Cells were treated as indicated and cytoplasmic extracts were made

as described below. For each experiment, 200,000 control cells and 200,000 cytoplasts were placed in separate wells of a LAB-TEK tissue culture slide (Nalge Nunc International), allowed to adhere, fixed in formaldehyde and stained with Hoescht dye.

A.3 Antibodies, Inhibitors and Oligonucleotides

Anti-Stat1 and Stat5 C-terminal sera and anti-Stat1 SH2 region serum were raised in rabbits as previously described (31, 167). Anti-IFN-γ receptor α chain monoclonal antibody (GIR-94) was the kind gift of Robert Schreiber. Anti-phosphotyrosine antibody (4G10) and a monoclonal antibody to the C-terminus of Stat1 were purchased from Upstate Biotechnology and Santa Cruz Biotechnology respectively. Anti-phosphorylated Stat1 serum (recognizing Stat1 phosphorylated on tyrosine 701) was purchased from New England Biolabs. Anti-SHP-1 polyclonal antiserum was the kind gift of Katherine Siminovitch.

Staurosporine (Sigma) was dissolved in DMSO and used at a final concentration of 500 nM. MG132 and lactacystin (the kind gifts of Alfred Goldberg and Julian Adams, MyoGenics) were dissolved in DMSO and used at final concentrations of 20 μM and 10 μM respectively. Actinomycin D and cycloheximide were dissolved in water and used at final concentrations of 2.5 μg/ml and 30 μg/ml respectively. Cytochalasin B was dissolved in DMSO at a concentration of 2 mg/ml.

Oligonucleotides for electrophoretic mobility shift assay (EMSA) probes (122, 168, 169):

β-casein	upper strand	5'-GATCAGATTTCTAGGAATTCAAATC-3'
	bottom strand	5'-GATCGATTTGAATTCCTAGAAATCT-3'
M67	upper strand	5'-GTCGACATTTCCCGTAAATC-3'
	bottom strand	5'-TCGAGATTTACGGGAAATG-3'

A.4 Cell Extracts, Immunoprecipitations and SDS-PAGE

When preparing cytoplasmic and nuclear extracts, cells were first lysed at 4°C by gently pipetting after 5 min in hypotonic buffer (20 mM Hepes, pH7.9, 10 mM KCl, 0.1 mM Na_3VO_4, 1 mM EDTA, 10% Glycerol, .5 mM PMSF, 1 μg/ml Aprotinin, 1 μg/ml Pepstatin, 1 μg/ml Leupeptin and 1 mM DTT) with 0.2% NP40. After centrifugation at 4°C (13k rpm in microfuge) for 10 seconds, supernatants were collected as cytoplasmic extracts. Nuclear extracts were prepared by resuspension of the crude nuclei in high-salt buffer (hypotonic buffer with 20% Glycerol and 420 mM NaCl) at 4°C for 30 min and the supernatants were collected after centrifugation at 4°C (13k rpm) for 5 min. Whole cell extracts were prepared by lysing cells in whole cell extract buffer (50 mM Tris, 280 mM NaCl, .5% NP-40, .2 mM EDTA, 2 mM EGTA, 10% glycerol, .5 mM PMSF, 1 μg/ml Aprotinin, 1 μg/ml Pepstatin, 1 μg/ml Leupeptin and 1 mM DTT and .1 mM Na_3VO_4) for 10 min at 4°C. Supernatants were collected after centrifugation at 4°C (13k rpm) for 10 min.

Immunoprecipitations were carried out by adding the precipitating antibody (5 μg of GIR-94, 3 μl of anti-Stat1 C-terminal antiserum or 3 μg of anti Stat1 C-terminal monoclonal antibody) to each extract and incubating for 1-2 hr at 4°C followed by incubation at 4°C with protein g-sepharose for 2 hr (in the case of GIR-94 or anti-Stat1 monoclonal antibody) or protein a-sepharose overnight (in the case of anti-Stat1 antiserum). Samples were then washed 3 times with whole cell extract buffer and then 2 times with PBS followed by resuspension in 2X Laemmli running buffer. Samples were then heated at 80°C for 4 min and subjected to SDS-PAGE on a 7% gel for the IFN-γ receptor α chain or a 6% gel for Stat1. For Western blots of Stat1, equal μg amounts of each extract were mixed with 2X Laemmli running buffer and heated to 80°C for 4 min and subjected to SDS-PAGE on a 6% gel.

A.5 Western Blotting

Following SDS-PAGE, proteins were transferred to nitrocellulose and blocked for 2 hr at room temperature with 5% BSA in TBST (TBS plus .05% Tween) if blotting with anti-phosphotyrosine antibody (4G10) or blocked with 5% milk in TBST if blotting with anti-Stat1 serum or anti-SHP-1 serum. 4G10 antibody was added at 1:4000 for overnight incubation at 4°C while anti-Stat1 C-terminal serum was added at 1:2500, anti-Stat1 SH2 region serum and anti-phosphorylated Stat1 serum were added at 1:2000, and anti-SHP-1 was added at 1:1000 for 2 hr at room temperature.

Membranes were then washed with TBST and incubated with a 1:4000 dilution of horseradish peroxidase conjugated goat anti-mouse (for 4G10) or goat anti-rabbit (for anti-Stat1, anti-phosphorylated Stat1 and anti-SHP-1) for 45 min, washed with TBST and subsequently developed using Renaissance chemiluminescence reagent (NEN-Dupont). Where indicated, membranes were stripped with a solution containing 2% SDS, 62.5 mM Tris pH 6.8 and .7% β-mercaptoethanol for 30 min at 50°C, washed extensively with TBST and blocked with 5% milk in TBST overnight at 4°C. Membranes were then reprobed with GIR-94 antibody (1 μg/ml) for 1 hr at room temperature, washed with TBST and then incubated with a 1:4000 dilution of horseradish peroxidase conjugated goat anti-mouse and subsequently developed using Renaissance chemiluminescence reagent.

A.6 Electrophoretic Mobility Shift Assay

EMSA was carried out on .25 X TBE, 4%, 29:1 acrylamide-bisacrylamide gels. The gels were prerun at 400 V in the cold room (4°C) until the voltage dropped to 10 mA (approximately 45 minutes). Labeled DNA probes were prepared through Klenow-catalyzed filling in of overhangs with ^{32}P labeled deoxyribonucleotides. For the DNA-binding reaction, 1 ng of probe, 2 μg of poly(dIdC) (Pharmacia) and equal μg amounts of each extract were incubated at room temperature for 15 minutes in a buffer containing 40 mM KCL, 20 mM Hepes (pH7.9), 1 mM $MgCl_2$, .5 mM

DTT, 4% Ficoll and 0.1 mM EDTA. For supershift experiments, 1 µl of 10 fold diluted antiserum in PBS was added to each binding reaction for 5 minutes at 4°C before addition of probe. The binding reactions were loaded onto the prerun gel and electrophoresis was continued for 2.5 more hours at 400 V in the cold room. Gels were then dried and exposed to film (122, 168-170)

A.7 Pulse-Chase Experiments

Bud-8 fibroblasts were cultured in methionine-free DMEM containing 1% fetal bovine serum and non-essential amino acids. 100 µCI/ml of ^{35}S-labeled methionine was added to each 10 cM plate for 2.5 hr. Label was then removed and fresh medium was added. At the indicated times, nuclear and cytoplasmic extracts were prepared and immunoprecipitation and SDS-PAGE was carried out as described above. Gels were then soaked in fixative (25% isopropanol, 10% acetic acid) for 35 min followed by soaking in Amplify (Amersham, Inc.) for 45 min. Gels were dried at 80°C for 1 hr and then exposed to film.

A.8 Quantitation using the PhosphorImager

The intensities of radioactive bands in dried gels were quantitated using a PhosphorImager (Molecular Dynamics, Inc.). For ^{35}S-labeling experiments, the band of interest in each lane was boxed and quantitated and an identical area above each band of interest

was boxed as background and subtracted. Data was expressed as a percent of the baseline (the value in the no treatment lane of the cytoplasmic extracts). For EMSAs, the value in the no treatment lane was subtracted from all the other values and data was expressed as a percent of the value indicated.

Appendix B References

1. Larner AC, Jonak G, Cheng Y-S, Korant B, Knight E Jr., Darnell JE Jr. Transcriptional induction of two genes in human cells by β interferon. Proc. Natl. Acad. Sci. USA 1984;81:6733-6737.

2. Larner AC, Chaudhuri A, Darnell JE Jr. Transcriptional induction by interferon. J. Biol. Chem. 1986;261:453-459.

3. Greenberg ME, Ziff EB. Stimulation of 3T3 cells induces transcription of the c-fos proto-oncogenes. Nature 1984;311:433-438.

4. Decker T, Lew DJ, Cheng Y-S, Levy DE, Darnell JE Jr. Interactions of alpha- and gamma-interferon in the transcriptional regulation of the gene encoding a guanylate-binding protein. EMBO J 1989;8:2009-2014.

5. Lodish HF, Darnell JE. Molecular cell biology. (3rd ed.) New York: Scientific American Books : Distributed by W.H. Freeman and Co., 1995:1 v. (various pagings).

6. Darnell JE Jr. Reflections on STAT3, STAT5, and STAT6 as fat STATs. Proc Natl Acad Sci U S A 1996;93(13):6221-4.

7. Ihle JN. Janus kinases in cytokine signalling. Philos Trans R Soc Lond B Biol Sci 1996;351(1336):159-66.

8. Darnell JE Jr., Kerr IM, Stark GM. Jak-STAT pathways and transcriptional activation in response to IFNs and other extracellular signaling proteins. Science 1994;264:1415-1421.

9. Darnell JE Jr. STATs and gene regulation. Science 1997;277:1630-1635.

10. Darnell JE Jr. Studies of IFN-induced transcriptional activation uncover the Jak-Stat pathway. J Interferon Cytokine Res 1998;18(8):549-54.

11. Horvath CM, Darnell JE. The state of the STATs: recent developments in the study of signal transduction to the nucleus. Curr Opin Cell Biol 1997;9(2):233-9.

12. Leonard WJ, O'Shea JJ. Jaks and STATs: biological implications. Annu Rev Immunol 1998;16:293-322.

13. Pellegrini S, Dusanter-Fourt I. The structure, regulation and function of the Janus kinases (JAKs) and the signal transducers and activators of transcription (STATs). Eur J Biochem 1997;248(3):615-33.

14. Levy D, Darnell JE Jr. Interferon-dependent transcriptional activation: Signal transduction without second messenger involvement? New Biologist 1990;2:923-928.

15. Schindler C, Darnell JE Jr. Transcriptional responses to polypeptide ligands: The JAK-STAT pathway. Annu. Rev. Biochem. 1995;64:621-51.

16. Baron S. Interferon : principles and medical applications. (1st ed.) Galveston, TX: University of Texas Medical Branch at Galveston Dept. of Microbiology, 1992:xi, 624.

17. Stark GR, Kerr IM, Williams BR, Silverman RH, Schreiber RD. How cells respond to interferons. Annu Rev Biochem 1998;67:227-64.

18. Friedman RL, Manly SP, McMahon M, Kerr IM, Stark GR. Transcriptional and post-transcriptional regulation of interferon-induced gene expression in human cells. Cell 1984;38:745-755.

19. Reich N, Evans B, Levy DE, Fahey D, Knight E Jr., Darnell JE Jr. Interferon-induced transcription of a gene encoding a 15 kDa protein depends on an upstream enhancer element. Proc. Natl. Acad. Sci. USA 1987;84:6394-6398.

20. Levy DE, Kessler DS, Pine R, Reich N, Darnell JE Jr. Interferon-induced nuclear factors that bind a shared promoter element correlate with positive and negative control. Genes & Devel. 1988;2:383-393.

21. Lew D, Decker T, Strehlow I, Darnell JE Jr. Overlapping elements in the GBP gene promoter mediate transcriptional induction by alpha and gamma interferon. Mol. Cell. Biol. 1991;11:182-191.

22. Decker T, Lew DJ, Mirkovitch J, Darnell JE Jr. Cytoplasmic activation of GAF, an IFN-γ regulated DNA binding factor. EMBO J 1991;10:927-932.

23. Dale C, Iman AMA, Kerr IM, Stark GR. Rapid activation by interferon α of a latent DNA-binding protein present in the cytoplasm of untreated cells. Proc. Natl. Acad. Sci. USA 1989;86:1203-1207.

24. Levy DE, Kessler DS, Pine RI, Darnell JE Jr. Cytoplasmic activation of ISGF3, the positive regulator of interferon-α stimulated transcription, reconstituted in vitro. Genes & Devel. 1989;3:1362-1372.

25. Schindler C, Fu X-Y, Improta T, Aebersold R, Darnell JE Jr. Proteins of transcription factor ISGF-3: One gene encodes the 91 and 84 kDA ISGF-3 proteins that are activated by inteferon-α. Proc. Natl. Acad. Sci. USA 1992;89:7836-7839.

26. Fu X-Y, Kessler DS, Veals SA, Levy DE, Darnell JE Jr. ISGF3, the transcriptional activator induced by interferon α, consists of multiple interacting polypeptide chains. Proc. Natl. Acad. Sci. USA 1990;87:8555-8559.

27. Fu X-Y, Schindler C, Improta T, Aebersold R, Darnell JE Jr. The proteins of ISGF-3: the interferon α-induced transcriptional activator, define a gene family involved in signal transduction. Proc. Natl. Acad. Sci. USA 1992;89:7840-7843.

28. Veals SA, Schindler C, Leonard D, Fu X-Y, Aebersold R, Darnell JE Jr., Levy DE. Subunit of an alpha-interferon-responsive transcription factor is related to interferon regulatory factor and Myb families of DNA-binding protein. Mol. Cell. Biol. 1992;12:3315-3324.

29. Bluyssen AR, Durbin JE, Levy DE. ISGF3 gamma p48, a specificity switch for interferon activated transcription factors. Cytokine Growth Factor Rev 1996;7(1):11-7.

30. Schindler C, Shuai K, Prezioso VR, Darnell JE Jr. Interferon-dependent tyrosine phosphorylation of a latent cytoplasmic transcription factor. Science 1992;257:809-815.

31. Shuai K, Schindler C, Prezioso VR, Darnell JE Jr. Activation of transcription by IFN-γ: tyrosine phosphorylation of a 91 kD DNA binding protein. Science 1992;259:1808-1812.

32. Mui AL-F, Wakao H, O'Farrell AM, Harada N, Miyajima A. Interleukin-3, granulocyte-macrophage colony stimulating factor and interleukin-5 transduce signals through two STAT5 homologs. EMBO J. 1995;14:1166-1175.

33. Zhong Z, Wen Z, Darnell JE Jr. Stat3 and Stat4: Members of the family of signal transducers and activators of transcription. Proc. Natl. Acad. Sci. USA 1994;91:4806-4810.

34. Wakao H, Gouilleux F, Groner B. Mammary gland factor (MGF) is a novel member of the cytokine regulated transcription factor gene family and confers the prolactin response. EMBO J. 1994;13:2182-2191.

35. Hou J, Schindler U, Henzel WJ, Ho TC, Brasseur M, McKnight SL. An interleukin-4-induced transcription factor: IL-4 Stat. Science 1994;265:1701-1706.

36. Akira S, Nishio Y, Inoue M, Wang X-J, Wei S, Matsusaka T, Yoshida K, Sudo T, Naruto M, Kishimoto T. Molecular cloning of APRF, a novel IFN-stimulted gene factor 3 p91-related transcription factor involved in the gp130-mediated signaling pathway. Cell 1994;77:63-71.

37. Waksman G, Kominos D, Robertson SR, Pant N, Baltimore D, Birge RB, Cowburn D, Hanafuaa H, Mayer BJ, Overduin M, Resh MD, Rios CB, Silverman L, Kuriyan J. Crystal structure of the phosphotyrosine recognition domain SH2 of v-src complexed with tyrosine-phosphorylated peptides. Nature 1992;358:646-653.

38. Shuai K, Horvath CM, Tsai-Huang LH, Qureshi S, Cowburn D, Darnell JE Jr. Interferon activation of the transcription factor Stat91 involves dimerization through SH2-phosphotyrosyl peptide interactions. Cell 1994;76:821-828.

39. Horvath CM, Wen Z, Darnell JE Jr. A STAT protein domain that determines DNA sequence recognition suggests a novel DNA-binding domain. Genes & Devel. 1995;9:984-994.

40. Schindler U, Wu P, Rothe M, Brasseur M, McKnight SL. Components of a Stat recognition code: evidence for two layers of molecular selectivity. Immunity 1995;2(6):689-97.

41. Becker S, Groner B, Muller CW. Three-dimensional structure of the Stat3beta homodimer bound to DNA. Nature 1998;394(6689):145-51.

42. Chen X, Vinkemeier U, Zhao Y, Jeruzalmi D, Darnell JE Jr., Kuriyan J. Crystal structure of a tyrosine phosphorylated STAT-1 dimer bound to DNA. Cell 1998;93(5):827-39.

43. Fu X-Y. A transcription factor with SH2 and SH3 domains is directly activated by an interferon α-induced cytoplasmic protein tyrosine kinase(s). Cell 1992;70:323-335.

44. Kaplan MH, Sun YL, Hoey T, Grusby MJ. Impaired IL12 responses and enhanced development of Th2 cells in Stat4 deficient mice. Nature 1996;382:174-177.

45. Thierfelder WE, Deursen JV, Yamamoto K, Tripp RA, Sarawar SR, Carson RT, Sangster MY, Vignali DAA, Doherty P, Grosveld G, Ihle JN. Requirement for Stat4 in IL-12 mediated responses of natural killer and T-cells. Nature 1996;382:171-174.

46. Kaplan MH, Schindler U, Smiley ST, Grusby MJ. Stat6 is required for mediating responses to IL-4 and for the development of Th2 cells. Immunity 1996;4:313-319.

47. Shimoda K, Deursen Jv, Sangster MY, Sarawar SR, Carson RT, Tripp RA, Chu C, Quelle FW, Nosaka T, Vignali DAA, Doherty PC, Grosveld G, Paul WE, Ihle JN. Lack of IL-4-induced Th2 response and IgE class switching in mice with disrupted Stat6 gene. Nature 1996;380:630-633.

48. Takeda K, Tanaka T, Shi W, Matsumoto M, Minami M, Kashiwamura S, Nakanishi K, Yoshida N, Kishimoto T, Akira S. Essential role of Stat6 in IL-4 signalling. Nature 1996;380:627-630.

49. Meraz MA, White JM, Sheehan KCF, Bach EA, Rodig SJ, Dighe AS, Kaplan DH, Riley JK, Greenlund AC, Campbell D, Carver-Moore K, DuBois RN, Clark R, Aguet M, Schreiber RD. Targeted disruption of the

Stat1 gene in mice reveals unexpected physiologic specificity in the JAK-STAT signaling pathway. Cell 1996;84:431-442.

50. Durbin JE, Hackenmiller R, Simon MC, Levy DE. Targeted disruption of the mouse Stat1 gene results in compromised innate immunity to viral disease. Cell 1996;84:443-450.

51. Takeda K, Noguchi K, Shi W, Tanaka T, Matsumoto M, Yoshida N, Kishimoto T, Akira S. Targeted disruption of the mouse Stat3 gene leads to early embryonic lethality. Proc. Natl. Acad. Sci. USA 1997;94:3801-3804.

52. Takeda K, Kaisho T, Yoshida N, Takeda J, Kishimoto T, Akira S. Stat3 activation is responsible for IL-6-dependent T cell proliferation through preventing apoptosis: generation and characterization of T cell- specific Stat3-deficient mice. J Immunol 1998;161(9):4652-60.

53. Garcia R, Jove R. Activation of STAT transcription factors in oncogenic tyrosine kinase signaling. J Biomed Sci 1998;5(2):79-85.

54. Muller M, Laxton C, Briscoe J, Schindler C, Improta T, Darnell JE Jr., Stark GR, Kerr IM. Complementation of a mutant cell line: Central role of the 91-kDa polypeptide of ISGF3 in the interferon-α and -γ signal transduction pathway. EMBO J 1993;12:4221-4228.

55. Zhang JJ, Zhao Y, Chait BT, Lathem WW, Ritzi M, Knippers R, Darnell JE. Ser727-dependent recruitment of MCM5 by Stat1alpha in

IFN-gamma-induced transcriptional activation. EMBO J 1998;17(23):6963-6971.

56. Bhattacharya S, Eckner R, Grossman S, Oldread E, Arany Z, D'Andrea A, Livingston DM. Cooperation of Stat2 and p300/CBP in signalling induced by interferon-α. Nature 1996;383:344-347.

57. Zhang JJ, Vinkemeier U, Gu W, Chakravarti D, Horvath CM, Darnell JE Jr. Two contact regions between Stat1 and CBP/p300 in interferon γ signaling. Proc. Natl. Acad. Sci. USA 1996;93:15092-15096.

58. Vinkemeier U, Cohen SL, Moarefi I, Chait BT, Kuriyan J, Darnell JE Jr. DNA binding of in vitro activated Stat1α, Stat1β , and truncated Stat1: Interaction between NH2 terminal domains stabilizes binding of two dimers to tandem DNA sites. EMBO J. 1996;15:5616-5626.

59. Xu XA, Sun YL, Hoey T. Cooperative DNA binding and sequence selective recognition conferred by the Stat amino terminal domain. Science 1996;273:794-797.

60. Wen Z, Darnell JE Jr. Mapping of Stat3 serine phosphorylation to a single residue (727) and evidence that serine phosphorylation has no influence on DNA binding of Stat1 and Stat3. Nucl. Acids Res. 1997;25: 2062-2067.

61. Wen Z, Zhong Z, Darnell JE Jr. Maximal activation of transcription of Stat1 and Stat3 requires both tyrosine and serine phosphorylation. Cell 1995;82:241-250.

62. Chung CD, Liao J, Liu B, Rao X, Jay P, Berta P, Shuai K. Specific inhibition of Stat3 signal transduction by PIAS3. Science 1997;278:1803-1805.

63. Liu B, Liao J, Rao X, Kushner SA, Chung CD, Chang DD, Shuai K. Inhibition of Stat1-mediated gene activation by PIAS1. Proc Natl Acad Sci U S A 1998;95(18):10626-31.

64. Leung S, Qureshi SA, Kerr IM, Darnell JE Jr., Stark GR. Role of STAT2 in the interferon-α/β signaling pathway. Mol. Cell. Biol. 1995;15:1312-1317.

65. Velazquez L, Fellows M, Stark GR, Pellegrini S. A protein tyrosine kinase in the interferon α/β signalling pathway. Cell 1992;70:313-322.

66. Muller M, Briscoe J, Laxton C, Guschin D, Ziemiecki A, Silvennoinen O, Harpur AG, Barbieri G, Witthuhn BA, Schindler C, Pellegrini S, Wilks AF, Ihle JN, Stark GR, Kerr IM. The protein tyrosine kinase JAK1 complements defects in interferon-α/β and -γ signal transduction. Nature 1993;366:129-136.

67. Watling D, Gushin D, Müller M, Silvennoinen O, Witthuhn BA, Quelle FW, Rogers NC, Schindler C, Stark GR, Ihle JN, Kerr IM. Complementation by the protein tyrosine kinase Jak2 of a mutant cell line defective in the interferon-γ signal transduction pathway. Nature 1993;366:166-170.

68. Ihle JN, Kerr IM. Jaks and Stats in signaling by the cytokine receptor superfamily. Trends. Genet. 1995;11:69-74.

69. McKendry R, John J, Flavell D, Muller M, Kerr IM, Stark GR. High frequency mutagenesis of human cells and characterization of amutant unresponsive to both α and β interferons. Proc. Natl. Acad. Sci. USA 1991;88:11455-11459.

70. Pellegrini S, John J, Shearer M, Kerr IM, Stark GR. Use of a selectable marker regulated by alpha interferon to obtain mutations in the signaling pathway. Mol. Cell. Biol. 1989;9:4605-4612.

71. Leaman DW, Pisharody S, Flickinger TW, Commane MA, Schlessinger J, Kerr IM, Levy DE, Stark GR. Roles of JAKs in activation of STATs and stimulation of c-fos gene expression by epidermal growth factor. Mol. Cell. Biol. 1996;16:369-375.

72. Bach EA, Aguet M, Schreiber RD. The IFN gamma receptor: a paradigm for cytokine receptor signaling. Annu Rev Immunol 1997;15:563-91.

73. Briscoe J, Rogers NC, Witthuhn BA, Watling D, Harpur AG, Wilks AF, Stark GR, Ihle JN, Kerr IM. Kinase-negative mutants of JAK1 can sustain interferon-gamma-inducible gene expression but not an antiviral state. EMBO J 1996;15(4):799-809.

74. Greenlund AL, Farrar MA, Viviano BL, Schreiber RD. Ligand-induced IFN-γ receptor tyrosine phosphorylation couples the receptor to its signal transduction system (p91). EMBO J. 1994;13:1591-1600.

75. Shuai K, Stark GR, Kerr IM, Darnell JE Jr. A single phosphotyrosine residue of Stat91 required for gene activation by interferon-γ. Science 1993;261:1744-1746.

76. Greenlund AC, Morales MO, Viviano BL, Yan H, Krolewski J, Schreiber RD. Stat recruitment by tyrosine-phosphorylated cytokine receptors: an ordered reversible affinity-driven process. Immunity 1995;2(6):677-87.

77. Boulikas T. Nuclear localization signals (NLS). Crit Rev Eukaryot Gene Expr 1993;3(3):193-227.

78. Sekimoto T, Imamoto N, Nakajima K, Hirano T, Yoneda Y. Extracellular signal-dependent nuclear import of Stat1 is mediated by nuclear pore-targeting complex formation with NPI-1, but not Rch1. EMBO J 1997;16(23):7067-77.

79. Heim MH, Kerr IM, Stark GR, Darnell JE Jr. STAT SH2 groups contribute to specific interferon signalling by the Jak-STAT pathway. Science 1995;267:1347-1349.

80. Stahl N, Farruggella TJ, Boulton TG, Zhong Z, Darnell JE Jr., Yancopoulos GD. Choice of STATs and other substrates specified by modular tyrosine-based motifs in cytokine receptors. Science 1995;267:1349-1353.

81. Fujitani Y, Hibi M, Fukada T, Takahashi-Tezuka M, Yoshida H, Yamaguchi T, Sugiyama K, Yamanaka Y, Nakajima K, Hirano T. An alternative pathway for STAT activation that is mediated by the direct interaction between JAK an dSTAT. Oncogene 1997;14:751-.

82. Mukherjee S, Ghosh RN, Maxfield FR. Endocytosis. Physiol Rev 1997;77(3):759-803.

83. Schmid SL. Clathrin-coated vesicle formation and protein sorting: an integrated process. Annu Rev Biochem 1997;66:511-48.

84. Hicke L. Ubiquitin-dependent internalization and down-regulation of plasma membrane proteins. Faseb J 1997;11(14):1215-26.

85. Hershko A, Ciechanover A. The ubiquitin system. Annu Rev Biochem 1998;67:425-79.

86. Goldberg AL. Functions of the proteasome: the lysis at the end of the tunnel. Science 1995;268:522-523.

87. Mori S, Heldin C-H, Claesson-Welsh L. Ligand-induced polyubiquitination of the platelet-derived growth factor β-receptor. J. Biol. Chem. 1992;267:6429-6434.

88. Strous GJ, van Kerkhof P, Govers R, Ciechanover A, Schwartz AL. The ubiquitin conjugation system is required for ligand-induced endocytosis and degradation of the growth hormone receptor. EMBO J 1996;15(15):3806-12.

89. Mori S, Tanaka K, Omura S, Saito Y. Degradation process of ligand-stimulated platelet-derived growth factor β-receptor involves ubiquitin-proteasome proteolytic pathway. J. Biol. Chem. 1995;270:29447-29452.

90. Govers R, van Kerkhof P, Schwartz AL, Strous GJ. Linkage of the ubiquitin-conjugating system and the endocytic pathway in ligand-induced internalization of the growth hormone receptor. EMBO J 1997;16(16):4851-8.

91. Klingmuller U, Lorenz U, Cantley LC, Neel BG, Lodish H. Specific recruitment of SH-PTP-1 to the erythropoietin receptor causes inactivation of JAK2 and termination of proliferative signals. Cell 1995;80:729-738.

92. Neel BG, Tonks NK. Protein tyrosine phosphatases in signal transduction. Curr Opin Cell Biol 1997;9(2):193-204.

93. Tonks NK, Neel BG. From form to function: signaling by protein tyrosine phosphatases [see comments]. Cell 1996;87(3):365-8.

94. David M, Chen HE, Goelz S, Larner AC, Neel BG. Differential regulation of the alpha/beta interferon-stimulated Jak/Stat pathway by the SH2 domain-containing tyrosine phosphatase SHPTP1. Mol Cell Biol 1995;15(12):7050-8.

95. Tsui HW, Siminovitch KA, DeSouza L, Tsui FWL. Motheaten and viable motheaten mice have mutations in the hematopoietic cell phosphatase gene. Nature Genet. 1993;4:124-129.

96. Shultz LD, Schweitzer PA, Rajan TV, Yi T, Ihle JN, Matthews RJ, Thomas ML, Beier DR. Mutations at the murine motheaten locus are within the hematopoietic cell protein-tyrosine phosphatase (Hcph) gene. Cell 1993;73:1445-1454.

97. Shultz LD, Rajan TV, Greiner DL. Severe defects in immunity and hematopoiesis caused by SHP-1 protein- tyrosine-phosphatase deficiency. Trends Biotechnol 1997;15(8):302-7.

98. Massa PT, Wu C. The role of protein tyrosine phosphatase SHP-1 in the regulation of IFN- gamma signaling in neural cells. J Immunol 1996;157(11):5139-44.

99. Starr R, Willson TA, Viney EM, Murray LJL, Rayner JR, Jenkins BJ, Gonda TJ, Alexander WS, Metcalf D, Nicola NA, Hilton DJ. A family of cytokine-inducible inhibitors of signalling. Nature 1997;387:917-921.

100. Yoshimura A, Ohkubo T, Kiguchi T, Jenkins NA, Gilbert DJ, Copeland NG, Hara T, Miyajima A. A novel cytokine-inducible gene CIS encodes an SH2-containing protein that binds to tyrosine-phosphorylated interleukin 3 and erythropoietin receptors. EMBO J 1995;14(12):2816-26.

101. Naka T, Narazaki M, Hirata M, Matsumoto T, Minamoto S, Aono A, Nishimoto N, Kajita T, Taga T, Yoshizaki K, Akira S, Kishimoto T. Structure and function of a new STAT-induced STAT inhibitor. Nature 1997;387:924-929.

102. Endo TA, Masuhara M, Yokouchi M, Suzuki R, Sakamoto H, Mitsui K, Matsumoto A, Tanimura S, Ohtsubo M, Misawa H, Miyazaki T, Leonor N, Taniguichi T, Fujita T, Kanakura Y, Komiya S, Yoshimura A. A new protein containing an SH2 domain that inhibits JAK kinases. Nature 1997;387:921-924.

103. Scheffner M, Huibregtse JM, Vierstra RD, Howley PM. The HPV-16 E6 and E6-AP complex functions as a ubiquitin-protein ligase in the ubiquitination of p53. Cell 1993;75(3):495-505.

104. Trier M, Staszewski LM, Bohmann D. Ubiquitin-dependent c-Jun degradation in vivo is mediated by the δ domain. Cell 1994;78:787-798.

105. Stancovski I, Gonen H, Orian A, Schwartz AL, Ciechanover A. Degradation of the proto-oncogene product c-Fos by the ubiquitin proteolytic system in vivo and in vitro: identification and characterization of the conjugating enzymes. Mol. Cell. Biol. 1995;15:7106-7116.

106. Kim TK, Maniatis T. Regulation of interferon γ activated STAT1 by the ubiquitin proteasome pathway. Science 1996;273:1717-1719.

107. David M, Grimley PM, Finbloom DS, Larner AC. A nuclear tyrosine phosphatase downregulates interferon-induced gene expression. Mol. Cell. Biol. 1993;13:7515-7521.

108. Haque SJ, Flati V, Deb A, Williams BR. Roles of protein-tyrosine phosphatases in Stat1 alpha-mediated cell signaling. J Biol Chem 1995;270(43):25709-14.

109. Lamb P, Haslam J, Kessler L, Seidel HM, Stein RB, Rosen J. Rapid activation of the interferon-gamma signal transduction pathway by inhibitors of tyrosine phosphatases. J Interferon Res 1994;14(6):365-73.

110. Ram PA, Waxman DJ. Interaction of growth hormone-activated STATs with SH2-containing phosphotyrosine phosphatase SHP-1 and nuclear JAK2 tyrosine kinase. J Biol Chem 1997;272(28):17694-702.

111. Caldenhoven C, vanDijh TB, Solari R, Armstrong J, Raaijnakers JAM, Lammers JWJ, Koenderman L, deGroot RR. Stat3beta, a splice variant factor STAT3, is a dominant negative regulator of transcription. J. Biol. Chem. 1996;271:31221-31227.

112. Schaefer TS, Sanders LK, Nathans D. Cooperative transcriptional activity of Jun and Stat3β, a short form of Stat3. Proc. Natl. Acad. Sci. USA 1995;92:9097-9101.

113. Schaefer TS, Sanders LK, Park OK, Nathans D. Functional differences between Stat3alpha and Stat3beta. Mol Cell Biol 1997;17(9):5307-16.

114. Moriggl RM, Gouilleux-Gruart V, Jahne R, Berchtold S, Gartmann C, Liu X, Hennighausen L, Sotiropoulos , Groner B, Gouilleux F. Deletion of the carboxyl-terminal transactivation domain of MGF-Stat5 results in sustained DNA binding and a dominant negative phenotype. Mol. Cell. Biol. 1996;16:5691-5700.

115. Shuai K, Liao JY, Song MM. Enhancement of antiproliferative activity of gamma interferon by the specific inhibition of tyrosine dephosphorylation of Stat1. Mol. Cell. Biol. 1996;16:4932-4941.

116. Strehlow I, Schindler C. Amino-terminal signal transducer and activator of transcription (STAT) domains regulate nuclear translocation and STAT deactivation. J Biol Chem 1998;273(43):28049-56.

117. Yang E, Wen Z, Haspel RL, Darnell JE Jr. The Linker Domain of Stat1 is Required for Interferon-g Driven Transcription. Submitted 1998;.

118. Bromberg JF, Horvath CM, Besser D, Lathem WW, Darnell JE Jr. Stat3 activation is required for cellular transformation by v-src. Mol. Cell. Biol. 1998;18(5):2553-58.

119. Su WC, Kitagawa M, Xue N, Xie B, Garofalo S, Cho J, Deng C, Horton WA, Fu XY. Activation of Stat1 by mutant fibroblast growth-factor receptor in thanatophoric dysplasia type II dwarfism. Nature 1997;386(6622):288-92.

120. Schindler C. Personal communication.

121. Silvennoinen O, Schindler C, Schlessinger J, Levy DE. Ras-independent growth factor signaling by transcription factor tyrosine phosphorylation. Science 1993;261:1736-1739.

122. Pallard C, Gouilleux F, Benit L, Cocault L, Souyri M, Levy D, Groner B, Gisselbrecht S, Dunsanter-Fourt I. Thrombopoietin activates

a STAT5-like factor in hematopoietic cells. EMBO J. 1995;14:2847-2856.

123. Horvath CM, Darnell JE Jr. The antiviral state induced by alpha interferon and gamma interferon requires transcriptionally active Stat1 protein. J. Virol. 1996;70:647-650.

124. Kessler DS, Levy DE. Protein kinase activity required for an early step in interferon-α signaling. J. Biol. Chem. 1991;266:23471-23476.

125. Tamaoki T. Use and specificity of staurosporine, UCN-01, and calphostin C as protein kinase inhibitors. Methods Enzymol 1991;201:340-7.

126. Ruegg UT, Burgess GM. Staurosporine, K-252 and UCN-01: potent but nonspecific inhibitors of protein kinases. Trends Pharmacol Sci 1989;10(6):218-20.

127. Yu CL, Burakoff SJ. Involvement of proteasomes in regulating Jak-STAT pathways upon interleukin-2 stimulation. J Biol Chem 1997;272(22):14017-20.

128. Callus BA, Mathey-Prevot B. Interleukin-3-induced activation of the JAK/STAT pathway is prolonged by proteasome inhibitors. Blood 1998;91(9):3182-92.

129. Lee CK, Bluyssen HA, Levy DE. Regulation of interferon-alpha responsiveness by the duration of Janus kinase activity. J Biol Chem 1997;272(35):21872-7.

130. Fenteany G, Standaert RF, Lane WS, Choi S, Corey EJ, Schreiber SL. Inhibition of proteasome activities and subunit-specific amino-terminal threonine modification by lactacystin. Science 1995;268:726-731.

131. Palombella VJ, Rando OJ, Goldberg AL, Maniatis T. The ubiquitin-proteasome pathway is required for processing the NF-κB 1 precursor protein and the activation of NF-κB. Cell 1994;78:773-785.

132. Rock KL, Gramm C, Rothstein L, Clark K, Stein R, Dick L, Hwang D, Goldberg AF. Inhibitors of the proteasome block the degradation of most cell proteins and the generation of peptides presented on MHC class I molecules. Cell 1994;78:761-771.

133. Soh J, Donnelly RJ, Kotenko S, Mariano TM, Cook JR, Wang N, Emanuel S, Schwartz B, Miki T, Pestka S. Identification and sequence of an accessory factor required for activation of the human Interferon γ receptor. Cell 1994;76:793-802.

134. Hemmi S, Böhni R, Stark G, DiMarco F, Aguet M. A novel member of the interferon receptor family complements functionality of murine interferon γ receptor in human cells. Cell 1994;76:803-810.

135. Farrar MA, Campbell JD, Schreiber RD. Identification of a functionally important sequence in the C terminus of the interferon-γ receptor. Proc. Natl. Acad. Sci. USA 1992;89:11706-11710.

136. Gilmour KC, Reich NC. Receptor to nucleus signaling by prolactin and interleukin 2 via activation of latent DNA-binding factors. Proc. Natl. Acad. Sci. USA 1994;91:6850-6854.

137. Gilmour KC, Pine R, Reich NC. Interleukin 2 activates STAT5 transcription factor (mammary gland factor) and specific gene expression in T lymphocytes. Proc Natl Acad Sci U S A 1995;92(23):10772-6.

138. Hou J, Schindler U, Henzel WJ, Wong SC, McKnight SL. Identification and purification of human Stat proteins activated in response to interleukin-2. Immunity 1995;2(4):321-9.

139. Gaffen SL, Lai SY, Xu W, Gouilleux F, Groner B, Goldsmith MA, Greene WC. Signaling through the interleukin 2 receptor beta chain activates a STAT-5-like DNA-binding activity. Proc Natl Acad Sci U S A 1995;92(16):7192-6.

140. Fujii H, Nakagawa Y, Schindler U, Kawahara A, Mori H, Gouilleux F, Groner B, Ihle JN, Minami Y, Miyazaki T, et al. Activation of Stat5 by interleukin 2 requires a carboxyl-terminal region of the interleukin 2 receptor beta chain but is not essential for the

proliferative signal transmission. Proc Natl Acad Sci U S A 1995;92(12):5482-6.

141. Gaffen SL, Lai SY, Ha M, Liu X, Hennighausen L, Greene WC, Goldsmith MA. Distinct tyrosine residues within the interleukin-2 receptor beta chain drive signal transduction specificity, redundancy, and diversity. J Biol Chem 1996;271(35):21381-90.

142. Gordon JA. Use of vanadate as a protein-phosphotyrosine phosphatase inhibitor. Meth. Enzymol. 1991;201:477-482.

143. Fernandez L, Flores-Morales A, Lahuna O, Sliva D, Norstedt G, Haldosen LA, Mode A, Gustafsson JA. Desensitization of the growth hormone-induced Janus kinase 2 (Jak 2)/signal transducer and activator of transcription 5 (Stat5)-signaling pathway requires protein synthesis and phospholipase C. Endocrinology 1998;139(4):1815-24.

144. Igarashi K, David M, Larner AC, Finbloom DS. In vitro activation of a transcription factor by gamma interferon requires a membrane-associated tyrosine kinase and is mimicked by vanadate. Mol. Cell. Biol. 1993;13:3984-3989.

145. Radzioch D, Hudson T, Boule M, Barrera L, Urbance JW, Varesio L, Skamene E. Genetic resistance/susceptibility to mycobacteria: phenotypic expression in bone marrow derived macrophage lines. J Leukoc Biol 1991;50(3):263-72.

146. Wigler MH, Weinstein IB. A preparative method for obtaining enucleated mammalian cells. Biochem Biophys Res Commun 1975;63(3):669-74.

147. Bossart W, Loeffler H, Bienz K. Enucleation of cells by density gradient centrifugation. Exp Cell Res 1975;96(2):360-6.

148. Gudas JM, Karenlampi SO, Hankinson O. Intracellular location of the Ah receptor. J Cell Physiol 1986;128(3):441-8.

149. LaFond RE, Kennedy SW, Harrison RW, Villee CA. Immunocytochemical localization of glucocorticoid receptors in cells, cytoplasts, and nucleoplasts. Exp Cell Res 1988;175(1):52-62.

150. Hagting A, Karlsson C, Clute P, Jackman M, Pines J. MPF localization is controlled by nuclear export. EMBO J 1998;17(14):4127-38.

151. Fukuda M, Gotoh I, Gotoh Y, Nishida E. Cytoplasmic localization of mitogen-activated protein kinase kinase directed by its NH2-terminal, leucine-rich short amino acid sequence, which acts as a nuclear export signal. J Biol Chem 1996;271(33):20024-8.

152. Engel K, Kotlyarov A, Gaestel M. Leptomycin B-sensitive nuclear export of MAPKAP kinase 2 is regulated by phosphorylation. EMBO J 1998;17(12):3363-71.

153. Celada A, Schreiber RD. Internalization and degradation of receptor-bound interferon-gamma by murine macrophages. Demonstration of receptor recycling. J Immunol 1987;139(1):147-53.

154. Gorin E, Goodman HM. Turnover of growth hormone receptors in rat adipocytes. Endocrinology 1985;116(5):1796-805.

155. Verdier F, Chretien S, Muller O, Varlet P, Yoshimura A, Gisselbrecht S, Lacombe C, Mayeux P. Proteasomes regulate erythropoietin receptor and signal transducer and activator of transcription 5 (STAT5) activation. Possible involvement of the ubiquitinated Cis protein. J Biol Chem 1998;273(43):28185-90.

156. Timms JF, Carlberg K, Gu H, Chen H, Kamatkar S, Nadler MJ, Rohrschneider LR, Neel BG. Identification of major binding proteins and substrates for the SH2- containing protein tyrosine phosphatase SHP-1 in macrophages. Mol Cell Biol 1998;18(7):3838-50.

157. Diamond RH, Cressman DE, Laz TM, Abrams CS, Taub R. PRL-1, a unique nuclear protein tyrosine phosphatase, affects cell growth. Mol Cell Biol 1994;14(6):3752-62.

158. McLaughlin S, Dixon JE. Alternative splicing gives rise to a nuclear protein tyrosine phosphatase in Drosophila. J Biol Chem 1993;268(10):6839-42.

159. Walton KM, Dixon JE. Protein tyrosine phosphatases. Annu Rev Biochem 1993;62:101-20.

160. Sun H, Charles CH, Lau LF, Tonks NK. MKP-1 (3CH134), an immediate early gene product, is a dual specificity phosphatase that dephosphorylates MAP kinase in vivo. Cell 1993;75(3):487-93.

161. Kumar A, Commane M, Flickinger TW, Horvath CM, Stark GR. Defective TNF-alpha-induced apoptosis in STAT1-null cells due to low constitutive levels of caspases [see comments]. Science 1997;278(5343):1630-2.

162. Gerace L. Nuclear export signals and the fast track to the cytoplasm. Cell 1995;82(3):341-4.

163. Wolff B, Sanglier JJ, Wang Y. Leptomycin B is an inhibitor of nuclear export: inhibition of nucleo- cytoplasmic translocation of the human immunodeficiency virus type 1 (HIV-1) Rev protein and Rev-dependent mRNA. Chem Biol 1997;4(2):139-47.

164. Fornerod M, Ohno M, Yoshida M, Mattaj IW. CRM1 is an export receptor for leucine-rich nuclear export signals [see comments]. Cell 1997;90(6):1051-60.

165. Ullman KS, Powers MA, Forbes DJ. Nuclear export receptors: from importin to exportin [comment]. Cell 1997;90(6):967-70.

166. Kappler JW, Skidmore B, White J, Marrack P. Antigen-inducible, H-2-restricted, interleukin-2-producing T cell hybridomas. Lack of independent antigen and H-2 recognition. J Exp Med 1981;153(5):1198-214.

167. Ghilardi N, Ziegler S, Wiestner A, Stoffel R, Heim MH, Skoda RC. Defective STAT signaling by the leptin receptor in diabetic mice. Proc Natl Acad Sci U S A 1996;93(13):6231-5.

168. Wagner BJ, Hayes TE, Hoban CJ, Cochran BH. The SIF binding element confers sis/PDGF inducibility onto the c-fos promoter. EMBO J. 1990;9:4477-4484.

169. Zhong Z. Ph.D. Thesis. The Rockefeller University, New York City 1995;.

170. Fried M, Crothers DM. Equilibria and kinetics of lac repressor-operator interactions by polyacrylamide gel electrophoresis. Nucl. Acids Res. 1981;9:6505-6525.

End